Uncertainties in Cancer Risk Coefficients for Environmental Exposure to Radionuclides

An Uncertainty Analysis for Risk Coefficients Reported in Federal Guidance Report No. 13

January 2007

Prepared by
D. J. Pawel[a]
R. W. Leggett[b]
K. F. Eckerman[b]
C. B. Nelson[a]

[a]Office of Radiation and Indoor Air
U.S. Environmental Protection Agency
Washington, DC 20460

[b]Oak Ridge National Laboratory
Oak Ridge, Tennessee 37831

Uncertainties in Cancer Risk Coefficients for Environmental Exposure to Radionuclides

An Uncertainty Analysis for Risk Coefficients Reported in Federal Guidance Report No. 13

Authors:
D. J. Pawel
R. W. Leggett
K. F. Eckerman
C. B. Nelson

PREFACE

Federal Guidance Report No.13 (FGR 13) provides cancer risk coefficients for various modes of environmental exposure to each of more than 800 radionuclides (EPA 1999), including inhalation of airborne activity and ingestion of activity in food or drinking water. A risk coefficient for inhalation or ingestion of a radionuclide is an estimate of the probability of radiogenic cancer mortality or morbidity per unit activity taken into the body. A risk coefficient may be interpreted either as the average risk per unit intake for persons exposed throughout life to a constant activity concentration of a radionuclide, or as the average risk per unit intake for persons exposed briefly to the radionuclide in an environmental medium. The risk coefficients in FGR 13 apply to an average member of the public in the sense that estimates of risk are averaged over the age and gender distributions of a hypothetical population whose survival functions and cancer mortality rates are based on recent data for the U.S.

Uncertainties in cancer mortality risk coefficients were assessed in FGR 13 for inhalation or ingestion of each of 11 radionuclides: ^{3}H, ^{60}Co, ^{90}Sr, ^{106}Ru, ^{125}Sb, ^{131}I, ^{137}Cs, ^{226}Ra, ^{232}Th, ^{234}U, and ^{239}Pu. Assigned levels of uncertainty were based on sensitivity analyses in which various combinations of plausible biokinetic and dosimetric models and radiogenic cancer risk models were used to generate alternative risk coefficients. Uncertainties relating to the validity of the linear-no-threshold hypothesis were not addressed in the analysis because this is not feasible. Also, the analysis did not address uncertainties associated with absorbed dose as a measure of cancer risk.

The present report updates the uncertainty analysis in FGR 13 for the cases of inhalation and ingestion of radionuclides and expands the analysis to all radionuclides addressed in that report. This analysis is in response to suggestions that the uncertainty analysis in FGR 13 should be expanded as an aid in determining the kinds of additional information that are most needed for improving confidence in risk assessments for exposure to environmental radionuclides.

As in FGR 13, results of the uncertainty analysis are given in terms of semi-quantitative "uncertainty categories" identified by letters A-E, with Category A representing the most narrowly determined risk coefficients, Category E representing the least well characterized coefficients, and Categories B, C, and D representing intermediate, increasing levels of uncertainty. Assignment of a risk coefficient to an uncertainty category was based on propagation of uncertainties in components of a simplified version of the complex computational model used in FGR 13 to calculate risk coefficients. The uncertainty in a risk coefficient was viewed as the net result of uncertainties in the following main components of the derivation: biokinetic models describing the biological behavior of ingested or inhaled radionuclides; specific energies that relate emissions from source organs to energy deposition in target organs; risk model coefficients representing the risk of cancer per unit absorbed dose to sensitive tissues from low-LET radiation at high dose and high dose rate; tissue-specific dose and dose rate effectiveness factor *(DDREF)*; and tissue-specific high-dose relative biological effectiveness *(RBE)*. The biokinetic models and specific energies together make up the dose model, and the

risk model coefficients, *DDREF*, and *RBEs* together make up the risk model. This formulation allows a convenient allocation of uncertainties associated with the models used to derive the risk coefficients.

Peer reviewers of this report were Dr. Andre Bouville of the U.S. National Institutes of Health, Dr. Lawrence Miller of the Department of Nuclear Engineering, University of Tennessee, and Dr. Wilson McGinn of the Environmental Sciences Division, Oak Ridge National Laboratory (ORNL). Dr. Bouville has chaired or served as a member of a number of committees of the U.S. National Council on Radiation Protection and Measurements (NCRP) and the International Commission on Radiological Protection (ICRP) concerned with uncertainties in radiation dose or risk estimates. Dr. Miller has been involved in investigations of uncertainties in dose estimators for environmentally important radionuclides including ^{90}Sr, ^{131}I, and ^{137}Cs. Dr. McGinn leads the Risk and Regulatory Analysis Group at ORNL and has experience in the area of uncertainties in risk estimators for chemical hazards.

The main comments received from the peer reviewers are paraphrased below. Each comment is followed by a summary of related changes made in the report or reasons for not making changes.

1) The section titled "Results" is too general. Presentation of results for a few radionuclides would be helpful.

Fifteen selected risk coefficients are now examined in Section 3 (Results), six for inhaled radionuclides and nine for ingested radionuclides. The main sources of uncertainty for each of these cases are summarized in a table.

2) The section titled "Discussion" should be expanded.

This section was expanded to provide a fuller discussion of the strengths and weaknesses of the analytical approach. Issues related to characterization of uncertainties in radiogenic cancer risk models were addressed at length because these models are indicated by the analysis to be the dominant source of uncertainty in most of the risk coefficients for inhalation or ingestion given in FGR 13.

3) Explain why relatively large uncertainties were assigned to risk coefficients for the extensively studied radionuclide ^{131}I while relatively small uncertainties were assigned to coefficients for some radionuclides such as ^{95}Zr for which little information is available.

Factors determining uncertainty categories for risk coefficients for ^{131}I, ^{95}Zr, and a number of other radionuclides representing different levels of information were examined and are now addressed in Section 3 (Results). Limitations of the methodology specific to the important radionuclide ^{131}I are further addressed in Section 4 (Discussion). In response to this review comment and the subsequent critical reexamination of the analytical methods, the methodology was revised slightly and uncertainty categories were recalculated for all cases addressed in the report. Based on the revised methods, the uncertainty categories for ingestion of ^{131}I and inhalation of soluble forms of ^{131}I were both revised from Category D (accurate within a factor

of 10) to Category C (accurate within a factor of 7).

4) Why were radon isotopes not considered?

As explained in Section 3 (Results), this report addresses only the risk coefficients tabulated in FGR 13. Ingestion or inhalation of radon was not considered in that document.

5) Why were standard methods of parameter uncertainty analysis not applied to the computational model used in FGR 13?

It is explained in Section 2 (Methods) that it is not feasible to apply the computational model used in FGR 13 in an uncertainty analysis for each of the thousands of risk coefficients tabulated in that document due to the complex model formulation involving numerous parameters that depend on time, age, or gender. It is also noted that a full-scale parameter uncertainty analysis is prohibitive even with the simplified computational model applied in this report because of the large number of cases to be considered and difficulties in assigning uncertainty distributions to some of the parameter values. For each risk coefficient, a limited analysis based on propagation of uncertainties was performed to assess the sensitivity of predictions of the simplified model to dominant sources of uncertainty in each of the parameter values. The typically dominant sources of uncertainty were determined by examination of a number of cases of inhalation or ingestion of specific radionuclides representing different levels and types of information.

6) Explain why much different uncertainty levels are assigned in some cases to different radioisotopes of the same element.

It is explained in Section 4 (Discussion) that the distribution of doses among sensitive tissues and the time period over which doses are delivered may differ radically for two different isotopes of the same element due to differences in radiological half-lives and types and energies of emitted radiations.

7) While the amount of work done to prepare the appendix describing alternative biokinetic models is enormous, the description of the models used in the three variants is often not clear.

The descriptions of nearly all models were expanded with the goal of making the appendix self-contained, i.e., understandable without the need to refer to other documents. Figures showing structures of different types of models have been added. Tables of parameter values were added in cases where descriptions in the text were inadequate.

The authors are grateful for the thoughtful comments from these reviewers. The reviews identified some important weaknesses in the methodology and improvements that could be made in the description of the methods and results. We believe that the efforts to address these problems led to a more strongly supported analysis and a better report.

CONTENTS

LIST OF TABLES

LIST OF TABLES (continued)

LIST OF FIGURES

ABSTRACT

Federal Guidance Report No. 13 (FGR 13) provides risk coefficients for estimation of the risk of cancer due to low-level exposure to each of more than 800 radionuclides. Uncertainties in risk coefficients were quantified in FGR 13 for 33 cases (exposure to each of 11 radionuclides by each of three exposure pathways) on the basis of sensitivity analyses in which various combinations of plausible biokinetic, dosimetric, and radiation risk models were used to generate alternative risk coefficients. The present report updates the uncertainty analysis in FGR 13 for the cases of inhalation and ingestion of radionuclides and expands the analysis to all radionuclides addressed in that report. The analysis indicates that most risk coefficients for inhalation or ingestion of radionuclides are determined within a factor of 5 or less by current information. That is, application of alternate plausible biokinetic and dosimetric models and radiation risk models (based on the linear, no-threshold hypothesis with an adjustment for the dose and dose rate effectiveness factor) is unlikely to change these coefficients by more than a factor of 5. In this analysis the assessed uncertainty in the radiation risk model was found to be the main determinant of the uncertainty category for most risk coefficients, but conclusions concerning the relative contributions of risk and dose models to the total uncertainty in a risk coefficient may depend strongly on the method of assessing uncertainties in the risk model.

1. INTRODUCTION

Federal Guidance Report No.13 (FGR 13) provides cancer risk coefficients for each of more than 800 radionuclides (EPA 1999). A risk coefficient for a radionuclide that exposes persons through a given environmental medium is an estimate of the probability of radiogenic cancer mortality or morbidity per unit activity inhaled or ingested or, in the case of external exposure, per unit time-integrated activity concentration in air or soil. A risk coefficient may be interpreted either as the average risk per unit intake for persons exposed throughout life to a constant activity concentration of a radionuclide, or as the average risk per unit intake for persons exposed briefly to the radionuclide, in an environmental medium. The risk coefficients in FGR 13 apply to an average member of the public, in the sense that estimates of risk are averaged over the age and gender distributions of a hypothetical population whose survival functions and cancer mortality rates are based on recent data for the U.S.

Uncertainties in cancer mortality risk coefficients were quantified in FGR 13 for inhalation or ingestion of ^{3}H, ^{60}Co, ^{90}Sr, ^{106}Ru, ^{125}Sb, ^{131}I, ^{137}Cs, ^{226}Ra, ^{232}Th, ^{234}U, or ^{239}Pu and for external exposure to each of these radionuclides and their progeny in soil. Assigned levels of uncertainty were based on sensitivity analyses in which various combinations of plausible biokinetic and dosimetric models and radiation risk models were used to generate alternative coefficients.

The present report updates the uncertainty analysis in FGR 13 for the cases of inhalation and ingestion of radionuclides and expands the analysis to all radionuclides addressed in that report. This analysis is in response to suggestions that the uncertainty analysis in FGR 13 needed to be expanded for the purpose of deciding what additional information is most needed for improving confidence in risk assessments.

As described in the next section, the complex computational approach used for generating risk coefficients in FGR 13 was simplified for this analysis. Computations in FGR 13 incorporated models for the biological behavior of elements in the human body, the doses to radiosensitive tissues from radiation originating in the body or in an external medium, and the age-specific excess cancer rates per unit dose to these tissues. Also incorporated were data that characterized the mortality and the usage of air, food, and water in the U.S. population. Data characterizing mortality and usage patterns are reasonably reliable. In contrast, biokinetic, dosimetric, and radiation risk models generally have been derived from less complete information and may have substantial uncertainties associated with their predictions. The present analysis considers only uncertainties that are associated with the biokinetic, dosimetric, and radiation risk models, and dose modifying factors such as the relative biological effectiveness (*RBE*) and dose and dose rate effectiveness factor (*DDREF*). *DDREF* is used to account for an apparent decrease of the risk of cancer per unit dose at moderate doses received over an extended period for most cancer sites compared with observations made at high, acutely delivered doses in epidemiologic studies such as that of the atomic bomb survivor cohort. Other than for the DDREF, the present assessment of uncertainty in a risk coefficient does not reflect the uncertainty associated with the linear no-threshold hypothesis underlying the radiation risk models used in this document.

The main results of this uncertainty analysis are tabulated for each of two broad modes of exposure: inhalation and ingestion. This differs from FGR 13 in which risk coefficients were tabulated for both ingestion in tap water and ingestion in food. However, since data on usage patterns are relatively reliable, uncertainties for both modes of ingestion should be similar for most radionuclides. This analysis was based on subjective probability distributions for parameters associated with the biokinetic, dosimetric, and risk models, and the *RBE* and *DDREF* dose modifying factors. Distributional assumptions for the parameters relating to *RBE* and *DDREF* paralleled those made in NCRP report 126 (NCRP 1997), and risk model distributional assumptions were based on an expert elicitation (NRC-CEC 1998). Choices of models, relevant parameters, and distributional assumptions for characterizing uncertainties in the biokinetics of radionuclides were derived in part by considering the extent to which assumptions and parameter values underlying ICRP models might be reasonably altered for a given element. The analysis did not consider uncertainties associated with absorbed dose as a measure of radiogenic cancer risk or idealized representations of the population and exposure.

Results of the uncertainty analysis are given in terms of broad, semi-quantitative "uncertainty categories" identified by letters A-E, with Category A representing the most narrowly determined risk coefficients, Category E representing the least well characterized coefficients, and Categories B, C, and D representing intermediate, increasing levels of uncertainty. The uncertainty category for a radionuclide and exposure mode was determined by the quotient Q_{95}/Q_5, where Q_5 and Q_{95} are the 5% and 95% sample quantiles of a set of risk coefficients generated by combining plausible variations of the biokinetic, dosimetric, and risk models and dose modifying factors used in FGR 13. The risk coefficient was assigned to Category A for Q_{95}/Q_5 less than 15; Category B for Q_{95}/Q_5 between 15 and 35; Category C for Q_{95}/Q_5 between 35 and 65; Category D for Q_{95}/Q_5 between 65 and 150; and Category E for Q_{95}/Q_5 greater than 150.

The proper interpretation of these intervals depends to some extent on the radionuclide. All values in the uncertainty interval from Q_5 to Q_{95} are within a factor of roughly $(Q_{95}/Q_5)^{1/2}$ of the risk coefficient given in FGR 13, provided the risk coefficient is near the geometric mean of Q_5 and Q_{95}. This would most likely occur for radionuclides for which the biokinetic and dosimetric models in FGR 13 were chosen to yield central estimates of dose per unit activity intake. For these radionuclides, risk coefficients in Category B, say, would likely be accurate within a factor of about 5 in the sense that application of alternate plausible biokinetic and dosimetric models, risk model coefficients (based on a linear, no-threshold model), dose and dose rate effectiveness factor (DDREF), and relative radiobiological effectiveness (RBE) for alpha particles appears unlikely to change the risk coefficient by more than this factor. Similarly a risk coefficient in Category D might be accurate within an order of magnitude. For some radionuclides, however, the accuracy of the risk coefficients would be less than this interpretation would suggest. For example, this may be the case for radionuclides for which the dosimetric and biokinetic models were based on conservative assumptions that are expected to overestimate the absorbed doses to some cancer sites.

2

2. METHODS

2.1. A simplified computational model

It is not feasible to apply the computational model used in FGR 13 in an uncertainty analysis for each of the thousands of risk coefficients tabulated in that document due to the complex model formulation involving numerous parameters that depend on time, age, or gender (see Chapters 3-7 of FGR 13). A simpler model was formulated with predictions consistently close to those of the more complicated model and having components that are easier to assess. For inhalation or ingestion of a radionuclide, the simpler model is

$$\text{Cancer Mortality Risk} = \Sigma \, [(d_i \, / \, a_i) + D_i \times b_i)] \, R_i \tag{1}$$

where d_i and D_i are, respectively, low- and high-LET absorbed doses for tissue i, integrated over a period of 20 y after acute intake of the radionuclide by an average adult; R_i is the age- and gender-averaged site-specific cancer mortality risk estimate for tissue i for low-LET uniform irradiation of the tissue at high dose and dose rate; a_i is the low-LET effectiveness factor at moderate dose or dose rate, i.e., the tissue-specific dose and dose rate effectiveness factor *(DDREF)*; and b_i is the biological effectiveness of high-LET radiation relative to high dose, high dose-rate low-LET radiation, i.e., the tissue-specific high-dose relative biological effectiveness (*RBE*). *DDREF* is used to account for an apparent decrease of the risk of cancer per unit dose at moderate doses received over an extended period for most cancer sites compared with observations made at high, acutely delivered doses in epidemiologic studies such as that of the atomic bomb survivor cohort. *RBE* refers to the relative biological effectiveness of alpha radiation in producing fatal cancers, compared with 200 kV x-rays at doses less than 0.2 Gy. The term "high dose *RBE*" is used here to refer to the relative biological effectiveness of alpha radiation to 200kV x- rays when both are received at doses greater than 0.2 Gy. Nominal values for *DDREF*, *RBE,* and high dose *RBE* are given in Table 1.

Table 1. Nominal values for *DDREF(a_i)* and *RBE (b_i)* used in this report, and high dose *RBE* for alpha particles

Tissue	DDREF (a_i)[a]	RBE (b_i)[a]	High dose RBE[b]
Breast	1	10	10
Red marrow	2	1	0.5
All others	2	20	10

[a]For doses < 0.2 Gy
[b]For doses ≥ 0.2 Gy

As illustrated in Figure 1 for the case of intake of radionuclides in drinking water, predictions of the simplistic model represented by Eq. 1 are generally close to the risk coefficients for intake of

radionuclides, although small, systematic differences may arise for a given mode of intake, and differences of 50% or more may occur in a few cases. In Figure 1, comparisons are in terms of the quotient A/B, where A is the cancer mortality risk for acute ingestion of a radionuclide by an average adult as predicted by Eq. 1, and B is the risk coefficient for that radionuclide.
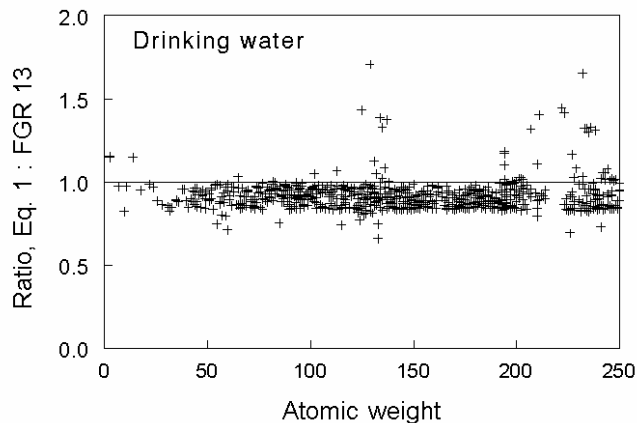
Figure 1. Comparison of predictions of cancer mortality based on Eq. 1 (simplistic estimate) with FGR 13 risk coefficients for intakes of radionuclides in drinking water (Table 2.2a of FGR 13).

Even with the simpler model, a full-scale parameter uncertainty analysis is prohibitive because of the large number of cases to be considered and difficulties in assigning uncertainty distributions to some of the parameter values of Eq. 1. For each risk coefficient, a limited analysis based on propagation of uncertainties was performed to assess the sensitivity of predictions of Eq. 1 to dominant sources of uncertainty in each of the parameter values d_i, a_i, D_i, R_i, and b_i. The uncertainties were propagated through assignment of uncertainty distributions to each of the parameter values and application of random simulation techniques to the model represented by Eq. 1 to generate a range of possible values of each risk coefficient. The 5% and 95% values from the generated range formed the basis for assigning a nominal uncertainty interval for each risk coefficient. This incorporated evaluation of subjective judgments derived from an expert elicitation (NRC-CEC 1998), previously published reports on uncertainties (such as NCRP 1997; EPA 1999), and additional subjective judgments of the authors.

Assignment of uncertainties to the values R_i (age- and gender-averaged risk model coefficients for high dose for tissues $i = 1, 2, ...$) was based on published judgments of nine independent experts on the health effects of radiation (NRC-CEC 1998). Uncertainty distributions assigned to the alpha *RBE*s *(b_i)*, and the *DDREFs (a_i)* were the same as in an EPA report on uncertainties from whole-body low-LET radiation (EPA 1999). Assigned uncertainties for the *RBE*s were based on ranges of values determined from experimental and epidemiological studies of the

4

relative carcinogenic effects of low- and high-LET radiation data, as discussed in recent documents (NAS 1988; NCRP 1990; ICRP 1991; EPA 1991; EPA 1999). Conclusions regarding uncertainties in *DDREF*s were based on subjective evaluations of evidence from animal studies and to some extent on epidemiological studies applied to competing dose-response models. Uncertainties for the parameter values R_i, a_i, and b_i were assumed to be independent of the radionuclide and exposure mode.

Characterization of uncertainties in the tissue-specific dose estimates d_i and D_i (respectively, low- and high-LET dose estimates for tissues $i = 1, 2...$) was more difficult. These uncertainties depend strongly on the radionuclide as well as the exposure mode. As described later, uncertainties in the values d_i and D_i were judged from results of a separate sensitivity analysis in which the typically dominant components of the ICRP's biokinetic and dosimetric scheme were varied within plausible ranges of values.

2.2. Assignment of uncertainties to components of the simplified model

2.2.1 Risk model coefficients for high dose and dose rate

The U.S. Nuclear Regulatory Commission (NRC) and the Commission of European Communities (CEC) conducted a joint study aimed at characterizing the uncertainties in predictions of the consequences of accidental releases of radionuclides into the environment (NRC-CEC 1997, 1998). As part of the exercise, nine experts were asked to provide 5%, 50%, and 95% quantiles of subjective probability distributions for the total number of radiation-induced cancer deaths and for the numbers of tissue-specific cancer deaths over a lifetime in a typical population of 100 million persons, each receiving a whole body dose of 1 Gy low LET radiation at a uniform rate over 1 min. With minor exceptions, the tissues considered in the NRC-CEC study are the same as those addressed in this report. In the present analysis, the uncertainty in site-specific cancer mortality risk estimates for high-dose, low-LET radiation was based on the judgments of the NRC-CEC experts. Results from the expert elicitation are summarized in Table 2.

In the present analysis, a set of site-specific distributions was used to represent the uncertainties in estimates of site-specific cancer deaths following a high dose of radiation at a high dose rate. For each cancer site, nine separate joint probability distributions representing uncertainty in risk per unit dose were constructed based on judgments of each of the nine experts. Each of these distributions was fit to the 5%, 50%, and 95% quantiles supplied by a given expert.

Table 2. Conclusions from nine experts concerning radiation-induced cancer deaths (in millions) over a lifetime in a population of 100 million persons, each receiving a whole body dose of 1 Gy low-LET radiation at a uniform rate over 1 min (NRC-CEC, 1998)

Cancer type	Expert								
	A	B	C	D	E	F	G	H	I
Bone	0.003	0	0.012	0.005	0	0.017	0.0044	0.0027	0.007
	0.018	**0.1**	**0.10**	**0.012**	**0.087**	**0.05**	**0.022**	**0.1**	**0.087**
	0.11	1.0	1.50	0.031	0.261	0.15	0.120	0.15	1.39
Breast	0.0184	0.44	0.02	0.382	0.851	0.207	0.18	0.10	0.22
	0.370	**1.1**	**1.1**	**0.994**	**1.135**	**0.62**	**0.34**	**1.4**	**0.568**
	0.770	2.8	5.0	2.59	1.70	1.87	0.64	4.2	1.25
Colon	0.14	0.16	0.25	0.341	0.08	0.035	0.51	0.065	0.35
	0.72	**0.92**	**1.1**	**0.886**	**0.92**	**0.7**	**1.5**	**1.1**	**0.92**
	3.68	2.26	4.0	2.30	1.84	2.8	3.6	2.0	2.02
Leukemia	0.43	0.64	0.4	0.355	0.336	0.600	0.40	0.020	0.59
	0.81	**1.0**	**1.1**	**0.851**	**1.001**	**1.05**	**0.66**	**1.5**	**1.0**
	1.50	1.5	3.5	2.04	2.00	1.85	1.00	1.8	1.44
Liver	0.055	0.018	0.018	0.028	0	0.43	0.020	0.003	0.005
	0.29	**0.055**	**0.065**	**0.073**	**0.055**	**1.3**	**0.049**	**0.08**	**0.055**
	1.55	0.12	0.25	0.190	0.11	3.80	0.120	0.17	1.21
Lung	0.79	0.014	1.0	0.791	1.12	0.58	0.41	0.80	1.3
	1.83	**3.4**	**3.5**	**2.057**	**3.373**	**1.8**	**1.0**	**3.8**	**3.37**
	4.20	6.4	10.0	5.35	5.06	5.25	2.4	8.6	7.42
Pancreas	0	0	0.03	0.162	0	0	0	0	0.01
	0.13	**0.21**	**0.25**	**0.421**	**0.205**	**0.27**	**0.22**	**0.165**	**0.0205**
	0.70	1.1	1.0	1.10	0.82	1.40	0.82	0.84	0.039
Skin	0.012	0	0.012	0.015	0.028	0	0.00043	0.0040	0.0056
	0.031	**0.056**	**0.08**	**0.038**	**0.056**	**0.05**	**0.0025**	**0.055**	**0.056**
	0.081	0.28	0.50	0.099	0.112	0.27	0.015	0.34	0.123
Stomach	0.12	0.032	0.06	0.156	0	0.58	0.18	0.03	0.0172
	0.50	**0.17**	**0.25**	**0.405**	**0.172**	**2.5**	**0.63**	**0.1**	**0.172**
	2.18	0.43	0.75	1.05	0.344	7.6	2.20	0.48	0.43
Thyroid	0.042	0	0.009	0.009	0.020	0.0475	0.030	0.005	0.0041
	0.19	**0.041**	**0.05**	**0.024**	0.041	**0.19**	**0.092**	**0.06**	**0.041**
	0.84	6.2	0.30	0.064	0.082	0.76	0.280	0.192	0.0779
Residual	1.52	0.48	0.50	1.52	0	1.15	0.77	1.20	0.70
	3.58	**1.8**	**2.25**	**3.964**	**1.787**	**4.6**	**1.9**	**2.2**	**1.79**
	8.45	4.5	10.0	10.3	7.15	13.8	3.9	14.0	3.93
All	5.43	3.4	3.0	3.74	2.94	6.80	4.0	3.5	3.5
	10.7	**8.8**	**9.85**	**9.73**	**8.83**	**13.3**	**7.3**	**7.5**	**8.83**
	21.1	14.0	30.0	25.3	17.7	27.0	12.0	35.0	19.4

In the Monte Carlo simulation used to propagate the uncertainties in components of the model represented by Eq. 1, a distribution of risk coefficients for a given radionuclide and exposure mode was first generated by giving equal weight to each expert's fitted distribution function; that is, an equal number of values were taken from each of the nine distributions. The ratio of the derived 95% to 5% uncertainty bounds was then calculated. A second set of calculations was performed to check whether the derived 5% to 95% uncertainty intervals were highly sensitive to judgments of individual experts, considering that judgments of one or two of the experts sometimes differed noticeably from judgments of the other seven or eight experts. For each tissue, uncertainty bounds were generated by excluding the risk per unit dose values associated with the first expert; the calculations were then repeated by eliminating risk values associated with the second expert; and so forth. The analysis revealed that the 5% to 95% interval based on eight experts was in many cases substantially narrower than the interval based on all nine experts. Because it was not evident whether the elimination of outlying judgments provided a more accurate assessment of current knowledge, the value used as a basis for assigning a risk coefficient to an uncertainty category was the geometric mean of two derived values: (1) the ratio of 95% to 5% uncertainty levels based on judgments of all nine experts; and (2) the smallest of the ratios of 95% to 5% uncertainty levels based on the opinions of eight experts.

2.2.2. Tissue-specific *DDREFs*

In FGR 13, a *DDREF* (identified as a_i in Eq. 1) of 2 was applied to all cancer sites except breast, for which a value of 1 was applied. The distributions used here for representing uncertainties in the *DDREF* are described in the EPA report on uncertainties from whole-body low-LET radiation (EPA 1999), and are based on the approach developed in NCRP Report No. 126 (1997). For all tissues combined, NCRP Report 126 applied a piecewise linear uncertainty distribution to the *DDREF* depicting 2 as the most likely value, 1 as one-fourth as likely as 2, 3 as half as likely as 2, and a value less than 1 or greater than 5 as unlikely (Figure 2).   In the present analysis, a distribution that places more weight on a *DDREF* value close to 1 and assigns a positive probability to *DDREF*s > 5 was assigned to cancer sites other than breast. The distribution is uniform from 1 to 2 and falls off exponentially for values greater than 2. The two parts of the distribution are normalized so that: (1) the probability density function is continuous and (2) the integrals of the uniform and exponential portions are each 0.5. Mathematically, this probability density for the *DDREF*, $f(x)$, can be written:

$$f(x) = 0.5, 1 \le x \le 2$$
$$f(x) = 0.5 \, e^{-(x-2)}, \, x > 2 \tag{2a}$$

This distribution is compared with NCRP's distribution in Figure 2. The probability density function for breast given in Eq. 2b is somewhat more narrow to reflect linear dose response

results observed in several study populations and the apparent invariance in risk with dose fractionation (Hrubec *et al.* 1989, NAS 1990, Howe 1992, Tokunaga *et al.* 1994).

$$f(x) = 2e^{(1-x)}, x > 1 \qquad\qquad (2b)$$
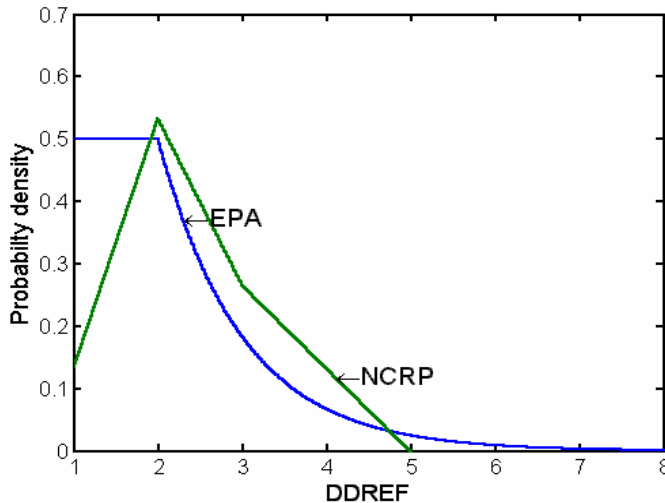
Figure 2. The probability distribution for DDREF applied in this analysis (curve labeled EPA) to tissues other than breast, compared with the distribution applied in NCRP Report 126 (1997) to all tissues combined. A narrower probability distribution was applied in this report to breast (see text).

2.2.3. Tissue-specific *RBE*s

In the derivation of the risk coefficients tabulated in FGR 13, alpha *RBE*s (identified as b_i in Eq. 1) of 1, 10, and 20 were applied to red marrow (leukemia), breast, and all other tissues, respectively. For this analysis, uncertainty distributions assigned to tissue-specific *RBE*s were the same as those described in the EPA report on uncertainties from whole-body low LET radiation (EPA 1999). For most tissues, the assigned distribution was lognormal with geometric mean equal to the square root of 50, and a 90% probability assigned to the interval from 2.5 to 20 (Figure 3). For leukemia, the uncertainty in *RBE* was represented using a uniform distribution between 0 and 1.

8
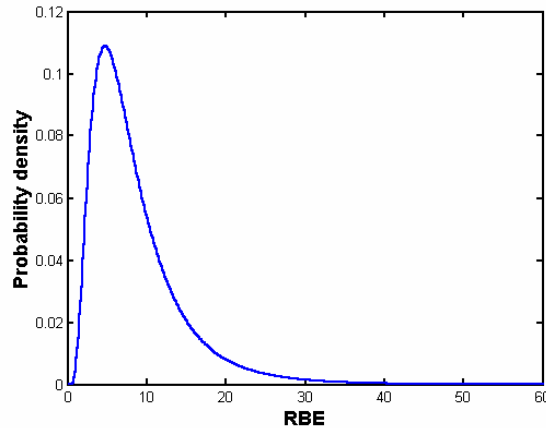
Figure 3. Probability distribution for RBE applied in this analysis to most tissues (see text).

2.2.4. Estimates of absorbed dose

Assignment of uncertainty distributions to the radionuclide-specific parameter values d_i and D_i (respectively, low- and high-LET dose estimates for tissues $i = 1, 2 ...$) for internally deposited radionuclides is particularly difficult because these values are end products of complex calculations involving a collection of uncertain biokinetic and dosimetric models and assumptions. Current biokinetic models for elements generally are not process models, and their parameter values often do not represent measurable quantities. Conversion from internally distributed activity to tissue doses involves the application of specific energies (*SE* values) for numerous pairs of target and source organs, and the uncertainty in a given *SE* value depends on the types and energies of emitted radiations. Even if the information were available to assign meaningful uncertainty distributions to all parameter values of all biokinetic and dosimetric models applied in this report, this would not be a feasible task due to the numerous cases considered.

In view of such difficulties, a systematic scheme was devised to produce computer-generated ranges of plausible dose estimates based on a limited number of plausible alternatives of the typically dominant components of the biokinetic and dosimetric models. The scheme consisted of identification of those components of the models that are usually the most dominant sources of uncertainty in absorbed dose estimates, based on relatively detailed sensitivity analyses for selected radionuclides; for each radionuclide addressed in this document, construction of a few substantially different but equally plausible variations of each of those dominant components; and, for each radionuclide addressed in this document, calculation of absorbed dose estimates using each combination of the constructed components, with all other aspects of the biokinetic and dosimetric models left unchanged.

The following components were judged to represent the dominant uncertainties in most situations: the fraction of inhaled material deposited in the respiratory tract (this was addressed

9

separately from d_i and D_i, as described later), the rate of absorption from the respiratory tract to blood, the gastrointestinal absorption fraction (f_1), the systemic biokinetic model, and *SE* values for certain combinations of source and target organs and radiation types. For inhalation of a radionuclide of a given absorption type, as many as 54 combinations were considered, i.e., all distinct combinations of 3 respiratory models, 3 systemic models, 3 f_1 values, and 2 sets of *SE* values. For ingestion of a radionuclide, 18 combinations were considered in initial dose calculations, i.e., all distinct combinations of 3 f_1 values, 3 systemic models, and 2 sets of *SE* values. The 18 sets of derived dose estimates were used to expand the number of possible values considerably based on an extended, continuous uncertainty distribution for f_1 and the assumption of a linear, tissue-specific relation between f_1 and the dose to each systemic tissue in the case of ingestion of a radionuclide.

The following paragraphs discuss uncertainties in the typically dominant components summarized above. It should be kept in mind that "uncertainty" refers in this report to the level of knowledge of a central value for the subpopulation of interest (e.g., adult males) for exposure to forms of radionuclides typically encountered in the environment. Thus, the uncertainty ranges assigned in this report to components of dosimetric models (e.g., f_1 values) generally are narrower than would be assigned to an unknown individual in the population or to intake of an unusual form of a radionuclide.

Specific energies (*SE* values) for various source and target organs

The *SE* values used to convert from a distribution of activity in the body to dose rates to tissues are known reasonably well in most cases but may represent an important source of uncertainty in dose estimates in some situations. For example, the uncertainty in the amount of emitted energy deposited in sensitive tissues may be large if the target organ is a walled organ such as the urinary bladder or various segments of the gastrointestinal tract, the source organ is the contents of the walled organ, and the radionuclide emits alpha or low-energy beta particles. The uncertainty may also be sizable in the situation in which the target organ is red marrow, the source organ is mineral bone, and the radionuclide is an alpha emitter.

In the ICRP's dosimetric scheme, the dose to a walled organ from alpha particles emitted in its contents is taken as 1% of the dose at the surface of the contents, and the dose from beta particles is assumed to be equivalent to the dose at the surface of the contents. For low-energy beta particles and all alpha particles, these assumptions seem likely to overestimate the dose to radiosensitive cells, which may lie some distance from the surface. For example, there may be virtually no dose to radiosensitive cells of the large intestine walls from alpha particles or low-energy beta particles emitted in the intestinal contents.

For an alpha emitter uniformly distributed in the mineral of trabecular bone, the absorbed fraction in the red marrow depends on the energy of the alpha particle and the proximity of the hematopoietic stem cells to the bone surface. Lacking information on the location of the hematopoietic stem cells, the ICRP assumes that the cells are uniformly distributed within the marrow space. If the sensitive cells were located at least 10 μm from the bone mineral surface,

the relevant absorbed fraction might be overestimated by a factor of 2-3, depending on the energy of the alpha particle.

Based on these considerations, an alternate set of *SE* values for adults was derived. In this alternate set, values *SE* (*T←S*) were reduced for: (1) walled organs *T*, contents *S*, and relatively non-penetrating radiations; (2) red marrow *T*, bone surface *S*, and alpha particles; and (3) red marrow *T*, bone volume *S*, and alpha particles. *SE* values for all other sources and targets were left unchanged. It was assumed that the dose to walled organs from alpha particles arising in the contents is zero. Reductions in *SE* values for low-energy beta particles were energy dependent and were based on methods of Poston *et al*. (1996a, 1996b). *SE* values for red marrow as the target organ and alpha emissions from bone surface or volume were reduced by 60% from the ICRP's nominal values. For each radionuclide, comparative dose calculations were made with the ICRP's *SE* values and this alternate set of *SE* values, together with the various combinations of biokinetic model components described above.

Systemic biokinetic models

For each element, two alternate systemic biokinetic models were constructed, in addition to the ICRP's current systemic biokinetic model. The alternate models were designed in an effort to represent distinctly different but equally plausible representations of the biological behavior of the element. For some elements, this could be achieved by leaving the model structure intact and varying selected parameter values. For other elements, alternate model structures were used. The three systemic biokinetic models assigned to each element are described in Appendix B.

Rate of absorption from the respiratory tract to blood

For the case of inhalation of a radionuclide in particulate form, a separate risk coefficient is given in FGR 13 for each of three main absorption types specified by the ICRP: Type F, corresponding to fast absorption; Type M, corresponding to an intermediate rate of absorption; and Type S, corresponding to slow absorption from the lungs to blood. Risk coefficients for a few radionuclides are also given for vapors or gases (Type V or G). Depending on a variety of factors including the half-life of the radionuclide, the risk coefficient for inhalation of a radionuclide may vary substantially from one absorption type to another. Although it was assumed in the analysis that the user has some basis for assigning an absorption type, situations may arise for which there is little or no information on the form of the airborne material. Comparison of the three risk coefficients for the three different absorption types gives some indication of the extent of the uncertainty in application of any one of these three coefficients arising from lack of information on the physico-chemical form of the airborne radionuclide. Such comparisons are left to the user.

Even if there is sufficient general information on the form of an airborne radionuclide to determine a most nearly appropriate absorption type, the problem remains that each absorption

type represents a wide range of absorption rates to blood (ICRP 1995b). For example, a material would be assigned to Type M if published data on laboratory animals suggest that the rate of absorption to blood falls between 0.069 d^{-1} and 0.001 d^{-1} (ICRP 1995b). Except for very short-lived radionuclides, such a wide range of absorption rates could correspond to a wide range of estimated doses to the lung due to differences in residence time in the lungs. Substantial differences in dose estimates for systemic organs may also occur due to differences in fractional absorption of activity to blood. The estimate of fractional absorption to blood changes when the estimated absorption rate is changed, due to the modeled competition between absorption to blood and mechanical clearance of activity from the thoracic portions of the respiratory tract in the direction of the mouth.

In this analysis it was assumed that the particle size is known to be approximately 1 μm (activity median aerodynamic diameter, or AMAD) and that the user has sufficient information to assign a generic absorption type (Type F, M, or S). It was considered, however, that a given absorption type is intended to represent a relatively wide range of absorption rates and that the actual absorption rate could be substantially different from the baseline parameter values specified by the ICRP for that absorption type.

For Type F material, the data set of dose estimates comprised calculations for each of three absorption rates from the various compartments to blood: 100 d^{-1} (baseline value), 2 d^{-1}, and 0.1 d^{-1}. For Type M, calculations were made for absorption rates of 0.05 d^{-1}, 0.005 d^{-1} (baseline value), or 0.0015 d^{-1}. For Type S, calculations were made for absorption rates of 0.001 d^{-1}, 0.0001 d^{-1} (baseline value), and 0.00002 d^{-1}. These ranges of absorption rates are patterned after criteria given by the ICRP for assigning an absorption type to an inhaled material (ICRP 1995b).

Fractional absorption from the respiratory tract to blood was not treated as an independent uncertainty but was assumed to be determined by the rate of absorption to blood and the half-life of the radionuclide. For long-lived radionuclides, the variations in absorption rates described in the preceding paragraph yield about a twofold variation in fractional absorption from the respiratory tract to blood for Type F or M and about a sevenfold variation for Type S. Variation is smaller for very short-lived radionuclides due to competition between absorption and radiological decay in the respiratory tract.

Fractional absorption from the gastrointestinal tract (f_1)

For each element, three f_1 values were chosen in an effort to span the range of likely values. One of the values was the ICRP's recommended value. If the ICRP's value represented a central estimate, then the other two values were chosen to represent the lower and upper ends of the plausible range of values. If the ICRP's value appeared to represent a cautiously high estimate, then the other two values were set to represent the lower end and a central value from the range of plausible values.

For inhalation cases, all dose calculations (54 sets) were based on the three selections of f_1, using all combinations of the f_1 values, 3 respiratory models, 3 systemic models, and 2 sets of *SE* values. For ingestion cases, the three selected f_1 values were used to derive 18 starting sets of dose estimates based on all combinations of the f_1 values, 3 systemic models, and 2 sets of *SE* values). This is illustrated in Table 3 for the case of for ingestion of [106]Ru, for which f_1 values of 0.005, 0.05 (the ICRP's value), and 0.07 were considered; the table shows the 18 derived dose estimates for two of the tissues addressed, colon and stomach. As described below, the 18 starter sets of dose estimates generated for the case of ingestion of a radionuclide were expanded to a larger set of possible values for ingestion of a radionuclide based on an extended, continuous uncertainty distribution for f_1, assuming a piecewise-linear relation between f_1 and doses to systemic tissues as supported by a number of case studies.

Table 3. Dose estimates for the colon and stomach for ingestion of [106]Ru

Combination	Systemic model	f_1-value	*SE* value	Colon dose (Gy/Bq)	Stomach dose (Gy/Bq)
1	Variation 1	0.005	ICRP	4.59e-08	1.69e-09
2	Variation 1	0.005	Low	3.84e-08	1.42e-09
3	Variation 1	0.05 (ICRP)	ICRP	4.44e-08	1.71e-09
4	Variation 1	0.05 (ICRP)	Low	3.71e-08	1.44e-09
5	Variation 1	0.07	ICRP	4.37e-08	1.72e-09
6	Variation 1	0.07	Low	3.66e-08	1.45e-09
7	ICRP	0.005	ICRP	4.60e-08	1.83e-09
8	ICRP	0.005	Low	3.85e-08	1.56e-09
9	ICRP	0.05 (ICRP)	ICRP	4.55e-08	3.13e-09
10	ICRP	0.05 (ICRP)	Low	3.83e-08	2.86e-09
11	ICRP	0.07	ICRP	4.54e-08	3.71e-09
12	ICRP	0.07	Low	3.83e-08	3.44e-09
13	Variation 2	0.005	ICRP	4.59e-08	1.76e-09
14	Variation 2	0.005	Low	3.84e-08	1.49e-09
15	Variation 2	0.05 (ICRP)	ICRP	4.49e-08	2.46e-09
16	Variation 2	0.05 (ICRP)	Low	3.77e-08	2.19e-09
17	Variation 2	0.07	ICRP	4.45e-08	2.77e-09
18	Variation 2	0.07	Low	3.74e-08	2.50e-09

For each radionuclide, a continuous distribution of possible f_1 values was assigned in the form of a trapezoid with the base representing the assumed range of possible values and the plateau (top, flat portion) representing the most likely range of values. Thus, a trapezoidal distribution of

13

possible f_1 values was defined by four numbers, $a < b < c < d$, where a and d represent the lowest and highest plausible values, respectively, and the interval from b to c represents the most likely range with all values in that range considered equally likely. The element-specific values a, b, c, and d were taken from Table C-1 of Appendix C, which summarizes the authors' assessments of uncertainties in f_1 values for ingestion of environmental radionuclides. For a given element, "Low" and "High" values in Table C-1 were used as the endpoints a and b, respectively, of the base of the trapezoid; the endpoints of the "Most Likely" interval indicated in Table C-1 were used as the endpoints b and c, respectively, of the plateau; and the height of the trapezoid is calculated as the value that gives a trapezoidal area of 1.0. As an illustration, the distribution of possible f_1 values for ruthenium is shown in Figure 4. In this case, $a = 0.001$, $b = 0.005$, $c = 0.07$, and $d = 0.15$, which are the values found in the columns Low, Most Likely (left and right endpoints), and High, respectively, of Table C-1.
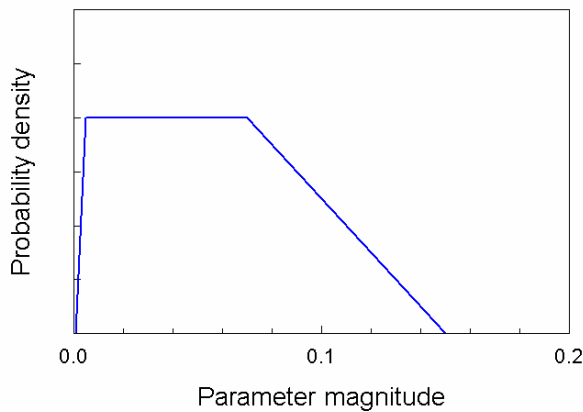
Figure 4. Trapezoidal distribution describing uncertainty in f_1 for ruthenium.

For a given radionuclide and each tissue, the starting set of 18 possible doses from ingestion was used to derive a random set of doses as follows. For a fixed combination of systemic biokinetic model and *SE* values, three different doses $\{D_A, D_B, D_C\}$ to the tissue corresponding to the three starting f_1 values $\{f_A, f_B, f_C\}$ were among the 18 derived dose values. A value f_X was chosen at random from the trapezoidal distribution for f_1, and the dose to the tissue corresponding to f_X was extrapolated from the line through those two points in the set $\{(f_A,D_A), (f_B,D_B), (f_C,D_C)\}$ with f_1 values closest to f_X. Doses for other tissues were then calculated using the same value for f_1. The process was repeated to generate as many as 2160 sets of dose values for each combination of a systemic biokinetic model and a *SE* value.

14

Fractional deposition in the respiratory tract

Although fractional deposition in the respiratory tract represents part of the uncertainty in tissue dose estimates for inhaled radionuclides, it was convenient to address this uncertainty outside the scheme described earlier for developing uncertainty ranges for values d_i and D_i. In contrast to other components of the biokinetic and dosimetric models, fractional deposition of inhaled material in the respiratory tract can be treated as a multiplicative component of the model represented by Eq. 1. That is, for the case of inhalation of a radionuclide, Eq. 1 may be rewritten as

$$\text{Cancer Mortality Risk} = DF \times \Sigma \; [(d_i / a_i) + D_i \times b_i)] \; R_i$$

where DF is the fraction of inhaled material deposited in the respiratory tract, and the values d_i and D_i are calculated for a unit deposition in the respiratory tract.

Because the values d_i and D_i in the above equation are based on the ICRP's assumed deposition fraction, DF_0 (approximately 0.48), for particle size 1 μm (AMAD), the uncertainty distribution for the factor DF in this equation must be normalized to DF_0. The uncertainty in the factor DF was represented by the trapezoidal distribution of unit area with base starting at $0.25/DF_0$ and ending at $0.75/DF_0$ and plateau starting at $0.4/DF_0$ and ending at $0.6/DF_0$.

Sources of uncertainties in tissue dose estimates that were not addressed

There are other sources of uncertainty in tissue dose estimates that are generally less important than those summarized above but not necessarily trivial. These include the rate of transit of material through the segments of the gastrointestinal tract, the initial distribution of inhaled material within the respiratory tract, the rate of mechanical transfer of material between the segments of the respiratory tract, the masses of the target organs, and the definition of lung dose. Lung dose is defined as a weighted average of the doses to three regions of the lungs: the bronchial region (BB), the bronchiolar region (bb), and the alveolar-interstitial (AI) region (ICRP 1994). Two plausible but substantially different sets of lung apportionment factors that have been considered are BB:bb:AI = 0.333:0.333:0.333 (the weights applied by the ICRP) and 0.6:0.3:0.1 (estimated regional distribution of spontaneous lung cancers). For a radionuclide that emits only alpha or low-energy beta radiation, these two sets of apportionment factors could yield lung doses that differ by up to a factor of 3, depending on the physical half-life, the assumed absorption type, and other factors. For most radionuclides, however, the estimate of lung dose is not highly sensitive to the choice of apportionment factors.

3. RESULTS

This chapter summarizes results of the Monte Carlo analysis of uncertainties in the mortality risk coefficients for ingestion and inhalation of radionuclides given in FGR 13. With minor exceptions the radionuclides addressed here and in the internal exposure scenarios in FGR 13 are the same as those addressed in ICRP Publication 72 (1996), which is a summary of the ICRP's dose coefficients for intake of radionuclides by members of the public. Some commonly encountered radionuclides excluded from ICRP Publication 72 and FGR 13 and hence from the present report are isotopes of radon and other noble gases. Both ICRP Publication 72 and FGR 13 address external exposure to isotopes of noble gases from submersion in contaminated air, however, because that is considered to be the dominant mode of exposure to these radionuclides in most situations.

As described in the previous section, conclusions concerning uncertainties in the risk coefficients given in FGR 13 for inhalation and ingestion of radionuclides are based on subjective judgments that were used for deriving inputs to a Monte Carlo simulation. In that simulation, various combinations of substantially different but plausible biokinetic and dosimetric models and radiation risk model coefficients were used to generate alternative risk coefficients. The results of the simulation may be thought of as measures of uncertainty or, perhaps more appropriately, measures of imprecision in risk coefficients in FGR 13, arising from typically dominant uncertainties associated with the underlying models.

In the analysis the uncertainty in a risk coefficient was viewed as the net result of uncertainties in five main components of the derivation:
    (1) biokinetic models, i.e., models describing the biological behavior of ingested or inhaled radionuclides;
    (2) *SE* values describing the relation of sites of decay of internally deposited radionuclides to sites of deposition of emitted energy;
    (3) risk model coefficients, i.e., numerical values representing the risk of cancer per unit absorbed dose to sensitive tissues from low-LET radiation at high dose and high dose rate;
    (4) tissue-specific dose and dose rate effectiveness factor *(DDREF)*;
    (5) tissue-specific high-dose relative biological effectiveness (*RBE*).
Items 1 and 2 together make up the dose model, and items 3-5 together make up the risk model.

The analysis did not address uncertainties associated with the use of a linear, no-threshold model for estimating radiogenic cancer at low doses, absorbed dose as a measure of radiogenic cancer risk, or idealized representation of the population.

The level of uncertainty associated with a dose model may vary with its application. For example, the uncertainty associated with predicted tissue doses following inhalation of a radionuclide may depend strongly on the availability of information on the chemical and physical characteristics of the carrier, which is needed to select the appropriate particle size and absorption type. Thus, to develop meaningful statements of uncertainty, it was necessary to specify the type and level of information available on the exposure. For consideration of risk

coefficients for inhalation of particulates it was assumed that the particle size is known to be approximately 1 μm (activity median aerodynamic diameter, or AMAD) and that the absorption type is known in the sense that there is sufficient general information on the form of the inhaled radionuclide to establish with reasonable confidence that this is the most nearly accurate absorption type. For example, it may be known that the radionuclide is in a readily soluble form indicative of Type F material or a highly insoluble form indicative of Type S material. It was considered in the analysis, however, that a given absorption type is intended to represent a relatively wide range of absorption rates and that the actual absorption rate could be substantially different from the baseline parameter values specified by the ICRP for that absorption type.

The results of the analysis are tabulated by radionuclide in Table D-1 (ingestion) and Table D-2 (inhalation) of Appendix D. As in FGR 13, which provides uncertainty statements for selected risk coefficients, judgments concerning the uncertainty in a risk coefficient are tabulated in terms of relatively broad, semi-quantitative "uncertainty categories" identified by letters *A-E*. The uncertainty category for a radionuclide and exposure mode was determined by the quotient Q_{95}/Q_5, where Q_5 and Q_{95} are the 5% and 95% sample quantiles of a set of risk coefficients generated by combining plausible variations of the biokinetic, dosimetric, and risk models and dose modifying factors used in FGR 13. A risk coefficient was assigned to Category A if Q_{95}/Q_5 <15; Category B if $15 \leq Q_{95}/Q_5 < 35$; Category C if $35 \leq Q_{95}/Q_5 < 65$; Category D if $65 \leq Q_{95}/Q_5 < 150$; and Category E if $Q_{95}/Q_5 \geq 150$. A risk coefficient in Category B, for example, is considered to be determined within a factor of about 5, in the sense that application of alternate plausible biokinetic and dosimetric models, risk model coefficients (based on a linear, no-threshold model), dose and dose rate effectiveness factor (*DDREF*), and relative radiobiological effectiveness (*RBE*) for alpha particles appears from this analysis to be unlikely to change the risk coefficient by more than this factor. Similarly, a risk coefficient in Category D is considered to be determined within an order of magnitude.

Table 4 lists the relative numbers of risk coefficients assigned to each of these uncertainty categories. For both the ingestion and the inhalation cases, most of the risk coefficients were assigned to Categories A and B, indicating that most of the risk coefficients appear on the basis of this analysis to have been determined within a factor of 5 or less by the models of FGR 13. Only 3% of the risk coefficients for ingestion and 1% of those for inhalation were assigned to the highest category (E), indicating that nearly all of the risk coefficients have been determined within an order of magnitude by the models applied in FGR 13.

An assessment was made of the relative contributions of different sources of uncertainty (individual items 1-5 listed above, or the dose model consisting of items 1 and 2, or the risk model consisting of items 3-5) to the total uncertainty in a risk coefficient. This was accomplished by repeating the analysis but varying only one of the sources at a time while fixing the other sources as they were applied in FGR 13 in the derivation of risk coefficients. This analysis suggested that the risk model is an important component of the overall uncertainty in most risk coefficients. Although the uncertainty in the dose model generally had some effect on determining the uncertainty category for a risk coefficient, the risk model was usually the main determinant of the category. As pointed out in the next section, however, the relative

17

contribution of risk and dose model uncertainties to the overall uncertainty in a risk coefficient may depend strongly on the method of assessing uncertainties in each type of model or the individuals or group performing the assessment.

Table 4. Relative numbers of risk coefficients assigned to uncertainty categories

Uncertainty category	Definition	% radionuclides in category	
		Ingestion	Inhalation
A	$Q_{95}/Q_5 < 15$	26	42
B	$15 \leq Q_{95}/Q_5 < 35$	51	42
C	$35 \leq Q_{95}/Q_5 < 65$	11	10
D	$65 \leq Q_{95}/Q_5 < 150$	8	5
E	$Q_{95}/Q_5 \geq 150$	3	1

The following idealized description of the results of the analysis has a number of exceptions but is descriptive of the relative importance of the dose and risk models in determining the overall uncertainty in a risk coefficient. The dose and risk models together determined the tissues that contributed most to a risk coefficient. That is, the dose model determined the tissues receiving highest doses, and the risk model involved multipliers that modified the doses to these tissues with regard to their importance as contributors to cancer risk. The products of dose and risk per unit dose for individual tissues are combined to give the risk coefficient. If the risk models for the dominant tissues (i.e., those contributing most to the risk coefficient) were relatively well established, the uncertainty category might be A or B, depending somewhat on the level of uncertainty in the dose model. If the risk models were moderately uncertain, the uncertainty category would likely be B or C, depending on the uncertainty in the dose model. If the risk models were highly uncertain, the uncertainty category might be C, D, or E, depending on the uncertainty in the dose model. If the dose model indicated that doses are relatively uniform among tissue, the derived uncertainty generally was small (Category A or B).

The different levels of uncertainty in the generally dominant component of the risk models, i.e., the risk model coefficients, are indicated in Table 5. (Uncertainties associated with the other two components of the risk models, i.e., the *DDREFs* and, for alpha emitters, the *RBEs*, are discussed in Section 2.) The risk model coefficients used in FGR 13 were inferred largely from epidemiological data on radiogenic cancer and involve uncertainties associated with extrapolation of these data to other populations and other radiation types. As discussed in Section 2, the magnitudes of uncertainties in the risk model coefficients were assessed on the basis of tissue-specific distributions generated from conclusions of nine researchers involved in an expert elicitation study (NRC-CEC 1998). As part of the exercise, the nine experts were asked to provide 5%, 50%, and 95% quantiles of subjective probability distributions for the total

number of radiation-induced cancer deaths and for the numbers of tissue-specific cancer deaths over a lifetime in a typical population of 100 million persons, each receiving a whole body dose of 1 Gy low LET radiation at a uniform rate over 1 min. Table 5 summarizes the conclusions of those experts. The measures of the uncertainties in tissue-specific risk model coefficients indicated in this table are the ratios of the 95% to 5% quantiles for all nine experts (fifth column) and the minimal ratios of the 95% to 5% quantiles for all combinations of eight of nine experts (last column).

Table 5. Spread of expert judgments concerning risk per unit dose for tissues. Nine experts were asked to provide 5%, 50%, and 95% quantiles of subjective probability distributions for radiation-induced cancer deaths (in millions) over a lifetime in a population of 100 million persons, each receiving a whole body dose of 1 Gy low LET radiation at a uniform rate over 1 min (NRC-CEC, 1998)

Cancer site	Combined judgments of all 9 experts				95% / 5% for 8 experts[a]
	5%	50%	95%	95% / 5%	
Leukemia[b]	0.437	0.968	1.87	4.28	3.95
Lung	0.636	2.51	6.69	10.5	8.71
Other	0.734	2.678	9.54	13.0	11.1
Breast	0.188	0.754	2.77	14.7	12.0
Colon	0.171	0.964	2.73	16.0	12.0
Thyroid	0.0073	0.0586	0.479	65.5	33.6
Stomach	0.0435	0.276	3.01	69.1	28.3
Liver	0.0158	0.0748	1.57	99.3	35.0
Bone	0.0046	0.0483	0.491	107	73.1
Skin	0.0014	0.0433	0.210	150	42.6
Total	4.06	9.51	24.0	5.90	5.54

[a]Smallest ratio obtained by omitting judgments of any one of the 9 experts.
[b]Dose to red marrow used to estimate risk of leukemia.

Based on these 95% to 5% ratios, the risk model coefficients seem relatively well known for red marrow (dose to red marrow was used to estimate risk of leukemia) and for uniform irradiation of the total body; moderately well known for lung, breast, colon, and "other" (collective tissues not explicitly identified in this list), and relatively poorly known for thyroid, stomach, liver, bone, and skin. These conclusions are based on the premise that judgments of as many as eight or nine experts will become less consistent between experts as the quality and quantity of information decreases. That is, the premise is that inconsistency in expert judgment is a valid measure of uncertainty in a quantity.

Table 6. Basis for uncertainty categories for selected risk coefficients

Case	Category	Main sources of uncertainty and comments
Ingestion of H-3 as tritiated water	A	Risk and dose models contribute ~ 80% and 20% of uncertainty, respectively. GI uptake virtually complete. Systemic biokinetics well known. Absorbed activity nearly uniformly distributed, yielding relatively low risk model uncertainty.
Inhalation of H-3 as vapor or tritiated water	A	Risk and dose models contribute ~ 80% and 20% of uncertainty, respectively. Absorption from respiratory tract rapid and virtually complete. Systemic biokinetics well known. Absorbed activity nearly uniformly distributed, yielding relatively low risk model uncertainty.
Ingestion of Co-60	B	Risk and dose models contribute ~ 70% and 30% of uncertainty, respectively. GI uptake and systemic biokinetics moderately well established. Dominant cancer site is colon. Risk model for colon moderately uncertain.
Inhalation of Co-60 (Type M)	B	Risk and dose models contribute ~ 70% and 30% of uncertainty, respectively. Fractional deposition in respiratory tract reasonably well known for 1-µm (AMAD) particles. Estimated lung dose sensitive to uncertainty in dissolution rate in lungs. Fractional absorption to blood and systemic biokinetics moderately well known. Dominant cancer site is lung followed by colon. Risk model moderately uncertain in both cases.
Ingestion of Sr-90	A	Risk and dose models contribute ~ 65% and 35% of uncertainty, respectively. GI uptake and systemic biokinetics well known. Dominant cancer type is leukemia; risk model is well established.
Inhalation of Zr-95 (Type M)	B	Risk and dose models contribute ~ 85% and 15% of uncertainty, respectively. Fractional deposition in respiratory tract reasonably well known for 1-µm (AMAD) particles. Estimated lung dose sensitive to uncertainty in dissolution rate in lungs. Fractional uptake to blood moderately well established. Systemic biokinetics overall not well known but doses to critical tissues are only moderately sensitive to these uncertainties. Dominant cancer site is lung followed by colon, red marrow (leukemia). Risk models moderately well established for lung, colon; well established for leukemia.
Ingestion of Ru-106	B	Risk and dose models contribute ~ 95% and 5% of uncertainty, respectively. GI uptake and systemic biokinetics not well known overall but dose to critical tissues only moderately sensitive to uncertainties. Dominant cancer site is colon. Risk model for colon moderately uncertain.

Table 6 (continued)

Ingestion of I-131	C	Risk and dose models contribute ~ 95% and 5% of uncertainty, respectively. GI uptake virtually complete. Systemic biokinetics reasonably well known for dominant cancer site (thyroid). Risk model for radiogenic thyroid cancer deaths highly uncertain, at least as indicated by results of the NRC-CEC expert solicitation study. Analysis based on updated, age-specific risk model might indicate much less uncertainty in risk coefficient.
Ingestion of Cs-137	A	Risk and dose models contribute ~ 85% and 15% of uncertainty, respectively. GI uptake virtually complete. Systemic biokinetics well known. Absorbed activity nearly uniformly distributed, yielding relatively low risk model uncertainty.
Inhalation of Cs-137 (Type F)	A	Risk and dose models contribute ~ 85% and 15% of uncertainty, respectively. Fractional deposition in respiratory tract reasonably well known for 1-µm (AMAD) particles. Fractional absorption to blood and systemic biokinetics well known. Absorbed activity nearly uniformly distributed, yielding relatively low risk model uncertainty.
Ingestion of Gd-148	E	Risk and dose models contribute ~ 80% and 20% of uncertainty, respectively; both models are highly uncertain. GI uptake known to be low but can be estimated only within order of magnitude. Systemic biokinetics broadly understood. Important cancer sites include bone and liver; risk model is highly uncertain in both cases.
Ingestion of Ra-226	C	Risk and dose models contribute ~90% and 10% of uncertainty, respectively. GI uptake and systemic biokinetics reasonably well established. Important cancer sites include bone, for which the risk model is highly uncertain, and colon, for which risk model is moderately uncertain.
Ingestion of U-234	C	Risk and dose models contribute ~90% and 10% of uncertainty, respectively. GI uptake and most of the important aspects of systemic biokinetics reasonably well known. Important cancer sites include colon, for which risk model is moderately well established, and bone, for which risk model is poorly established.
Inhalation of U-234 (Type M)	C	Risk and dose models contribute ~80% and 20% of uncertainty, respectively. Fractional deposition in respiratory tract reasonably well known for 1-µm (AMAD) particles. Fractional uptake to blood moderately well established. Dominant cancer sites are lung and colon, for which risk model is moderately well established. Risk models less well established for other important sites such as bone.
Inhalation of Pu-238 (Type S)	B	Risk model contributes ~98% of uncertainty. Fractional deposition in respiratory tract reasonably well known for 1-µm (AMAD) particles. Fractional absorption from respiratory or gastrointestinal tract to blood not well established. Systemic biokinetics reasonably well established. Risk coefficient relatively insensitive to uncertainties in absorption and systemic biokinetics. Lung is dominant tissue at risk. Risk model for lung moderately uncertain.

The relative contributions of uncertainties in the dose model and risk model to the total uncertainty in a risk coefficient are illustrated in Table 6 for 15 risk coefficients. The different cases addressed in Table 6 represent all five uncertainty categories considered in the analysis, a wide range of uncertainty levels in both the dose models and the risk models, and a number of different tissues at risk. In each of these 15 cases, the risk model accounted for at least 65% and as much as 98% of the quantified uncertainty in the risk coefficients. Although it is difficult to assess the relative uncertainties associated with the risk versus dose models, a reasonable conclusion would be that for each of these radionuclides the risk model is an important component of the overall uncertainty in the risk coefficient.

4. DISCUSSION

Characterization of uncertainties in estimates of cancer risk from environmental exposure to radionuclides is a complex problem that has received little attention in the literature. The problem is particularly complicated for internally deposited radionuclides because each radionuclide presents a unique combination of issues associated with deposition and retention in the respiratory tract, the rate and level of absorption from the respiratory or gastrointestinal tract to blood, the time-dependent distribution and retention of the parent radionuclide and any radioactive progeny in systemic tissues, and the types and energies of emitted radiations. Conclusions drawn for a given radionuclide may not apply to other radioisotopes of the same element due to differences in the types of radiation emitted and differences in radiological half-lives that may result in changes in the time-frame over which the dose is received. For example, uncertainties in dose estimates may be much smaller for short-lived isotopes than longer-lived isotopes because the biokinetics of an element may be well understood for times close to intake, when a short-lived radionuclide delivers its dose, but poorly understood for times remote from intake, when a long-lived radionuclide may deliver most of its dose. Conclusions drawn for intake of a certain chemical form of a radionuclide may not apply to other chemical forms due to differences in retention properties in the respiratory tract or in the level of absorption to blood from the respiratory or gastrointestinal tract. For such reasons, an analysis of uncertainties in risk coefficients that addresses radionuclide-specific issues in detail is not feasible for the comprehensive set of radionuclides considered in FGR 13.

The uncertainty categories for risk coefficients tabulated in this report were based on a simplistic model in which the risk per unit activity for each type of radiation (high-LET or low-LET) is expressed as the product of three components: 1) the risk per absorbed dose received by target tissues (for low-LET high dose and dose rate radiation); 2) modifying factors applied to the first component to account for type of radiation, dose, and dose rate; and 3) the absorbed dose per unit activity. This formulation allows a convenient allocation of uncertainties associated with the models used to derive the risk coefficients and is a logical extension of formulations in previous evaluations of uncertainties in risks from whole-body irradiation (NCRP 1997; EPA 1999).

Uncertainties relating to the validity of the linear-no-threshold hypothesis were not addressed because this is not feasible. Also, the analysis did not consider uncertainties associated with absorbed dose as a measure of radiogenic cancer risk or idealized representations of the population and exposure.

The approach was designed as an efficient way of estimating the sensitivity of each of thousands of risk coefficients tabulated in Federal Guidance Report 13 to uncertainties in the underlying dose and risk models. For any given risk coefficient the results of this analysis could be refined and potentially improved by addressing components of the more sophisticated computational scheme used in Federal Guidance Report 13 and focusing on information and sources of uncertainty most relevant to the radionuclide and its dominant cancer sites. This is particularly true of radionuclides that deliver their dose over a relatively short period after intake and show

strong age dependency with regard to dose per unit intake or cancer risk per unit dose for the dominant cancer sites. For example, for ingested ^{131}I the simplistic age-independent risk model used in the present report does not take account of the strong multiplicative age dependencies associated with thyroid dose and thyroid cancer risk per unit dose, nor does it take account of recent information on thyroid cancers related to ^{131}I exposure following the Chernobyl accident.

The approach used here is not appropriate for radon, for which risks projections are from analyses of cohorts of miners and relate risk to exposure rather than absorbed dose. Risk coefficients for intake of radon were not given in Federal Guidance Report 13 and are not considered in the present document.

Issues relating to the use of the expert elicitation for characterizing uncertainties in risk per absorbed dose (NRC-CEC, 1997) should be highlighted because these uncertainties were frequently judged to be the dominant contribution to total uncertainty in risk coefficients. NRC-CEC (1997) gives a description of the process and how the experts were chosen. Briefly, the experts were chosen in order "to provide a wide diversity of expertise and experience." We did not attempt to weight the opinions of the experts, because information that might be used for the weighting was not yet available. The two most important steps for combining the results from the experts were (1) to construct probability distributions representing the subjective judgment of each expert for the proportion of fatal cancers that would result from a specific dose to each tissue, and (2) to average the resulting probability densities. Approaches for combining expert opinion are discussed by Clemen and Winkler (1999). They concluded that, in general, simple approaches for combining probability distributions, such as our averaging of probability densities derived for each expert, often perform as well or better than more complex approaches.

Our results indicate that the sensitivity to the choice of experts for the elicitation is greater for risk per absorbed dose for individual tissues than for the combined risk per absorbed dose to all tissues. Thus, results from our uncertainty analysis for radionuclides such as [3]H (tritium), for which the absorbed dose is similar for most tissues, would be largely independent of the choice of experts or how the experts are weighted. For other radionuclides, for which the dominant cancer site category would typically be either colon, leukemia, stomach, thyroid, or residual, the assigned uncertainties might sometimes change with a different choice of experts or weighting scheme, but most likely by at most by one uncertainty category. It would appear that for radionuclides with the largest uncertainties, our uncertainty categorization would be especially robust to the choice of experts, since the uncertainties relating to the models for absorbed dose predominate in those cases.

The uncertainty intervals in Table 5 for risk per absorbed dose derived from the expert elicitation tend to be wider than comparable intervals derived from results from alternative sources such as the BEIR VII report (NRC 2006) or the Interactive Radio-Epidemiological Program (IREP) (IREP 2006). BEIR VII is the most recent comprehensive review by the National Academy of Sciences of health risks from low levels of ionizing radiation. IREP is a publicly available computer software program used by the Department of Labor to determine the probability that a cancer was caused by radiation. (Neither BEIR VII nor IREP was available at the time that the

methods of the present report were designed.) Table 7 compares the ratio of 95% to 5% uncertainty bounds derived from IREP for excess relative risk (ERR) – the proportional increase in cancer risk over background due to radiation – to the ratio of 95% to 5% uncertainty bounds for lifetime risk projections in BEIR VII and the expert elicitation. Note that IREP does not calculate lifetime risk projections, but ratios of uncertainty bounds for ERR and lifetime risk should be similar. For purposes of comparison results in Table 7 do not incorporate uncertainties associated with DDREF, which based on our analyses would be much smaller than uncertainties associated with risk per absorbed dose. For DDREF, the approach used for our uncertainty calculations was less complicated than in IREP and similar to what was done in BEIR VII.

Table 7. Comparison of IREP, BEIR VII, and expert elicitation based ratios of 95% to 5% uncertainty bounds for either excess relative risk (ERR) or lifetime risk projections of radiogenic risk to the U.S. population[a,b]

Site	IREP				BEIR VII		Expert elicitation	
	Males		Females				All 9	Excluding
	Age at Exposure		Age at Exposure		Males	Females	experts	1 "outlier"
	20y	30y	20y	30y				
Breast			4.2	4.6		1.8	14.7	12.0
Colon	7.2	6.3	7.3	5.0	4.8	4.2	16.0	12.0
Liver	12.8	13.0	9.5	9.7	21.5	48.4	99.3	35.0
Lung	4.8	4.8	3.8	3.8	3.9	3.4	10.5	8.7
Bone	5.0	4.5	4.2	3.7			107.0	73.1
Stomach	221.0	126.0	15.6	19.4	43.8	36.2	69.1	28.3
Thyroid	15.4	17.1	15.4	17.1	9.3	9.1	65.5	33.6
Other	5.5	5.0	5.4	4.8	3.0	2.8	13.0	11.1
Leukemia	20.0	5.5	18.0	5.4	6.4	8.2	4.3	4.0
All solid					1.8	1.5		

[a]Uncertainty intervals from IREP version 5.5.1 (obtained online at http://www.niosh-irep.com/irep_niosh) are for excess relative risk (ERR) per mSv at attained age 70 y, and age at exposure 20 or 30y. The BEIR VII and expert elicitation based intervals are for lifetime risks for populations of mixed ages.

[b]The uncertainty intervals incorporate uncertainties relating to sampling variation, assigned doses in the atomic bomb cohort, transportation of risks, but not uncertainties relating to DDREF. In BEIR VII the uncertainty associated with transportation of risks is assumed to be 0 for female breast cancer.

From Table 7, the ratios of uncertainty bounds typically are two to three times wider based on the expert elicitation than from either BEIR VII or IREP. The wider uncertainty intervals from the expert elicitation reflect differences in subjective judgment among the experts, whereas unified approaches were used to derive the results for both IREP and BEIR VII. The ratios for uncertainty intervals from individual experts (Table 2) were substantially smaller than the ratios reflecting the aggregate judgments of the experts (Table 7) and often comparable to the ratios from IREP and BEIR VII.

It is not clear whether the application of either IREP or BEIR VII rather than the NRC-CEC

expert elicitation study would yield a more strongly supported categorization of uncertainties in risk coefficients. The expert elicitation might better reflect similarly valid but differing opinions on risk for some types of cancers, but conclusions of IREP or BEIR VII might be superior for cancers for which some experts might not have been well informed. In particular, results from IREP and BEIR VII tended to be based more on results from the A-bomb survivors, and in our opinion the intervals are particularly well formulated for the many cancers sites for which A-bomb survivor cohort is the dominant source of information. In addition, both IREP and BEIR VII benefited from more thorough review processes. On the other hand, use of the expert elicitation has the advantages that the derived uncertainty intervals are generally less likely to underestimate uncertainties, and the intervals may reflect a more balanced approach for sites for which sources of data other than the A-bomb data should be considered.

The most divergent results in Table 7 are for bone cancer (BEIR VII versus the expert elicitation) and breast cancer (IREP versus the expert elicitation). IREP grouped bone cancer with "other and ill-defined sites", based on the judgment that the data on the relatively few A-bomb survivors with bone cancer did not provide an adequate basis for estimating risk or associated uncertainty. This may have led to unrealistically narrow intervals; many of the cancers among A-bomb survivors were categorized as "other or ill-defined", and sampling variation for this category was relatively small. In contrast, the uncertainty for radiogenic bone cancer would likely be smaller than suggested from expert elicitation results. Some experts apparently overestimated bone cancer risk using results from Mays and Speiss (1984) without properly accounting for the approximately 7.5-fold difference between endosteal and skeletal dose (EPA 1994).   For breast cancer, BEIR VII (in contrast to IREP) considered as negligible "transport" uncertainties relating to the use of risk estimates derived in part on results from Japanese A-bomb survivor population. In the case of leukemia, the uncertainty interval based on the aggregate judgment from the expert elicitation is narrower than the intervals from IREP or BEIR VII. It may be that the experts were all, or nearly all, strongly influenced by a set of calculations regarding leukemia that had been presented to the committee (NRC-CEC 1997).

In contrast to the uncertainties relating to risk per absorbed dose, the uncertainties relating to dose per unit intake were assessed using the judgment of two of the authors of the present report. Thus, our characterization of uncertainties for dose per unit intake did not reflect differences in judgment that may exist among other experts, which is a factor that should be considered before concluding that the risk model is the dominant source of uncertainty in a risk coefficient for a particular radionuclide and mode of intake.

APPENDIX A: COMBINING EXPERT OPINIONS
ON RISKS FROM WHOLE BODY IRRADIATION

Uncertainty distributions representing the combined expert opinions on risk per unit absorbed dose were obtained by 1) fitting a distribution to the 5th, 50th, and 95th percentile values for each expert, and 2) averaging the density functions associated with each expert.

Fitting distributions to percentile values

For each expert, we assumed that risk per unit dose (Y) for a specified cancer site is related to a normal random variable X with mean (μ) and standard deviation (σ) by a power transformation given by:

$$x = \frac{y^{\lambda} - 1}{\lambda} \quad (\lambda \neq 0)$$

$$x = \log(y) \quad (\lambda = 0).$$

Values for μ, σ, and λ were then chosen to be consistent with the 5th, 50th, and 95th percentile values provided by the expert. In fact, the transformed values (x) associated with each cancer site were assumed to follow a multivariate normal distribution. A simple correlation structure was assumed between cancer sites so that the corresponding quantiles for the total risk per unit dose – the tissue-specific risks summed over all sites – were as consistent as possible with the quantile values provided by the expert.

Composite distributions

A composite distribution, for the combined opinions of the nine experts, was derived by simply averaging the density functions fitted for each expert. Alternate composite distributions were obtained by averaging the fitted density functions from each set of eight experts. As described in the text, for each radionuclide the analysis was based on the composite distribution for all nine experts and the alternate composite distribution that results in the smallest ratio of upper to lower uncertainty bounds.

APPENDIX B: UNCERTAINTIES IN SYSTEMIC BIOKINETICS OF RADIONUCLIDES AND VARIANTS OF ICRP SYSTEMIC BIOKINETIC MODELS USED IN ANALYSIS

The ICRP uses systemic biokinetic models to predict the behavior of radionuclides that have been absorbed to blood. These models are generally specific to an element rather than to particular isotopes of that element. In a few cases, different systemic biokinetic models are provided for different forms of an element taken into the body. For example, different models are given for organic and inorganic sulfur.

This appendix summarizes the biokinetic database for each of the elements addressed in this report and describes variants of the ICRP's biokinetic models used to examine the sensitivity of dose estimates to uncertainties in the systemic biokinetics of radionuclides. In each case, a "low variant" and a "high variant" of the ICRP's systemic biokinetic model for a typical adult is provided. The low and high variants were usually constructed by the authors but in some cases were selected from existing biokinetic models for an element. Ideally, a low or high variant model would produce a reasonable lower bound or upper bound, respectively, of the cumulative activity of each radionuclide in each tissue of the body. Depending on the complexity of the biokinetics of an element, however, it may be difficult to identify plausible alternative models A and B for an element such that A yields lower estimates of cumulative activity than B for all radioisotopes of an element and all tissues of the body. The low and high variants given below were generally constructed or selected with specific radioisotopes of an element and specific repositories in mind and may not preserve the ideal order (low variant < ICRP model < high variant) of cumulative activities for all isotopes of an element and all tissues of the body.

Except where otherwise indicated, the following summaries are based on information provided in the following reports or papers: ICRP 1979, 1980, 1981, 1987, 1988, 1989, 1993, 1995a, 1995b; Leggett 1992; Leggett *et al*.1994; Leggett *et al*. 1998.

^{3}H as tritiated water (HTO)

There is a large data base on whole-body retention of ^{3}H in adult humans exposed to HTO, and there have been several detailed studies of the behavior of HTO in laboratory animals (ICRP 1989). It has been established that ^{3}H is fairly uniformly distributed in the body and that the retention can be described as a sum of 2-3 exponential terms. The dominant, short-term component closely approximates the turnover of body water, and the longer-term components, apparently representing a relatively small portion of the cumulative activity, appear to represent tritium incorporated into tissues. The consistency in reported means of the short-term half-time in largely adult male study groups indicate that the typical short-term half-time is reasonably well established for this portion of the population. The equivalence of the short-term component with the turnover of body water, as supported by observations on adult male humans and laboratory animals, provides a means of extending the model to adult females with some confidence. Thus, a combination of different types of data leads to reasonably high confidence in estimates of cumulative activity of ^{3}H in the body after intake of HTO by the typical adult.

In the ICRP's systemic model for tritiated water in the adult, 97% of absorbed tritium is assigned to a compartment with half-time 10 d and 3% to a compartment with half-time 40 d (ICRP 1989, 1993).

Low variant: Model half-times are decreased by a factor of 1.5

High variant: Model half-times are increased by a factor of 1.5.

Organically bound ^{3}H (OBT)

Data on different animal species indicate that the biokinetics of OBT depends strongly on the compound ingested but that intake of OBT generally results in considerably greater accumulated activity in the body than intake of the same activity level of tritiated water. For example, tritium incorporation into tissues of rats, rabbits, pigs, and calves exposed for an extended period to OBT in food was generally 4-10 times higher than after similar exposure to tritiated water (Kirchmann *et al*. 1977; Rochalska and Szot 1977; Pietrzak-Flis *et al*., 1978; 1982). Etnier *et al*. (1984) concluded from a review of biokinetic data for tritium that intake of OBT in food could result in absorbed doses up to about five times higher than intake of tritiated water. Because available data on the biokinetics of OBT vary considerably with the compound administered, and because the ICRP's model for OBT is based mainly on observations of the behavior of selected compounds in laboratory animals, the model for OBT seems considerably less reliable than that for tritiated water. Absorbed doses based on these models are about 2.5 times higher for OBT than for tritiated water. Dose coefficients based on acute uptake of a unit activity of tritium taken into the adult body in organically bound form could overestimate true values by a factor of 1.5-2 or could underestimate true values by a factor of 3 or more.

In the ICRP's systemic model for organically bound tritium in the adult, 50% of absorbed tritium is assigned to a compartment with half-time 10 d and 50% to a compartment with half-time 40 d (ICRP 1989, 1993).

Low variant: The compartmental fractions representing fast and slow removal are changed from 0.5 and 0.5 to 0.8 and 0.2, respectively. The removal half-times for both compartments are divided by 1.5.

High variant: The compartmental fractions are left at 0.5 and 0.5, but the short-term half-time is increased to 15 d and the long-term half-time to 120 d.

Beryllium

Biokinetic data on beryllium have been reviewed by the ICRP (1981) and Thorne *et al*. (1986). There are relatively extensive data for laboratory animals, including mice, rats, rabbits, hamsters, dogs, and monkeys, but there is little direct information on the biokinetics of beryllium in man. Limited data on beryllium in human tissues suggest that concentrations typically are highest in lung, brain, and bone. Data on laboratory animals indicate that beryllium is concentrated mainly in bone, to a lesser extent in liver and kidneys, and to a small extent in all tissues. Integrated whole-body retention does not appear to vary greatly with species, being about 635 d in mice, 700 d in rats, 1340 d in monkeys, and 710 d in dogs. Systemic beryllium appears to be excreted mainly in urine, although some results suggest that fecal excretion represents a non-trivial portion of total excretion. Deposition and excretion appear to depend on route of entry, chemical form, and size of dose. Data on the systemic behavior of beryllium seem consistent with the biokinetics of calcium in the human body, as described in the ICRP's current systemic model for calcium (ICRP, 1995b). For example, in monkeys, cumulative urinary and fecal excretion of ^{7}Be at 6 d were 18.1 and 10.6%, respectively, compared with calcium model predictions of 17.4% and 11.3% for ^{7}Be. In rats, (effective) total-body retention of ^{7}Be at 71 d after administration was 17% of the injected amount, and 93% of the body burden was in bone; the calcium model applied to ^{7}Be predicts total-body retention of 14%, of which 97% is in bone. Beryllium may be retained longer than calcium in some soft tissues such as liver and spleen, but this may be due in part to rapid formation of colloids with injected Be and may not be applicable to slowly absorbed Be. Beryllium is generally assumed to be a bone-volume seeker because it is in the alkaline earth family, but the possibility cannot be excluded that it is more nearly a bone-surface seeker.

In the ICRP's systemic model for beryllium in the adult (ICRP 1981, 1994b), beryllium leaves blood with a half-time of 0.25 d, with 40% going to excretion pathways (urinary bladder contents or upper large intestine contents), 40% going to mineral bone from which it is removed with a half-time of 1500 d, 16% to a soft-tissue compartment with removal half-time 15 d, and 4% to a soft-tissue compartment with removal half-time 500 d. Activity removed from all compartments goes to excretion pathways. A urinary to fecal excretion ratio of 1:1 is assigned (ICRP, 1994b). Beryllium is assumed to be uniformly distributed within the volume of bone.

Low variant: The calcium model from ICRP Publication 71 is used as a low variant. That model assigns ~14% of activity leaving plasma to trabecular bone surface, ~11% to cortical bone surface, 58% to fast-turnover soft tissues, 10% to intermediate-term soft tissues, 0.005% to soft tissues with tenacious retention, 4% to urinary bladder contents (urinary fraction), and 3% to the contents of the upper-large intestine (fecal fraction). Translocation in the bone and removal from bone to plasma are described by the ICRP's generic bone model for bone-volume seekers (ICRP, 1993).

High variant: The model structure is the same as that of the ICRP's model for beryllium used in ICRP Publication 30 (1981), but beryllium is assumed to be a surface seeker rather than a volume seeker. Activity leaving blood is divided as follows: 60% is assigned to bone surfaces (equally divided between trabecular and cortical surfaces), 15% to fast turnover soft tissue, 5% to slow turnover soft tissue, and 20% to excretion. A urinary to fecal excretion ration of 1:1 is assigned. The removal half-times to excretion are 5 y for trabecular bone surface, 20 y for cortical bone surface, 15 d for fast soft tissue, and 1500 d for slow soft tissue.

Carbon

The model adopted in ICRP Publication 56 (1989) for carbon is based mainly on ^{14}C injection data for human subjects and rats and balance data for humans exposed to environmental ^{14}C. The biokinetics of carbon appears to depend strongly on the administered compound. Estimates of carbon retention derived from observations of various metabolites in different organs and tissues are highly variable (ICRP 1981). Studies on autopsy samples of persons exposed to ^{14}C from fallout indicate that bone collagen and bone mineral retain carbon with a biological half-time in excess of 5 y, but bone is not a significant reservoir for carbon and normally would receive only a tiny fraction of activity reaching the systemic circulation. Long-term studies on patients suffering from various diseases indicate four or more components of retention with biological half-lives ranging from a few hours to 70 d after injection with glycine or acetate compounds. In rats administered various ^{14}C compounds, most activity was removed rapidly from the body, but components of retention with half-times up to 126 d were demonstrated for fat and muscle.

In the ICRP's model for carbon (ICRP 1989, 1993), the biological half-life adopted for the adult, 40 d, is based on balance considerations, assuming a single whole-body carbon pool. This is intended to yield a realistic whole-body dose for ^{14}C labeled metabolites and seems likely to overestimate doses from most other ^{14}C labeled compounds. Dose estimates for injection of ^{14}C ($T_{1/2}$ = 5730 y) into the adult, based on the ICRP's biokinetic model for carbon, seem unlikely to underestimate true central values by more than a factor of 2 but conceivably could overestimate true central values for some ^{14}C compounds by a factor of 5 or more. These estimates of reliability should apply equally to organ dose coefficients and to the effective dose.

There are only two carbon isotopes that are of interest here. One of these, ^{11}C, has a half-life of about 20 min. The other, ^{14}C, has a half-life of about 5730 y. For these two extremely different half-lives, it suffices to consider simplistic high and low variants.

Low variant: Carbon is removed from blood with a half-time of 5 min, with 50% going to excreta and 50% to tissues. Carbon is removed from tissues to excreta with a half-time of 20 d.

High variant: Carbon is removed from blood with a half-time of 0.25 d, with 10% going to excretion, 0.1% to trabecular bone volume, 0.1% to cortical bone volume, and the rest to Other. Removal half-times to excretion are 5 y for trabecular bone volume, 20 y for cortical bone volume, and 60 d for Other.

Fluorine

The only isotope of fluorine considered in this report is ^{18}F, which has a half-life of 109.8 min. Therefore, only the short-term behavior of fluorine is of interest here.

The ICRP model (ICRP 1980) depicts rapid and complete uptake of fluorine by bone, and no removal from bone. As pointed out in ICRP Publication 53 (1987), however, a substantial portion of fluorine reaching blood is distributed throughout extracellular fluids, and a substantial portion is excreted in urine. The following models are recycling models. In each case the initial skeletal uptake is considerably lower than the peak skeletal content. The compartment Other in these models represents extracellular fluids of soft tissues.

Low variant: Fluorine is removed from blood with a half-time of 5 min, with 25% going to bone surfaces, 50% to Other, and 25% to the urinary bladder contents. Fluorine moves from Other to Blood with a half-time of 5 min.

High variant: Fluorine is removed from blood with a half-time of 20 min, with 30% going to bone surfaces, 30% to Other, and 40% to kidneys. Fluorine moves from Other to Blood with a half-time of 20 min and from kidneys to urinary bladder contents with a half-time of 1 h.

Sodium

The turnover rate of sodium has been studied extensively in man and laboratory animals (ICRP 1980). Total-body sodium is described as exchangeable and non-exchangeable pools, with the latter associated largely with mineral bone. Exchangeable sodium is assumed to be a uniformly mixed pool with a half-time determined by uptake (~intake) and the size of the exchangeable pool. This yields an estimated half-time of ~10 d for adult humans, with an error of 50% or more due to uncertainties in typical intake of sodium and the size of the exchangeable pool in the adult population. Some error may also occur from the assumption that the pool is uniformly mixed. The greatest uncertainties in the biokinetics of sodium are associated with the behavior in bone.

The ICRP model for sodium (ICRP 1980, 1994b) assigns 30% of the uptake to skeleton and assumes 99% is removed with a half-life of 10 d and 1% with a half-time of 500 d, so that 0.3% of the uptake is assumed to be retained fairly tenaciously in bone. Available data do not clearly reveal the initial uptake by bone, the fraction that is tenaciously retained, or the retention time. Two constraints are that the skeleton contains about 30-50% of total-body sodium long after the beginning of continuous intake, and the concentration of sodium in the total body is about 1 g/kg.

Low variant: Sodium is removed from blood at the rate 20 d^{-1}. The skeleton receives 10% of systemic uptake, loses 99% of this to excreta with a half-time of 10 d, and loses the remaining 1% with a half-time of 20 y. The removal half-time from other tissues to excreta is 10 d. The division between urine and feces is the same as in the ICRP model.

High variant: Sodium is removed from blood at the rate 20 d^{-1}. The skeleton receives 40% of uptake, loses 98% with a half-time of 10 d, and loses the remaining 2% with a half-time of 300 d; the removal half-time from other tissues to excreta is 15 d. The division between urine and feces is the same as in the ICRP model.

Magnesium

Magnesium-28 ($T_{1/2}$ = 20.9 h) is the only isotope of magnesium considered here. Therefore, interest here is in the short-term kinetics of magnesium. Studies on man have indicated two components of retention with half-times on the order of 0.25 and 35 d (ICRP 1981). Magnesium is concentrated in bone to a large extent, but this may occur gradually as a result of low deposition and tenacious retention in bone rather than as a result of high initial deposition. For consideration of ^{28}Mg it is not useful to address extended uptake in bone in the high and low variant models. Magnesium-28 decays to ^{28}Al, which represents much of the deposited energy in this chain. Aluminum-28 is short-lived ($T_{1/2}$ = 2.24 m), and its distribution in the body appears to be broadly similar to that of magnesium. Therefore, potential migration of ^{28}Al from systemic ^{28}Mg is not expected to be an important source of error in dose estimates.

In the ICRP's systemic model for magnesium (ICRP 1981, 1994b), activity leaves blood with a biological half-time of 0.25 d, with 10% going to the urinary bladder contents, 10% to the upper large intestine contents, 40% to mineral bone, and 40% to remaining tissues (Other). Magnesium is assumed to deposit uniformly on bone surfaces.

Low variant: Activity leaves blood with a half-time of 0.25 d, with 10% depositing on bone surfaces, 30% in the urinary bladder contents, and 60% in Other. The removal half-time from all compartments to excreta is 35 d. Aluminum-28 produced in the body is assigned the same kinetics as magnesium.

High variant: Activity leaves blood with a half-time of 0.25 d, with 50% depositing on bone surfaces, 10% in the urinary bladder contents, and 40% in Other. The removal half-time to excretion is 35 d for all compartments. Aluminum-28 produced in the body is assigned the same kinetics as magnesium.

Aluminum

Data on laboratory animals indicate that aluminum is distributed throughout all tissues but appears to be preferentially concentrated in the skeleton (ICRP 1981). It is not evident whether the behavior in the skeleton is more nearly like that of a bone-surface seeker such as plutonium or a bone-volume seeker such as calcium.

Studies involving healthy human subjects who received [26]Al citrate by intravenous injection indicate that about 40% of administered aluminum is retained after 1 d, 27% after 5 d, and 4% after 3 y (Priest *et al*. 1995; Talbot *et al*. 1995). A biological half-time of 7 y was estimated for the long-term component, but this was based on observations on only one subject.
In the ICRP's model for aluminum (ICRP 1981,1994b), 30% of aluminum leaving blood is deposited in bone and 70% is uniformly distributed in other tissues. The content of bone is uniformly distributed on bone surfaces at all times after deposition. The biological half-life in all tissues is 100 d, based on comparison of daily intake and the total body content given in ICRP Publication 23 (1975).

Low variant: The ICRP's model for aluminum is modified by assuming that 70% of activity leaving blood is removed to the urinary bladder contents, 5% is deposited in bone, and 25% is uniformly distributed in other tissues. Retention in any tissue is described as a sum of three exponential terms. Fractions 0.6, 0.2, and 0.2 are removed with half-times of 5 d, 50 d, and 3 y, respectively. Activity in bone is assumed to reside in bone volume at all times.

High variant: The high variant for aluminum is based on the ICRP's model for the chemically similar element gallium (ICRP 1981, 1994b), but deposition in the skeleton is reduced and the long-term retention half-time is increased compared with gallium to reflect apparent differences between aluminum and gallium while obtaining reasonable upper-bound estimates for aluminum. Specifically, aluminum is assumed to leave blood with a half-time of 0.25 d, with 30% going to mineral bone, 9% to liver, 1% to spleen, and 60% to Other. Each of these tissues is divided into compartments with rapid removal, representing 30% of activity deposited in the tissue, and slow removal, representing the other 70%. The removal half-times from these compartments to excretion pathways are 1 d and 200 d, respectively. Activity deposited in bone is assumed to be uniformly distributed on bone surfaces. A urinary to fecal excretion ratio of 1:1 is assigned.

Silicon

Information on the systemic kinetics of silicon comes mainly from studies on small animals and comparison with its close chemical analogue, germanium, which also appears to be a close physiological analogue in many respects (ICRP 1981). Apparently a substantial portion of absorbed silicon or germanium is excreted in urine during the first two days. In experiments on guinea pigs, two components of retention were found for silicon, with half-times of about 5 d and 100 d. Some studies on rats indicate rapid elimination of germanium from all tissues (half-life of a day or less) while others suggest retention of a small percentage of the absorbed or injected amount in bone, liver, and kidneys for several days.

According to the ICRP's model for silicon (ICRP 1981, 1994b), activity leaves blood with a biological half-time of 0.25 d and is uniformly distributed in body tissues. Fractions 0.4 and 0.6 of deposited activity are removed to excretion pathways with half-times of 5 d and 100 d, respectively. A urinary to fecal excretion ratio of 1:1 is assigned. Radioactive progeny produced in the body are assigned the biokinetics of silicon.

The following high and low variants are applied to germanium as well as silicon.

Low variant: The removal half-time from blood is 0.25 d. Of activity leaving blood, 5% deposits on bone surfaces, 5% in liver, 5% in kidneys, 45% in Other, 36% in the urinary bladder contents, and 4% in the upper large intestine contents. Activity is removed from tissues with a half-time of 2 d. Activity that is promptly excreted or removed from tissues transfers directly to the urinary bladder contents or upper large intestine contents. A urinary to fecal excretion ratio of 9:1 is assigned. Radioactive progeny produced in the body are assigned the biokinetics of silicon.

High variant: The removal half-time from blood is 0.25 d. Of activity leaving blood, 30% goes to excretion pathways and the rest is uniformly distributed in all tissues, with fractions 0.4 and 0.6 removed with half-times of 0.5 d and 100 d, respectively. Activity that is promptly excreted or removed from tissues transfers directly to the urinary bladder contents or upper large intestine contents. A urinary to fecal excretion ratio of 9:1 is assigned. Independent kinetics is assumed for radioactive progeny; that is, the biokinetics of a radionuclide produced in the body is described by the ICRP's model for that radionuclide (rather than that of the parent).

Phosphorus

The important isotopes of phosphorus have half-lives of at most a few weeks. The biokinetics of phosphorus during the first several weeks is reasonably well known (ICRP 1979). Behavior of phosphorus during this period is broadly similar to that of calcium, the main apparent difference being faster removal of phosphorus than calcium from soft tissues.

In the ICRP's biokinetic model for phosphorus (ICRP 1979, 1994b), activity leaves blood with a half-time of 0.5 d. The initial distribution of activity is as follows: 15 % goes to excretion pathways, 30% goes to mineral bone, and 55% is uniformly distributed in remaining tissues (Other). Other is divided into two compartments, one receiving 15% of activity leaving blood and having a removal half-time of 2 d, and the second receiving 40% and having a half-time of 19 d. The removal half-time from bone is 500 d. Activity that is promptly excreted or removed from tissues transfers directly to the urinary bladder contents or upper large intestine contents. A urinary to fecal excretion ratio of 9:1 is assigned. Phosphorous isotopes with half-life less than 15 d are assumed to be uniformly distributed on bone surfaces, and all others are distributed in bone volume.

The ICRP's assumption that phosphorus decays either entirely on bone surfaces or entirely in bone volume, depending on the half-life of the isotope, could lead to sizable errors in estimates of dose to bone tissues for some phosphorus isotopes. Use of the ICRP's calcium model as a starting point may give a better representation of the behavior of skeletal phosphorus, i.e., transfer to and from plasma and movement of phosphorus from bone surfaces to bone volume.
.
Low variant: This is the ICRP's "bone-volume" model for phosphorus (regardless of the half-life of the phosphorus isotope), with deposition in bone volume reduced from 30% to 20%, the percentage going to the rapid turnover soft-tissue compartment increased from 15% to 25%, and the half-time of the other soft-tissue compartment reduced from 19 d to 10 d. The prompt excretion percentage remains at 15%.

High variant: This is the ICRP's model for calcium (ICRP 1995b) (see the discussion for calcium), with the removal half-time from the intermediate-term soft-tissue compartment (called ST1) to blood changed from 4 d to 7 d. This modified calcium model closely approximates the ICRP model for phosphorus over the first four months after injection of phosphorus and may give a better representation of the behavior of skeletal phosphorus, i.e., transfer to and from plasma and movement of phosphorus from bone surfaces to bone volume.

Inorganic Sulfur

The biokinetics of inorganic sulfur has been studied in laboratory animals and human subjects. It appears that most of the sulfur reaching blood is excreted within a few hours, but there is a slower phase with removal half-time of at least a week and perhaps a few months.

In the ICRP's current model for inorganic sulfur (ICRP 1993) , the slower phase of removal represents 15% of sulfur leaving blood and has a removal half-time to excretion of 20 d. Further, a long-term component representing 5% of sulfur reaching blood, and having a removal half-time to excretion of 2000 d, is included in the ICRP model to reproduce total-body sulfur in Reference Man (140 g) (ICRP 1975).

Low variant: Sulfur is removed from blood with a half-time of 0.25 d, with 90% going to urinary bladder contents and 10% going being uniformly distributed in the body. Sulfur is removed from tissues to urine with a half-time of 20 d.

High variant: Sulfur is removed from blood with a half-time of 0.25 d, with 70% going to urinary bladder contents and 30% going being uniformly distributed in the body. Two retention components are assumed for the uniformly distributed sulfur: 25% is removed with a half-time of 100 d and 5% is removed with a half-time of 1,000 d.

Organic sulfur

Most information on the biokinetics of organic sulfur comes from studies on rats. Rapid urinary excretion does not appear to occur for sulfur incorporated into amino acids and other organic forms of sulfur.

In the ICRP's model for organic sulfur (ICRP 1993), activity is uniformly distributed in the body and removed with a biological half-time of 140 d.

Low variant: Sulfur leaves blood with a half-time of 0.25 d and is uniformly distributed throughout the body. The removal half-time from tissues to urine is 50 d.

High variant: Sulfur leaves blood with a half-time of 0.25 d and is uniformly distributed throughout the body. The removal half-time from tissues to urine is 300 d.

Chlorine

The ICRP's model for chlorine (1980, 1994b) assumes uniform distribution in the body and elimination with a half-time of 10 d. The model is based on a study on two healthy human subjects and comparison with the chemically and apparently physiologically similar element bromine, which has also been studied in humans.

Low variant: The removal half-time is reduced to 5 d.

High variant: The removal half-time is increased to 20 d.

Potassium

The biokinetics of potassium has been studied extensively in man and laboratory animals and is well understood (Leggett and Williams 1986). Potassium is distributed heterogeneously in the body during the first few hours after administration but gradually attains a more nearly uniform distribution. Skeletal muscle contains somewhat higher concentrations than most other tissues at equilibrium (Leggett and Williams 1986).

The ICRP's biokinetic model for potassium (1980, 1994b) assumes uniform distribution of potassium in the body and a removal half-time of 30 d. Half of the losses from the body are in urine and half in feces. The rate of removal from blood is 1000 d^{-1}, corresponding to a half-time of about 1 min.

There is much evidence that potassium is excreted primarily in urine, in contrast to the ICRP's assumption of equal losses in urine and feces (Leggett and Williams 1986). The assumption of a uniform distribution in the body may be appropriate for relatively long-lived potassium isotopes but not short-lived isotopes. For example, there is elevated uptake of potassium in the kidneys and liver soon after intake.

Low variant: Potassium leaves blood at the rate 100 d^{-1} and is uniformly distributed in the body. The removal half-time to excretion is 20 d, with 90% of losses in urine and 10% in feces.

High variant: This model accounts for the elevated uptake of potassium by liver and kidneys soon after absorption to blood in an attempt to account for elevated doses to these tissues from short-lived potassium isotopes. Potassium leaves blood at the rate 500 d^{-1}. Of potassium leaving blood, 10% goes to a compartment in liver called Liver 1, from which it is removed to blood with a half-time of 0.1 d; 2.5% goes to a compartment called Liver 2, from which it is removed to excretion with a half-time of 40 d; 10% goes to a compartment in kidneys called Kidneys 1, from which it is removed to blood with a half-time of 0.01 d; 0.4% goes to a compartment called Kidneys 2, from which it is removed to excretion with a half-time of 40 d; and the remainder is uniformly distributed in other tissues and removed to excretion with a half-time of 40 d. A urinary to fecal excretion ratio of 9:1 is assigned.

Calcium

The biokinetic database for calcium was reviewed by Leggett (1992) and is summarized in ICRP Publication 71 (1995b). The database includes a considerable amount of information obtained in controlled studies on human subjects and laboratory animals. That information is supplemented by much human and animal data on physiological analogues of calcium, particularly strontium.

The ICRP's systemic biokinetic model for calcium (ICRP 1995b) is a physiologically based model that has been used by the ICRP as a starting point for modeling the biokinetics of a number of radionuclides that follow the movement of calcium in bone. The generic model structure for calcium and several physiologically similar elements (e.g., strontium, barium, and radium) is shown in Figure B-1. Transfer coefficients used in the ICRP's model for calcium are given in Table B-1.

The generic structure was originally designed for application to the alkaline earth elements (Leggett, 1992) but was generalized for application to less complete physiological analogues of calcium, such as lead and uranium. For example, the red blood cell compartment (RBC) is not applied to the alkaline earth elements but is needed to describe the biokinetics of lead, which appears to behave similarly to calcium in bone but, unlike calcium, has a high affinity for red blood cells. The liver and kidneys are included as separate compartments mainly for applications to relatively heavy elements such as lead, radium, and uranium, which may accumulate to a greater extent in liver or kidneys than in other soft tissues.

In the ICRP's model for calcium, soft tissues are divided into three compartments corresponding to fast, intermediate, and slow return of activity to plasma (compartments ST0, ST1, and ST2, respectively). These soft tissue compartments are defined on a kinetic basis rather than an anatomical or physiological basis, but ST0 may correspond roughly to interstitial fluids plus some rapidly exchangeable cellular calcium; ST1 may be a composite of several pools with slower exchange rates, including mitochondrial calcium, cartilage calcium, and exchangeable dystrophic calcium (e.g., arterial plaque and calcified nodes); and ST2 may be associated with relatively nonexchangeable ("dystrophic") calcium that gradually accumulates in the human body.

Some of the transfer rates describing movement of activity in the skeleton are generic and others are element specific. Bone is divided into cortical and trabecular bone, and each of these bone types is further divided into bone surfaces and bone volume. Bone volume is viewed as consisting of two pools, one that exchanges with activity in bone surface for a period of weeks or months and a second, non-exchangeable pool from which activity can be removed only by bone restructuring processes. Activity depositing in the skeleton is assigned to bone surface, from which it is removed with an element-specific half-time on the order of days. Over a period of days a portion of the activity on bone surfaces moves to exchangeable bone volume and the rest returns to plasma. Activity leaves exchangeable bone volume with an element-specific half-time, on the order of a few weeks or months. Part of the activity leaving exchangeable bone volume is assigned to rapidly exchanging bone surfaces and the rest to non-exchangeable bone volume, from which it is assumed to be removed to plasma only by bone resorption. The rate of removal from non-exchangeable bone volume is assumed to be the rate of bone turnover and hence is independent of the element. Different turnover rates apply to cortical and trabecular bone (ICRP 2002).

Calcium is assumed to be lost from the body only by urinary or fecal excretion. Activity going to urine is first transferred from plasma to the urinary bladder contents, and activity going to feces is first transferred from plasma to the contents of the upper large intestines. The biliary excretion pathway is of limited importance for the alkaline earth elements and is not addressed explicitly in the model for calcium.
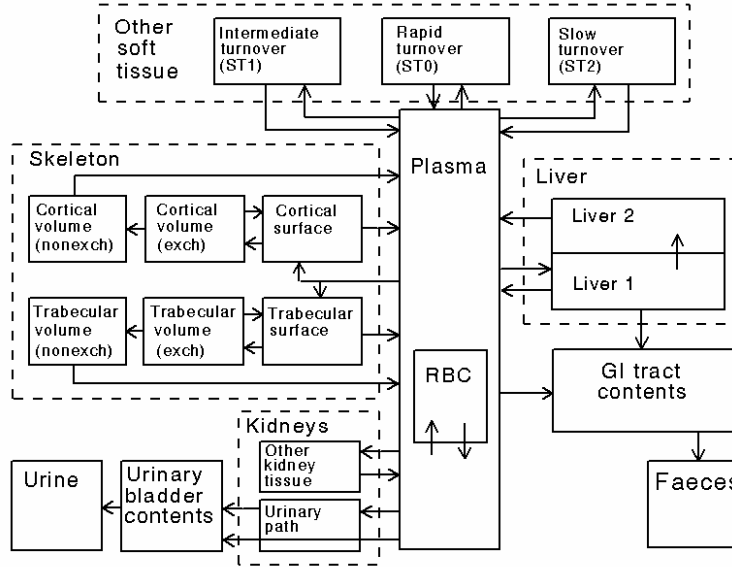
Figure B-1. The ICRP's generic model structure for elements that follow the movement of calcium in bone (ICRP 1993).

Low variant: The model structure is the same as that of the ICRP's model (Figure B-1). Deposition fractions are the same as in the ICRP's model. These can be determined from Table B-1 based on the removal rate from plasma of 15 d^{-1}; for example, the deposition fraction for soft-tissue compartment ST0 is 8.7 d^{-1}/ 15 d^{-1} = 0.58, meaning that 58% of activity leaving plasma deposits in ST0. The transfer coefficients from the intermediate- and long-term soft-tissue compartments to blood are, respectively, 1.5 times and 3 times the ICRP's values shown in Table B-1. The transfer coefficients from bone compartments are 2 times the ICRP's values shown in Table B-1. Independent kinetics of chain members is assumed; i.e., radionuclides produced in the body are assigned their characteristic biokinetics (as indicated by ICRP models) rather than the biokinetics of the parent calcium isotope.

High variant: The model structure is the same as that of the ICRP's model (Figure B-1). Deposition fractions are the same as in the ICRP's model. The transfer coefficients from the intermediate- and long-term soft-tissue compartments to blood are, respectively, 0.667 times and 0.333 times the ICRP's values shown in Table B-1. The transfer coefficients from bone compartments are 0.5 times the ICRP's values shown in Table B-1. Independent kinetics of chain members is assumed.

Table B-1. Transfer coefficients (d^{-1}) in the ICRP's model for calcium.[a]

Path of movement	Transfer coefficient (d^{-1})
Plasma to urinary bladder contents	6.0000E-01
Plasma to upper large intestine contents	4.5000E-01
Plasma to trab bone surface	2.0800E+00
Plasma to cort bone surface	1.6700E+00
Plasma to ST0	8.7000E+00
Plasma to ST1	1.5000E+00
Plasma to ST2	7.5000E-04
Trabecular bone surface to plasma	5.7800E-01
Trabecular bone surface to exch volume	1.1600E-01
Cortical bone surface to plasma	5.7800E-01
Cortical bone surface to exch volume	1.1600E-01
ST0 to Plasma	2.9000E+00
ST1 to Plasma	1.7330E-01
ST2 to Plasma	3.8000E-04
Exch trabecular bone volume to surface	2.7730E-03
Exch to nonexch trabecular bone volume	4.1590E-03
Exch cortical bone volume to surface	2.7730E-03
Exch to nonexch cortical bone volume	4.1590E-03
Nonexch cortical bone volume to plasma	8.2190E-05
Nonexch trabecular bone volume to plasma	4.9320E-04

[a] exch = exchangeable, nonexch = nonexchangeable

Scandium

Biokinetic data on scandium were reviewed in ICRP Publication 30 (1981). Experimental studies on laboratory animals and human subjects indicate that most of injected scandium is retained in the body for several months or years. The distribution has varied considerably from one experiment to another, but it is evident that a substantial portion of systemic scandium resides in the liver and skeleton. It is not known whether the skeletal behavior of scandium more nearly approximates that of a bone-surface seeker or bone-volume seeker.

In the ICRP's biokinetic model for scandium (1981, 1994b), activity leaves blood with a half-time of 0.25 d, with 40% going to bone, 30% to liver, and 10% to spleen, and 10% is uniformly distributed in other tissues (Other). Each of these regions is divided into two retention components representing fractions 0.1 and 0.9 of the deposit and having removal half-times of 5 d and 1500 d, respectively. Scandium isotopes are assumed to be uniformly distributed in bone volume.

Low variant: The low variant model is a modification of the ICRP's calcium model (ICRP 1995b; also see above discussion on calcium biokinetics). In contrast to the calcium model, the liver is treated explicitly as a site of uptake and retention of scandium. Activity assigned to skeleton in the calcium model is divided evenly between skeleton and liver in this low variant model for scandium. Activity lost from liver enters plasma. Removal from liver to plasma is assigned a half-time of 5 y. The removal rates from ST0 and ST1 to plasma in the calcium model are decreased by an order of magnitude.

High variant: This is the ICRP's model for the chemically related element yttrium (ICRP 1981, 1994b). The model is described in a later discussion of yttrium biokinetics.

Titanium

Information on the systemic biokinetics of titanium comes mainly from studies on rodents and lambs, although there is information on the content and distribution of stable titanium in man (ICRP 1981). Short-term data on lambs indicate a fairly high uptake of titanium by the skeleton, but longer-term studies on mice indicate that there is no preferential accumulation of titanium in any tissue. Based on the body content and daily intake of titanium, and assuming a gastrointestinal absorption fraction of 0.01, the ICRP (1981) estimated a biological half-time of 600 d for total-body titanium. A biological half-time of 640 d was determined in experimental studies on mice (Friberg *et al*. 1986), but the agreement with the ICRP value may be fortuitous, given the sizable uncertainty in the ICRP's f_1 value for titanium.

In the ICRP's biokinetic model for titanium (ICRP 1981, 1994b), activity leaves blood with a half-time of 0.25 d and is uniformly distributed throughout all organs and tissues including bone. It is removed from the body with a biological half-time of 600 d, with half the losses going to urine and half to feces.

Low variant: This is the same as the ICRP's model for titanium except that a removal half-time of 300 d is assigned. Radioactive progeny of titanium isotopes produced in the body are assigned the biokinetics of titanium.

High variant: This is the same as the ICRP's model for titanium except that a removal half-time of 6000 d is assigned. Radioactive progeny of titanium isotopes produced in the body are assigned the biokinetics of titanium.

Vanadium

Information on the systemic biokinetics of vanadium comes mainly from studies on mice, rats, and rabbits (ICRP 1981). It appears that there is rapid excretion of a substantial portion of absorbed vanadium, largely in urine. Vanadium is distributed throughout the body but accumulates to a greater extent in the skeleton than other organs. Using balance considerations based on data from Reference Man (ICRP 1975), the ICRP postulated a long-term component of retention with removal half-time in excess of 5000 d.

In the ICRP's model for vanadium (ICRP 1981, 1994b), activity leaves the transfer compartment with a half-time of 0.25 d, with 70% going to excretion pathways and 25% to bone, and 5% is uniformly distributed in other tissues (Other). The removal half-time from any tissue is 10,000 d, with half the losses going to urine and half to feces.

Low variant: Vanadium leaves blood with a half-time of 0.25 d, with 70% moving to excretion pathways, 10% depositing on bone surfaces, and 20% uniformly distributed throughout the other tissues (Other). Vanadium moves from bone surfaces to bone volume with a half-time of 1 d and is removed from cortical and trabecular bone volume to excretion with half-times of 20 y and 5 y, respectively. Vanadium is removed from other tissues to excretion with a half-time of 1000 d. A urinary to fecal ratio of 9:1 is assigned.

High variant: Vanadium leaves blood with a half-time of 0.25 d, with 30% depositing on bone surfaces, 30% distributing uniformly in other tissues, and 40% going to excretion pathways. Vanadium is removed from all tissues to excretion pathways with a half-time of 1000 d. A urinary to fecal ratio of 9:1 is assigned.

Chromium

The behavior of chromium has been studied in human subjects and laboratory animals (ICRP 1980, Thorne et al. 1986). Experimental studies indicate that the systemic biokinetics of chromium depends strongly on the chemical form administered. An estimated 25-45% of chromium absorbed to blood is rapidly excreted, largely in urine. In rats, 43% of chromium injected as $CrCl_3$ was excreted with a half-time of 0.5 d, 32% with a half-time of about 6 d, and 25% with a half-time of about 85 d. It appears that chromium is preferentially deposited in bone. The retention time in bone is not known. It is not known if chromium behaves more like a bone-surface seeker or a bone-volume seeker.

In the ICRP's model for chromium (ICRP 1980, 1994b), chromium leaves blood with a half-time of 0.5 d, with 30% moving to excretion pathways, 5% to bone, and 65% distributing uniformly in other tissues. Activity removed from tissues is assigned to excretion pathways. A urinary to fecal excretion ratio of 1:1 is assigned. The removal half-time from bone is 1000 d. Other tissues are divided into two retention components representing 40% and 25% of activity leaving blood and having removal half-times of 6 and 80 d, respectively. Chromium isotopes with half-life less than 15 d are assumed to be uniformly distributed on bone surfaces, and all others are distributed in bone volume.

Low variant: This is a modification of the ICRP's model described above in which 40% of activity leaving blood is assigned to excretion pathways and the rest is uniformly distributed in other tissues (Other). Two retention components are assigned. Half of the uniformly distributed chromium is removed to excretion pathways with a half-time of 6 d and half is removed with a half-time of 80 d. Radioactive progeny produced in the body are assigned the biokinetics of chromium.

High variant: This is a variation of a model described by Thorne et al. (1986). Whole body retention is described by R(t)=0.95[0.35exp(-0.693t/0.6) + 0.26exp(-0.693t/13) + 0.39exp(-0.693t/200)] + 0.05exp(-0.693t/10,000). The last term refers to retention in bone, and the first three terms describe retention in other tissues. Of the 95% depositing in other tissues, fractions 0.02, 0.02, 0.04, 0.02, and 0.9 deposit in lung, liver, kidneys, spleen, and all other tissues. Radioactive progeny produced in the body are assigned the biokinetics of chromium.

Manganese

Characterization of the systemic biokinetics of manganese is complicated by considerable interspecies variation in the behavior of manganese and by a dependence on levels of manganese and iron in diet (ICRP 1979). Short-term (60-d) studies of whole-body retention of injected manganese in human subjects indicate that approximately one-third is lost with a biological half-time of about 4 d and the remainder with is lost with a half-time of about 38 d. Studies involving mice, rats, monkeys, and dogs indicate that at most a few percent of the injected amount is retained after several months, with bone and brain having a slower rate of loss than other tissues.

The ICRP model has a maximum retention half-time of 40 d for any organ, including the skeleton, and seems more likely to underestimate than overestimate the true integrated activity of long-lived manganese isotopes in the body. In that model, it is assumed that, of manganese leaving blood, 35% goes to bone from which it is removed to excreta with a half-time of 40 d, 10% and 15% go to liver compartments 1 and 2 with removal half-times of 4 and 40 d, and 20% and 20% go to soft-tissue compartments 1 and 2 with removal half-times of 4 and 40 d. Skeletal manganese is assumed to reside on bone surfaces.

Low variant: This model is the same as the ICRP model, except that manganese is considered to be a bone volume seeker. Activity first deposits on bone surfaces but moves with a half-time of 1 d to bone volume. Radioactive progeny are assigned the biokinetics of manganese.

High variant: This model starts with the ICRP model, but 1% of manganese leaving blood is assumed to be uniformly distributed in a soft-tissue compartment that loses activity to excreta with a half-time of 1 y, and 10% of manganese leaving bone surface is assigned to bone volume, from which activity is removed to excreta with a half-time of 10 y. Radioactive progeny are assigned the biokinetics of manganese.

Iron

The systemic biokinetics of iron has been studied extensively in human subjects and laboratory animals and is reasonably well understood (ICRP 1995, Leggett et al. 2000). However, typical losses of iron from the body have not been determined with much precision, due mainly to difficulties in measuring the minuscule daily losses.

The current ICRP model for iron was introduced in Publication 69 (ICRP 1995a). This model predicts greater integrated activities of long-lived iron isotopes in most compartments than does the model given in ICRP Publication 30, Part 2 (ICRP 1980). Only two of the iron isotopes considered in this report have radioactive daughters, ^{52}Fe and ^{60}Fe. The daughter of ^{52}Fe, ^{52m}Mn, has a half-life of only 21 min, but ^{60}Co in the ^{60}Fe chain has a half-life of 5.3 y and might migrate appreciably from iron.

Low variant: This is the iron model of ICRP Publication 30 (ICRP 1980). Independent kinetics of chain members is assumed for ^{60}Fe only.

High variant: This is a modification of the ICRP's current iron model (ICRP 1995) in which transfer coefficients to excretion pathways are reduced by a factor of 2. Independent kinetics of chain members is assumed for ^{60}Fe only.

Cobalt

Data on the systemic biokinetics of cobalt are summarized in ICRP Publication 67 (1993) and by Leggett et al. (1998). Whole-body retention of inorganic cobalt in the adult can be estimated reasonably well from human data, but less is known about the time-dependent distribution in the human body. Information on the internal distribution of inorganic cobalt comes mainly from animal data, which cannot be extrapolated to man with high confidence due to apparent species differences in the biokinetics of cobalt. For example, the long-term retention component, representing roughly 10% of absorbed cobalt in humans, appears to be larger in human subjects than other studied species, and the difference cannot be explained by metabolic rate or body size. Limited comparisons of data for man and laboratory animals suggest that the liver may be a more important long-term repository for inorganic cobalt in humans than in other studied species, but it is a considerably less important storage site for inorganic cobalt than for labeled vitamin B_{12}.

The biokinetics of labeled vitamin B_{12} in human subjects varies with the method of administration (ICRP 1987). When administered by methods that seem most nearly applicable to environmental exposure (e.g., oral administration of small quantities without later injection of a flushing dose of vitamin), most of the absorbed activity is retained over a period of months or years, and a substantial portion of the absorbed activity accumulates in the liver. For example, the ICRP model for this mode of administration (ICRP 1987) assumes that 60% of the absorbed activity is taken up by the liver and retained with a half-time of 500 d, and the residual fraction is distributed throughout the body and eliminated with half-lives of 1 d (25%) and 500 d (75%).

An estimate of the long-term half-time may depend on the observation period and may vary from a few months soon after administration to a few years at times remote from administration (Thomas *et al*. 1976).

According to the biokinetic model for cobalt given in ICRP Publication 67 (ICRP 1993), activity leaves blood with a half-time of 0.5 d, with fractions 0.5 and 0.05 going to excretion and liver, respectively, and 0.45 uniformly distributed among the other organs and tissues. Fractions 0.6, 0.2, and 0.2 of activity translocated from blood to tissues are retained with biological half-times of 6, 60, and 800 d, respectively. Cobalt leaving tissues is assumed to be lost directly to excreta. This model is based on data for human subjects and laboratory animals exposed under controlled conditions to inorganic forms of cobalt. As a model for exposure to environmental cobalt, it involves substantial uncertainties stemming mainly from the problems that the biokinetics of cobalt varies from one animal species to another as well as with the form of cobalt taken into the body. Most data on man are for inorganic forms of cobalt or vitamin B_{12}, and it is not evident which, if either, of these forms should be used as a basis for modeling the biokinetics of environmental cobalt. The use of a model for inorganic cobalt might be appropriate for some exposure pathways such as ingestion of water or inhalation of airborne cobalt but inappropriate for other pathways such as ingestion of certain foods. In this regard, data of Inaba *et al.* (1982) for rats indicate that the biokinetics of orally administered ^{60}Co incorporated in freshwater fish was similar to that of orally administered vitamin B_{12} labeled with ^{58}Co and unlike that for orally administered cobalt in inorganic form.

Two high-variant models are given below, one for inhalation and one for ingestion. The high-variant model for ingestion is based on the consideration that the biokinetics of cobalt ingested in food could be more nearly like that of vitamin B_{12} than that of inorganic cobalt.

Low variant: Cobalt is uniformly distributed in the body. Removal half-times for short and intermediate components are as in the ICRP's model for cobalt (ICRP 1993), but the long-term component is reduced to 600 d. Independent kinetics of ^{55}Fe as a daughter of ^{55}Co is assumed.

High variant for inhalation: This model is a modification of the ICRP's model for cobalt that assigns greater uptake by the liver. It is assumed that the liver receives 30% of cobalt leaving blood, other tissues receive 40%, and the rest is promptly excreted. Independent kinetics of ^{55}Fe as a daughter of ^{55}Co is assumed.

High variant for ingestion: This model is a modification of the ICRP's systemic model for labeled vitamin B_{12} taken orally (ICRP 1987). It is assumed that 60% of the absorbed activity is taken up by the liver and retained with a half-time of 2 y, and the residual fraction is distributed throughout the body and eliminated with half-lives of 1 d (25%) and 2 y (75%). Independent kinetics of ^{55}Fe as a daughter of ^{55}Co is assumed.

Nickel

The systemic biokinetics of nickel has been studied in laboratory animals, particularly rats and rabbits, and to some extent in human subjects (ICRP 1981, Thorne et al. 1986). Nickel is rapidly taken up by the kidneys, but renal retention may be transient and related to the high urinary clearance. Nickel that is not promptly excreted appears to be retained tenaciously, but the retention time has not been clearly established. A retention half-time of 1200 d has been estimated from data on daily intake and total body content. Nickel does not appear to have an affinity for the skeleton.

In the ICRP's biokinetic model for nickel (ICRP 1993), activity leaved blood with a half-time of 0.25 d, with 68% going to excretion pathways and 2% to kidneys, and 30% uniformly distributed in other tissues (Other). The removal half-time from all tissues to excretion pathways is 1200 d. A urinary to fecal excretion ratio of 20:1 is assigned.

Low variant: Nickel leaves blood with a half-time of 0.5 d, with 2% going to kidneys, 75% going to the urinary bladder, and 23% uniformly distributed in body tissues. The removal half-time from kidneys is 0.1 d and the removal half-time from other tissues is 400 d. All excretion is in urine. Independent kinetics of chain members is assumed.

High variant: Nickel leaves blood with a half-time of 0.5 d, with 10% going to kidneys, 50% going to the urinary bladder, and 40% uniformly distributed in body tissues. The removal half-time from kidneys to urine is 1 d. The removal half-time from body tissues to excretion pathways is 10 y. A urinary to fecal ratio of 4 is assigned. Independent kinetics of chain members is assumed.

Copper

There have been several studies of the biological behavior of copper in human subjects as well as laboratory animals (ICRP 1980). Copper is distributed among all tissues but appears to concentrate to a greater extent in liver, brain, and pancreas than in other tissues. It is removed from the system largely in bile, with apparently little biliary copper being reabsorbed. The removal half-time from the human body has been estimated to be about four weeks on the basis of data for normal human subjects receiving radiocopper by intravenous injection. A slightly longer half-time of about 40 d has been estimated from data on daily intake of copper and total-body copper.

The ICRP model for copper (ICRP 1980, 1994b) assigns fractions 0.1, 0.1, 0.006, and 0.794 to liver, brain, pancreas, and other tissues, respectively, and assumes a removal half-time of 40 d from each compartment to excretion. With regard to dose estimates for short-lived isotopes of copper, this model may understate the importance of liver uptake at early times. Much of the absorbed copper binds to albumin in blood, and most of the copper from albumin is transported into the liver. External measurements indicate that there is little loss from liver during the period from one to three days after intravenous injection of copper. Copper apparently is slowly

metabolized in the liver and re-enters blood in a protein-bound form that is transported to various tissues. The following models were designed to address only the uncertainties in the early behavior of copper, because isotopes of copper have half-lives of at most a few days. These models would not be appropriate for application to stable copper.

Low variant: Copper leaves blood with a half-time of 0.25 d. Liver, brain, pancreas and other tissues receive fractions 0.3, 0.05, 0.01, and 0.64. The removal half-time from all tissues to excretion is 20 d.

High variant: Copper leaves blood with a half-time of 0.1 d, with 80% going to liver and 20% uniformly distributed in other tissues. The removal half-time from all tissues to excretion is 40 d. This model would not accurately describe the long-term behavior of copper but is a plausible model with regard to the distribution of copper during the first few days after uptake, which is the period of interest for the short-lived ^{64}Cu.

Zinc

Data on the systemic biokinetics of zinc were reviewed in ICRP Publication 67 (1993). The systemic biokinetics of zinc has been studied extensively in laboratory animals. Data also exits on whole-body retention and excretion rates in man, and there is information on the distribution of zinc in man. Selection of an appropriate biokinetic model is complicated by an apparent species dependence in the time-dependent distribution of zinc. It is evident that skeleton and liver are both important repositories for zinc in man, but deposition fractions for these organs are not known with much certainty. Zinc and lead tend to behave similarly in the environment, and there is some evidence of similar behavior in the skeleton and other sites in the body. However, there are also major differences in the behavior of lead and zinc in the body, most notably with regard to red blood cells, which represent a major repository for lead but not for zinc.

In the ICRP's biokinetic model for zinc (ICRP 1993), activity leaves plasma with a half-time of 0.25 d. It is assumed that 20% of activity leaving blood deposits in the skeleton, with 19.5% being retained with a half-time of 400 d and 0.5% with a half-time of 10,000 d. The remaining 80% is uniformly distributed throughout other tissues and retained with biological half-times of 20 d (30%) and 400 d (70%). Zinc isotopes with half-life less than 15 d are assumed to be uniformly distributed on bone surfaces, and all others are assumed to be distributed in bone volume. Activity removed from bone or other tissues is assigned to excretion pathways. A urinary to fecal excretion ratio of 1:4 is assigned.

Low variant: Zinc is uniformly distributed in the body, with 30% removed to excreta with a biological half-time of 20 d and 70% removed to excreta with a half-time of 1 y. The biokinetics of zinc is assigned to radioactive progeny produced in the body.

High variant: This is a modification of the ICRP's model for Pb in ICRP Publication 67 (ICRP 1993), but the amount assumed to be deposited in red blood cells in the Pb model is divided evenly between liver and intermediate-term soft-tissue compartment ST1, and the removal half-time from ST1 to blood is assumed to be 1 y. The biokinetics of zinc is assigned to radioactive progeny produced in the body.

Gallium

The systemic biokinetics of gallium has been studied in laboratory animals and, to some extent, in human subjects (ICRP 1981; Priest *et al*. 1995). Interpretation of the data is complicated by an apparent dependence of biological behavior on the amount of stable gallium administered as carrier. Some data suggest that gallium could be a bone seeker and other data suggest a fairly uniformly distribution in the body.

In the ICRP's biokinetic model for gallium (ICRP 1981), fractions 0.3, 0.09, and 0.01 of activity leaving the transfer compartment are deposited in mineral bone, liver, and spleen, respectively. The remaining fraction is distributed uniformly throughout all other organs and tissues. For any tissue, fractions 0.3 and 0.7 are retained with biological half-lives of 1 and 50 d, respectively. The isotopes of gallium considered in this report are relatively short-lived (half-lives ranging from several minutes to several hours). Dose estimates for these isotopes of are not particularly sensitive to uncertainties in the systemic biokinetics of gallium.

Low variant: Gallium leaves blood with a half-time of 0.25 d and is uniformly distributed in the body. A retention half-time of 0.5 d is assigned to 30% of the distributed activity and a half-time of 50 d is assigned to the other 70%. The biokinetics of gallium is assigned to radioactive progeny produced in the body.

High variant: This is similar to the ICRP model, but bone is assumed to take up twice as much gallium as indicated in the ICRP model (60% vs 30%). This additional 30% in bone is taken from gallium not assigned explicit organs. The biokinetics of gallium is assigned to radioactive progeny produced in the body.

Germanium

Information on the systemic kinetics of germanium comes mainly from studies on small animals and comparison with its close chemical analogue, silicon, which also appears to be a close physiological analogue in many respects (ICRP 1981, Mehard and Volcani 1975, Taylor *et al*. 1992). Apparently a substantial portion of absorbed silicon or germanium is excreted in urine during the first two days. In experiments on guinea pigs, two components of retention were found for silicon, with half-times of about 5 d and 100 d (ICRP 1981). Some studies on rats indicate rapid elimination of germanium from all tissues (half-life of a day or less) while others suggest retention of a small percentage of the absorbed or injected amount in bone, liver, and kidneys for several days.

In the ICRP's model for germanium (ICRP 1981, 1994b), activity leaves blood with a half-time of 0.25 d, with 50% depositing in the kidneys and 50% uniformly distributed in other tissues (Other). Removal half-times of 0.02 and 1 d are assigned to kidneys and other tissues, respectively. Activity leaving tissues moves to excretion pathways. A urinary to fecal excretion ratio of 1:1 is assigned.

Low variant: The removal half-time from blood is 0.25 d. Of activity leaving blood, 5% deposits on bone surfaces, 5% in liver, 5% in kidneys, 45% in Other, 36% in the urinary bladder contents (subsequently lost in urine), and 4% in the upper large intestine contents (subsequently lost in feces). Activity is removed from tissues to urine with a half-time of 2 d. Radioactive progeny are assigned the biokinetics of germanium.

High variant: The removal half-time from blood is 0.25 d. Of activity leaving blood, 30% moves to excretion pathways and the rest is uniformly distributed in all tissues, with fractions 0.4 and 0.6 removed with half-times of 0.5 d and 100 d, respectively. A urinary to fecal ratio of 9:1 is assigned. Independent kinetics is assumed for chains, using the daughters' baseline (ICRP) models.

Arsenic

Biokinetic data on arsenic have been reviewed by the ICRP (1981) and Thorne et al. (1986). Interpretation of the data for modeling purposes is complicated by its dependence on chemical form and animal species. The time-dependent distribution and residence time in the human body cannot be modeled with much confidence.

In the ICRP's model for arsenic (1981, 1994b), arsenic leaves blood with a half-time of 0.25 d, with 35% going to excretion pathways, 7% to liver, 1.5% to kidneys, and 0.5% to spleen, and 56% is uniformly distributed in other tissue. Within each of these regions, fractions 0.4 and 0.6 are retained with biological half-times of 1 and 10 d, respectively. A urinary to fecal excretion ratio of 1:1 is assigned. Some data suggest that the half-time of the longest-term component could be substantially greater than 10 d.

Low variant: Arsenic is uniformly distributed in the body, with 40% and 60% having removal half-times of 1 d and 10 d, respectively, as indicated in the ICRP model. Radioactive progeny are assigned the biokinetics of arsenic.

High variant: The ICRP's model for the chemically related element antimony is applied (ICRP 1995a). That model is described later in the discussion on antimony. Radioactive progeny are assigned the model for the parent.

Selenium

The systemic biokinetics of selenium has been studied extensively in laboratory animals and man (ICRP 1995a). Selenium is distributed throughout all tissues but is most highly concentrated in the liver and kidneys. Animal studies suggest that there also may be elevated uptake by the spleen, pancreas, and gonads. An estimated 10-20% of injected selenium is excreted in the first few days, roughly one-third to one-half is excreted over the next few weeks, and the remainder is excreted over a period of months.

In the ICRP's model selenium (ICRP 1995a), activity leaves blood with a half-time of 0.25 d. The model assigns 25% of the activity leaving blood to liver, 10% to kidneys, 1% to spleen, 0.5% to pancreas, 0.1% to testes, 0.02% to ovaries, and 63.4% to other tissues. For each tissue, 10% is removed with a half-time of 3 d, 40% with a half-time of 30 d, and 50% with a half-time of 200 d. A urinary to fecal excretion ratio of 2:1 is assigned.

Low variant: This is a modification of the ICRP's model in which removal half-times from all tissue compartments are divided by 2.

High variant: This is a modification of the ICRP's model in which removal half-times from all tissue compartments are multiplied by 2.

Bromine

The systemic biokinetics of bromine is similar to that of chloride (ICRP 1980). The ICRP model for bromine (ICRP 1980, 1994b) is based on measurements of the retention of bromide in human subjects and comparison with the chemically and apparently physiologically similar element chlorine, which has also been studied in humans. Daughters arising in bromine chains, other than radioisotopes of bromine, represent little of the total energy in the chain.

In the ICRP model (ICRP 1980, 1994b), bromine leaves blood with a half-time of 0.25 d and is uniformly distributed in the body. It is removed from tissues to excretion pathways with a half-time of 10 d. A urinary to fecal excretion ratio of 1:1 is assigned.

Low variant: The removal half-time is reduced to 5 d. Radioactive progeny produced in the body are assigned the biokinetics of the parent, except that krypton produced in the body is assumed to escape from the body without decay.

High variant: The removal half-time is increased to 20 d. Krypton produced in the body is assumed to escape from the body without decay.

Rubidium

Rubidium is chemically and physiologically similar to potassium and has been examined extensively in comparative studies of the behavior of the alkali metals (Leggett and Williams 1988). Rubidium is nearly uniformly distributed in the body by 1 d after introduction to blood but shows relatively high concentrations in the liver and kidneys in the first few minutes or hours. Removal half-times from the body on the order of 30-60 d have been estimated from studies on healthy adult humans (ICRP 1980, Leggett and Williams 1988).

In the ICRP's model for rubidium (ICRP 1980, 1994b), activity leaves blood with a half-time of 0.25 d, with 25% depositing in bone and 75% distributing uniformly in other tissues. The removal half-time from bone or other tissues to excretion pathways is 44 d. Rubidium isotopes are assumed to be uniformly distributed in bone volume at all times after deposition in bone. A urinary to fecal excretion ratio of 3:1 is assigned.

The assumption of elevated uptake of rubidium by bone appears to have been based on erroneous data (Leggett and Williams 1988). It can be traced to a typographical error in ICRP Publication 23 (1975) indicating tenfold higher skeletal content of stable rubidium than intended.

Low variant: Rubidium leaves blood at the rate 100 d^{-1} and is uniformly distributed in the body. The removal half-time from tissues to excretion pathways is 35 d. The urinary to fecal excretion ratio is 3:1. Krypton produced *in vivo* is assumed to escape from the body without decay. Otherwise, radioactive progeny are assigned the biokinetics of the parent.

High variant: Rubidium leaves blood at the rate 500 d^{-1}. Of rubidium leaving blood, 10% goes to a compartment in liver called Liver 1, from which it is removed to blood with a half-time of 0.1 d; 2.5% goes to a compartment called Liver 2, from which it is removed to excretion (U:F=3) with a half-time of 55 d; 10% goes to a compartment in kidneys called Kidneys 1, from which it is removed to blood with a half-time of 0.01 d; 0.4% goes to a compartment called Kidneys 2, from which it is removed to excretion with a half-time of 55 d; and the remainder is uniformly distributed in other tissues and removed to excretion with a half-time of 55 d. Krypton produced in vivo is assumed to escape from the body without decay. Otherwise, radioactive progeny are assigned the kinetics of the parent.

Strontium

Data on the systemic biokinetics of strontium are summarized by Leggett (1992) and in ICRP Publication 67 (1993). There is much information on the systemic biokinetics of strontium in man, but the heterogeneity of these data complicates the characterization of the typical biokinetics of strontium. A large database related to the transfer of ^{90}Sr from food and milk to the human skeleton was developed in the 1950s and 1960s, but interpretation of these environmental data is complicated by the facts that measured skeletal burdens were accumulated over an extended period and depend on assumptions concerning fractional uptake of ^{90}Sr from the gastrointestinal tract. More easily interpreted data are available from controlled studies on

human subjects. Data on the behavior of strontium in laboratory animals, particularly beagles, help to clarify the behavior of strontium at early times after intake. Because strontium is a close physiological analogue of calcium, data from controlled studies of calcium in humans provide supporting information for selection of parameter values for strontium.

The structure of the ICRP's biokinetic model for strontium (ICRP 1993) is the generic structure for calcium-like elements (Figure B-1). The ICRP's transfer coefficients for strontium are listed in Table B-2.

Table B-2. Transfer coefficients (d^{-1}) in the ICRP's model for strontium.[a]

Path of movement	Transfer coefficient (d^{-1})
Plasma to urinary bladder contents	1.7250E-01
Plasma to upper large intestine contents	5.2500E-01
Plasma to trab bone surface	2.0800E+00
Plasma to cort bone surface	1.6700E+00
Plasma to ST0	7.5000E+00
Plasma to ST1	1.5000E+00
Plasma to ST2	3.0000E-03
Trabecular bone surface to plasma	5.7800E-01
Trabecular bone surface to exch volume	1.1600E-01
Cortical bone surface to plasma	5.7800E-01
Cortical bone surface to exch volume	1.1600E-01
ST0 to Plasma	2.5000E+00
ST1 to Plasma	1.1600E-01
ST2 to Plasma	3.8000E-04
Exch trabecular bone volume to surface	4.3000E-03
Exch to nonexch trabecular bone volume	4.3000E-03
Exch cortical bone volume to surface	4.3000E-03
Exch to nonexch cortical bone volume	4.3000E-03
Nonexch cortical bone volume to plasma	8.2190E-05
Nonexch trabecular bone volume to plasma	4.9320E-04

[a]exch = exchangeable, nonexch = nonexchangeable

Low variant: The model structure is the same as that of the ICRP's model for strontium (Figure B-1). Transfer coefficients describing outflow from plasma are also the same as in the ICRP's model. The transfer coefficients from the intermediate- and long-term soft-tissue compartments to blood are, respectively, 1.5 times and 5 times the ICRP's values. The transfer coefficients from all bone compartments are 2 times the ICRP's values. Independent kinetics of chain members is assumed. The model for rubidium as a daughter is not the ICRP's model (which includes bone as a repository for rubidium); rather, it is assumed that rubidium leaves blood at the rate 100 d^{-1} and is uniformly distributed in the body.

High variant: The model structure is the same as that of the ICRP's model (Figure B-1). Transfer coefficients describing outflow from plasma are also the same as in the ICRP's model. The transfer coefficients from the intermediate- and long-term soft-tissue compartments to blood are, respectively, 0.667 times and 0.2 times the ICRP's values. The transfer coefficients from all bone compartments are 0.5 times the ICRP's values. Independent kinetics of chain members is assumed. The model for rubidium as a daughter is not the ICRP's model; rather, it is assumed that rubidium leaves blood at the rate 100 d^{-1} and is uniformly distributed in the body.

Yttrium

The biokinetics of yttrium has been studied in laboratory animals and human subjects (ICRP 1980, Etherington et al., 1989). Typically, three-fourths or more of absorbed yttrium is tenaciously retained in the body. The skeleton appears to be the most important repository, but 10-15% of the amount reaching blood deposits in the liver. The chemistry of yttrium resembles that of the actinides. Therefore, yttrium is expected to bind to bone surfaces. Because yttrium isotopes have half-lives ranging from a few minutes to about 100 d, it is only the relatively short-term kinetics that is of importance with regard to internal dosimetry.

In the ICRP's biokinetic model for yttrium (ICRP 1980, 1994b), yttrium leaves blood with a half-time of 0.25 d, with 25% going to excretion pathways (dividing equally between urinary bladder and upper large intestine contents), 50% to bone, and 15% to liver. The remaining 10% is distributed uniformly in remaining tissues. Yttrium entering tissues is permanently retained. Yttrium deposited in the skeleton is uniformly distributed on bone surfaces.

Low variant: This is a modification of the ICRP's model for strontium (described earlier) in which the liver is treated explicitly as a site of uptake and retention of activity. Yttrium is assumed to be initially distributed the same as strontium, except that 15% of yttrium leaving blood is assumed to go to liver; this amount is subtracted from deposition in the rapid-turnover soft-tissue compartment, ST0, in the strontium model. Yttrium in liver is assumed to be removed to the contents of the upper large intestine with a half-time of 1 y. Removal from all other soft-tissue compartments is assumed to be 10 times slower than indicated by the strontium model. There is assumed to be no removal of yttrium from bone surfaces. Because chain members generally are short-lived, have kinetics broadly similar to yttrium, or represent little of the total energy in the chain, it suffices to assume that radioactive progeny have the same kinetics as the parent. .

High variant: This is the same as the ICRP's model for thorium (described later). Radioactive progeny are assigned the biokinetics of the parent.

Zirconium

Data on the systemic biokinetics of zirconium were reviewed by the ICRP (1989) and Leggett et al. (1998). The only potentially useful data on the systemic biokinetics of zirconium in humans consist of short-term measurements of activity in blood and urine of a seriously ill subject injected with [89]Zr citrate. The best available quantitative animal data for this element come from studies on rats at different stages of life, adult mice, and adult guinea pigs. These data indicate that bone is a major repository for zirconium, but the data are highly variable and do not reveal a clear distribution between bone and soft tissues or a precise pattern of excretion of zirconium. Due to the paucity of zirconium-specific data on man and the scatter in data for other species, there is increased reliance on chemical analogy in this case. The behavior of zirconium is broadly similar to that of yttrium but appears to be more closely related to that of hafnium, a close chemical analogue. Relatively detailed and easily interpreted biokinetic data on hafnium have been developed in recent years for rats, hamsters, and marmosets and may provide some insight into the behavior of zirconium.

In the ICRP's model for zirconium (ICRP 1989, 1993), activity leaves blood with a half-time of 0.25 d with 50% depositing uniformly on bone surfaces and 50% depositing uniformly in remaining tissues. The half-time of removal from tissues to excretion pathways is 10,000 d for bone and 7 d for other tissues. A urinary to fecal excretion ratio of 5:1 is assigned.

Low variant: This is the same as the low variant model for yttrium described earlier. Independent kinetics of chain members is assumed.

High variant: Zirconium leaves blood with a half-time of 0.25 d, with 60% going to bone surface, 10% to liver, 20% to other tissues, 8% to urinary bladder contents, and 2% to the contents of the upper large intestine. The removal half-time from liver to upper large intestine contents 10 y. The removal half-times from trabecular and cortical bone surface to blood are 5 y and 20 y, respectively. The removal half-time from other soft tissues to blood is 100 d. Radioactive progeny are assigned the biokinetics of zirconium.

Niobium

Data on the systemic biokinetics of niobium were reviewed by the ICRP (1989). Information comes from radioisotope injection data on laboratory animals, including mice, rats, guinea pigs, dogs, monkeys, swine, and sheep. Data on the time-dependent systemic distribution are variable but indicate that the skeleton accumulates a non-trivial portion of systemic activity and that the liver and kidneys concentrate niobium to a greater extent than most soft tissues (ICRP 1989). Autoradiographic data on mice indicate that [95]Nb in bone is distributed throughout the bone volume by 4 d after injection (Backström *et al.* 1967). In rats, all tissues appeared to lose niobium at roughly the same rate. Retention times in the ICRP's model for niobium were based largely on a study of the comparative metabolism of niobium in mice, rats, monkeys, and dogs (Furchner and Drake 1971). The first component of retention accounted for about 50% of the activity entering blood and had a biological half-time on the order of 6 d in all four species, but

the half-time of the second component varied considerably (mice, 450 d; rats, 175 d; dogs, 150 d; monkeys, 100 d). Results reported by other workers suggest a fast component representing 25-50% of the systemic deposit and having a half-time on the order of 1-3 d, and a slower component representing 50-75% of the deposit and having a half-time of 45-95 d (ICRP 1989). Estimates of doses from intake of niobium isotopes are relatively insensitive to assumptions concerning the biokinetics of chain members.

In the ICRP's biokinetic model for niobium (ICRP 1989, 1993), activity leaves blood with a half-time of 0.25 d, with 40% depositing in bone, 20% in liver, and 3% in kidneys. The remaining 37% distributes uniformly in other tissues (Other). For each of these regions, half of the deposited activity is removed with a half-time of 6 d and half is removed with a half-time of 200 d. Niobium isotopes with half-life less than 15 d are uniformly distributed on bone surfaces, and all others are distributed uniformly in bone volume. A urinary to fecal excretion ratio of 5:1 is assigned.

Low variant: The low variant model is the ICRP's model for the chemically similar element tantalum as a volume seeker (described later), but removal half-times of 1 and 50 d, respectively, are assigned to the two retention components in soft tissues. Radioactive progeny are assigned the kinetics of the parent..

High variant: This is the same as the ICRP's model for niobium except that the long-term half-time in each organ is increased from 200 d to 500 d. Radioactive progeny are assigned the kinetics of the parent..

Molybdenum

Data on the systemic biokinetics of molybdenum were reviewed in ICRP Publication 67 (1993). Information comes from studies of its time-dependent distribution and retention in various non-human species, its distribution in human subjects exposed only to natural levels of environmental molybdenum, and the retention and excretion of molybdenum isotopes by human subjects. Development of a systemic biokinetic model for molybdenum is complicated by species differences in metabolism and a high variability in retention that is apparently due in large part to a dependence on the level of molybdenum in diet. There are similarities in the biological behavior of molybdenum, tungsten, and phosphorus (Leggett, 1997a), probably due to similar tendencies of these elements to form oxyanion compounds in physiological systems. It has been found, for example, that tungstate or molybdate can substitute for phosphate in bone. Tungsten has been used frequently as an experimental analogue of molybdenum because it is the element most chemically similar to molybdenum, is the best known biological antagonist of molybdenum, and is the only agent capable of producing experimental molybdenum deficiency in animals by preventing incorporation of molybdenum into certain enzymes.

In the ICRP's model for molybdenum (ICRP 1993), activity leaves blood with a half-time of 0.25 d and is divided among tissues as follows: bone, 10%; liver, 25%; kidney, 5%, other tissues, 60%. The removal half-time from bone is 10,000 d. Retention in other regions is divided into two components with fractions 0.1 and 0.9 removed with half-times of 1 and 50 d, respectively. Activity removed from tissues transfers directly to the urinary bladder contents or upper large intestine contents. A urinary to fecal excretion ratio of 8:1 is assigned. Molybdenum isotopes of half-life less than 15 d are uniformly distributed on bone surfaces, and all others are distributed in bone volume.

Low variant: The low variant is a modification of a recently published model for tungsten (Leggett 1997a) described later in the discussion of tungsten. With reference to the tungsten model, the fraction going from plasma to urinary bladder contents is reduced from 0.75 to 0.25, the fraction going from plasma to liver is increased from 0.04 to 0.2, and the fraction going from plasma to intermediate-term soft-tissue retention is increased from 0.0225 to 0.3625. Radioactive progeny are assigned the biokinetics of the parent..

High variant: The high variant model is a modification of the ICRP's model for molybdenum. All removal half-times are increased by a factor of 2. Radioactive progeny are assigned the biokinetics of the parent.

Technetium

Data on the systemic biokinetics of technetium were reviewed in ICRP Publication 67 (1993). The behavior of technetium has been studied in human subjects as well as laboratory animals and seems reasonably well characterized. Data for human subjects indicate that technetium may accumulate to some extent in the thyroid, gastrointestinal tract, and liver. There is no evidence of avid retention by any tissues.

In the ICRP's model for technetium (ICRP 1993), activity leaves blood with a half-time of 0.02 d and is divided among tissues as follows: thyroid, 4%; stomach wall, 10%; liver, 3%; other tissues, 83%. The removal half-time from thyroid is 0.5 d. Retention in other regions is divided into three components with fractions 0.75, 0.20, and 0.05 removed with half-times of 1.6, 3.7, and 22 d, respectively. Activity removed from tissues transfers to the urinary bladder contents and upper large intestine contents. A urinary to fecal excretion ratio of 1:1 is assigned.

Low variant: This is a modification of the ICRP's model for technetium. Uptake by thyroid is reduced from 4% to 1%, with the difference distributed among compartments of Other. All transfer coefficients from tissue compartments are multiplied by 2.

High variant: This is a modification of the ICRP's model for technetium. All transfer coefficients from tissue compartments are divided by 2.

Ruthenium

Data on the systemic biokinetics of ruthenium were summarized in ICRP Publication 56 (1989) and by Leggett et al. (1998). Information comes mainly from studies on laboratory animals, including mice, rats, guinea pigs, rabbits, cats, dogs, and monkeys. Reported long-term retention half-times range from about 200 d to about 1600 d and show no trend with body mass. Whole-body retention of ruthenium has also been measured in a controlled study in which a healthy human subject ingested different chemical forms of ^{103}Ru or ^{106}Ru at different times. The estimated long-term half-time in this subject is within the range of values indicated by the animal data. Data on the systemic distribution of ruthenium come mainly from studies on rodents and suggest a somewhat uniform distribution, with the main exception being an elevated concentration in the kidneys in the early weeks after injection. Because members of ruthenium chains generally are short-lived, have kinetics broadly similar to ruthenium, or represent little of the total energy in the chain, it suffices to assume that radioactive progeny behave the same as the parent ruthenium isotope.

In the ICRP's model for ruthenium (ICRP 1989, 1993), activity leaves blood with a half-time of 0.3 d, with 15% moving to excretion pathways (urinary bladder contents and upper large intestine contents) and 85% distributing uniformly throughout the body. The 85% retained in tissues is divided into three retention components representing 35%, 30%, and 20% of outflow from blood and having removal half-times of 8, 35, and 1000 d, respectively. Activity removed from tissues transfers to excretion pathways. A urinary to fecal excretion ratio of 4:1 is assigned.

Low variant: This is a model developed by Runkle *et al*. (1980) as a fit to measurements of ^{106}Ru in systemic tissues and excreta of rats exposed to ^{106}RuO$_4$ by inhalation or ingestion (Figure B-2). Radioactive progeny are assigned the biokinetics of the parent.

High variant: This model is based on broadly consistent whole-body retention data for dogs (Furchner *et al*. 1971) and a human subject (Yamagata *et al*. 1969, 1971) and on the distribution of systemic activity observed in guinea pigs (Burykina 1962). Activity is removed from blood with a half-time of 0.25 d, with fractions 0.2, 0.05, 0.2, 0.1, 0.35, and 0.1 going to urinary bladder contents, small intestine contents, liver (Liver 1), kidneys (Kidney 1), other soft tissues (Other 1), and bone surface, respectively. Activity leaves Liver 1, Kidney 1, Other 1, and bone surface with a half-time of 5 d. Of activity leaving Liver 1 or Other 1, 90% returns to blood and 10% moves to a long-term compartment of the same tissue (Liver 2 or Other 2, respectively). Of activity leaving Kidney 1, 98% returns to blood and 2% moves to a long-term compartment in the kidneys (Kidney 2). Of activity leaving bone surface, 75% returns to blood and 25% moves to bone volume. Activity moves from Liver 2 to the small intestine contents with a half-time of 100 d, from Kidney 2 to Kidney 1 with a half-time of 100 d, from Other 2 to Other 1 with a half-time of 500 d, and from bone volume to bone surface with a half-time of 1000 d. Radioactive progeny are assigned the biokinetics of the parent.

Other 0.06 Blood 0.04 Skeleton
1 1
0.05 0.2 0.2 0.05
2 2

Kidney 0.09 0.05 Liver
1 1
0.025 0.2 0.2 0.05
2 2
0.007

1.5 GI Tract

Urine 3.5 Feces
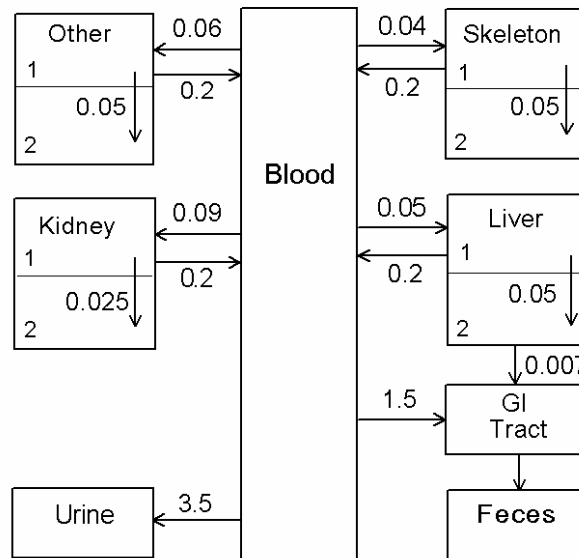
Figure B-2. Systemic biokinetic model for ruthenium developed by Runkle et al. (1980) and used in this report as the low variant for ruthenium. The transfer coefficients shown are in units of d^{-1}, i.e., fraction transferred per day.

Rhodium

In ICRP Publication 30, Part 2 (1980), it is stated that "There appears to be no information available concerning the distribution and retention of rhodium in any mammalian species." However, Durbin (1957) summarized data on the behavior of rhodium in rats during the first few days after administration of carrier-free [105]Rh by various routes. Distribution and excretion at these times were similar to that observed for the chemically-similar element ruthenium.

The ICRP's model for rhodium (ICRP 1980, 1994b) is the same as that for the chemically similar element ruthenium (described earlier).

Low variant: This is a modification of the low variant for ruthenium described earlier. All transfer coefficients describing outflow from tissue compartments are increased by a factor of 2.

High variant: This is a modification of the high variant for ruthenium described earlier. All transfer coefficients describing outflow from tissue compartments are decreased by a factor of 2.

Palladium

Information on the systemic biokinetics of palladium comes mainly from studies on rats (ICRP 1981). The data indicate that the behavior of palladium during the early days or weeks after intake is broadly similar to that of several other elements in Group VIIIA of the period chart, including platinum, ruthenium, rhodium, and iridium. The limited studies of palladium have not

59

revealed a long-term retention component such as observed for ruthenium, for example, but the possibility of long-term retention should not be dismissed.

In the ICRP's model for palladium (ICRP 1981, 1994b), activity leaves blood with a half-time of 0.25 d, with 30% going to excretion pathways (urinary bladder contents and upper large intestine contents), 45% to liver; 15% to kidneys, 7% to bone, and 3% to Other. The retention half-time in all tissues is 15 d. Activity removed from tissues transfers to excretion pathways. A urinary to fecal excretion ratio of 1:1 is assigned. Palladium isotopes with half-life less than 15 d are uniformly distributed on bone surfaces, and all others are distributed in bone volume.

Low variant: This is the same as the low variant for rhodium (described earlier).

High variant: This is the same as the high variant for platinum (described later).

Silver

The systemic biokinetics of silver has been studied in human subjects and laboratory animals (ICRP 1993) but cannot be characterized with much certainty due to inconsistencies in the database. Data for humans indicate considerable uptake by the liver and skin. Some but not all animal studies indicate that silver is concentrated in the liver. Retention times in the body have varied widely from one study to another. It appears that much of the absorbed amount is removed in a few days. A portion of absorbed silver may be retained for several weeks in the liver or perhaps other tissues, and a fraction of a percent may be retained in the body for an extended period.

In the ICRP model for silver (ICRP 1993), activity leaves blood with a half-time of 0.25 d. The model assigns 50% of activity leaving blood to liver and 50% to other tissues. Of silver going to any tissue, fractions 0.1, 0.8, and 0.1 are assumed to be removed with half-times of 3.5 d, 50 d, and 500 d, respectively. Activity removed from tissues transfers to the urinary bladder contents and upper large intestine contents. A urinary to fecal excretion ratio of 1:20 is assigned.

Low variant: Silver is removed from blood with a half-time of 0.25 d, with 50% going to liver and 50% to other tissues. Activity deposited in all tissues is removed to the upper large intestine contents with a half-time of 20 d.

High variant: This is a modification of the ICRP's model for silver. The long-term component of retention in tissues is increased to 5000 d and other parameter values are left unchanged.

Cadmium

The systemic biokinetics of cadmium has been investigated in laboratory animals, in controlled studies on human subjects, and through comparisons of intake, body burden, and excretion of stable cadmium (ICRP 1980, Friberg et al. 1986). It has been established that cadmium is concentrated in the liver and kidneys more than in other tissues, and has a long retention time in the body.

In the ICRP's model for cadmium (ICRP 1980, 1994b), activity leaves blood with a half-time of 0.25 d, with 30% going to liver, 30% to kidneys, and 40% to Other. The removal half-time from all tissues is 25 y. A urinary to fecal excretion ratio of 1:1 is assigned.

Low variant: Cadmium leaves blood with a half-time of 0.25 d, with 10% going to liver, 20% to kidneys, 50% to other tissues, and 20% to excretion pathways. The removal half-time from any compartment to excretion pathways is 10 y. A urinary to fecal excretion ratio of 1:1 is assigned.

High variant: Cadmium leaves blood with a half-time of 0.25 d, with 30% going to liver, 30% to kidneys, and 40% to other tissues. The removal half-time from any compartment to excretion is 40 y. A urinary to fecal excretion ratio of 9:1 is assigned.

Indium

The systemic biokinetics of indium has been studied only in small animals, including mice, rats, and rabbits (ICRP 1980, Friberg et al. 1986). The biological behavior varies with the chemical form injected. Indium apparently is distributed throughout all tissues, with perhaps somewhat higher concentrations in kidney and liver than other organs over an extended period. Data on rats suggest fairly slow excretion, with perhaps 25% of the body burden lost over the first 30 d and less than 5% over the next 30 d.

In the ICRP's biokinetic model for indium (ICRP 1980, 1994b), activity leaves blood with a half-time of 0.25 d, with 30% depositing in red bone marrow, 20% in liver, 7% in kidneys, 1% in spleen, and 42% in Other. There is assumed to be no biological removal from tissues.

Low variant: Indium leaves blood with a half-time of 0.25 d and is distributed uniformly throughout the body. It is removed from all tissues to excretion pathways with a half-time of 1 y. A urinary to fecal excretion ratio of 1:3 is assigned.

High variant: Indium leaves blood with a half-time of 0.25 d, with 25% going to liver, 10% to kidneys, 10% to red marrow, and 55% to Other. The removal half-time from all tissues is 50 y. Activity removed from tissues enters the upper large intestine and is removed in feces.

Tin

The systemic biokinetics of tin has been studied in rats, mice, monkeys, and dogs (ICRP 1981, Friberg et al. 1986). During the first few days after uptake to blood, about 20-60% is cleared in urine and a much smaller amount is cleared in feces. Tin accumulates in the skeleton, with possibly one-fourth of the total-body burden distributed among soft tissues. It has not been established whether tin remains on bone surfaces or enters bone volume.

In the ICRP's model for tin (ICRP 1981, 1994b), activity leaves blood with a half-time of 0.25 d, with 35% depositing in bone, 15% in Other, and 50% in excretion pathways (urinary bladder contents and upper large intestine contents). Activity deposited in tissues is divided into three retention components, with fractions 0.2, 0.2, and 0.6 removed with half-times 4, 25, and 400 d, respectively. Activity removed from tissues transfers to excretion pathways. A urinary to fecal excretion ratio of 1:1 is assigned. Tin isotopes with half-life less than 15 d are uniformly distributed on bone surfaces, and all others are distributed in bone volume.

Low variant: This is a modification of the ICRP's model for lead (ICRP 1993) described later. The red blood cell compartment is removed from the model and the deposition in that compartment (40% of the amount leaving plasmal) is divided among urine, feces, bone surface, and intermediate-term soft tissues. Of tin leaving plasma, the fraction 0.25 goes to urinary bladder contents, 0.06 to upper large intestine contents, 0.006 directly to excreta, 0.25 to bone surface (divided as in the lead model), 0.06 to intermediate-term soft tissues, 0.002 to long-term soft tissues, 0.02 to Liver 1, 0.035 to Kidneys 1, 0.00035 to Kidneys 2, and the remainder to rapid-turnover soft tissues. Transfers out of the various tissue compartments are the same as in the lead model, except that the removal half-time from intermediate soft tissues to blood is 10 d.

High variant: This is a modification of the ICRP's model for tin described above. Deposition fractions are changed from 0.5 to 0.3 for excretion pathways, 0.35 to 0.45 for bone, and 0.15 to 0.25 for other tissues. Activity in bone is assigned to bone surface. The long-term removal half-time for all compartments is changed from 400 d to 800 d.

Antimony

Despite the availability of data on the biological behavior of antimony in mice, rats, hamsters, rabbits, cows, dogs, and monkeys, and some scattered data on human subjects (ICRP 1995a), the systemic biokinetics of this element in humans cannot be modeled with much confidence. Interpretation of data for both laboratory animals and man is complicated by a sizable variability with the chemical form of antimony taken in and with route of exposure. Extrapolation of data from laboratory animals to man is complicated by a species dependence in the internal distribution of antimony. Information for man comes from measurements of excretion following accidental or controlled exposure to antimony and a few autopsy measurements in occupationally or environmentally exposed persons. The occupational and environmental data are difficult to interpret due to uncertainties in the level and time-course of exposure. The

environmental data are also suspect due to the questionable reliability of reported measurements of low-level environmental antimony in food and human tissues.

In the ICRP model it is assumed that antimony leaves blood with a half-time of 0.25 d. Of activity leaving blood, 20% is assigned to excretion pathways (urinary to fecal ratio of 1:4), 40% to bone, 5% to the liver, and 35% to other tissues. For each organ, it is assumed that fractions 0.85, 0.15, and 0.05 are removed to excretion pathways with half-times of 5 d, 100 d, and 5000 d, respectively. There is much uncertainty, however, regarding the distribution of antimony in the body, particularly during the first few days after intake. Also, the long-term retention time of 5000 d was used to account for the estimated content of stable antimony in man and is highly uncertain due to the questionable reliability of the reported organ contents. Finally, there is some question as to whether bone is an important repository for antimony in man.

Low variant: The ICRP's model for the chemically similar element arsenic (described earlier) is used as the low variant. That model (ICRP 1981, 1994b) depicts elevated accumulation in liver, kidneys, and spleen but not skeleton, and assumes a removal half-time of 10 d or less for all compartments. Independent kinetics of chain members is assumed.

High variant: This is a modification of the ICRP's model for antimony described above. The short-term removal half-time from each tissue (5 d, applicable to 85% of activity entering tissues) is increased to 10 d. Radioactive progeny are assigned the biokinetics of the parent.

Tellurium

Data on the systemic behavior of tellurium was reviewed in ICRP Publication 67 (1993). Information on the behavior of absorbed tellurium in humans consists mainly of autopsy measurements on environmentally-exposed subjects and urinary excretion rates of isotopes of tellurium ingested by volunteers. The autopsy data indicate that bone contains nearly all of the total-body tellurium, but the accuracy of the analytical technique has been questioned. Also, interpretation of the data depends on uncertain information on the level of tellurium in the diet. Data for rats, guinea pigs, sheep, and swine (Wright and Bell 1966, ICRP 1979, ICRP 1993) yield highly variable estimates of the bone content during the first few days after exposure, with most values falling in the range 5-35% of the injected or absorbed amount. The animal data indicate that the liver may contain more tellurium than the skeleton in the first several days after injection, but this pattern may be reversed at later times because of relative rapid loss from the liver and slow loss from the skeleton. There appears to be rapid excretion of half or more of absorbed tellurium. Although the systemic biokinetics of tellurium in humans is poorly characterized, the effective dose is not highly sensitive to these uncertainties for short-lived isotopes of tellurium such as ^{132}Te ($T_{1/2}$ = 78 h).

In the ICRP's model for tellurium (ICRP 1993), activity leaves blood with a half-time of 0.8 d and is divided among tissues as follows: bone, 25%; thyroid, 0.2%; kidney, 2.3%, Other, 22.5%; excretion pathways (urinary bladder contents and upper large intestine contents), 50%. The removal half-time from bone is 10,000 d and from soft tissue compartments is 20 d. Activity removed from tissues transfers to excretion pathways. A urinary to fecal excretion ratio of 4:1 is assigned. Tellurium isotopes are uniformly distributed on bone surfaces.

Low variant: Tellurium is removed from blood with a half-time of 0.8 d, with 60% going to excretion pathways, 5% to bone surface (divided evenly between cortical and trabecular), 0.2% to thyroid, 2% to kidneys, and the remainder to Other. A urinary to fecal excretion ratio of 4:1 is assigned. Tellurium on bone surface moves to bone volume with a half-time of 1 d and is removed from cortical and trabecular bone volume to excretion with half-times of 20 y and 5 y, respectively. Tellurium is removed from soft tissues to excretion with a half-time of 10 d. Independent kinetics of chain members is assumed for chains involving iodine; otherwise, radioactive progeny are assigned the kinetics of tellurium.

High variant: Tellurium is removed from blood with a half-time of 0.8 d, with 30% going to excretion pathways, 40% to bone surface (divided evenly between cortical and trabecular), 0.5% to thyroid, 5% to kidneys, 10% to liver, and the remainder to Other. A urinary to fecal excretion ratio of 4:1 is assigned. Tellurium is removed from bone surface to excretion with a half-time of 10,000 d. Tellurium is removed from soft tissues to excretion with a half-time of 40 d. Independent kinetics of chain members is assumed for chains involving iodine; otherwise, radioactive progeny are assigned the kinetics of tellurium.

Iodine

There is a large body of information on uptake and retention of iodine by the human thyroid (ICRP 1989; Stather and Greenhalgh 1983), but reported thyroidal uptake fractions and biological half-times are highly variable. This high variability appears to be due largely to a strong dependence of the biokinetics of absorbed radioiodine on the level of stable iodine in the thyroid. Large differences in values reported by investigators from different countries have been attributed to the high variability in the concentration of iodine in foods in different countries. However, substantial variability in thyroidal uptake fractions and biological half-times is also seen among members of relatively homogeneous populations, at least over the short term.

For relatively short-lived isotopes of iodine such as ^{131}I, uncertainty in the biological half-time in the thyroid is not an important source of uncertainty in the absorbed dose to the thyroid, because the estimated lower bound of the retention time is long compared with the radiological half-life of [131]I. A more important consideration is the level of thyroidal uptake of absorbed ^{131}I, which may be increased substantially in persons with low intake of iodine in food (ICRP 1989).

In an investigation of the imprecision in age-specific estimates of dose to the thyroid from intake of ^{131}I, Dunning and Schwarz (1981) examined the variability in reported age-specific values for uptake and retention of iodine by the thyroid. Their data relate to the variability in iodine biokinetics rather than the uncertainty in the central value but provide some insight regarding the accuracy with which typical values might be estimated.

The structure of the ICRP's systemic model for iodine is shown in Figure B-3. The model depicts different distributions of absorbed and recycled iodine, i.e., immediately after absorption to blood and after loss from the thyroid gland to blood. In the model, the removal half-time from blood is 0.25 d. Of iodine atoms entering blood for the first time, 30% are deposited in the thyroid gland and 70% move to the urinary bladder contents. Iodine is removed from the thyroid gland with a biological half-time of 80 d in the adult. Organic iodine returning to blood from the thyroid is taken up and metabolized in tissues (Other) and is returned to the plasma pool as inorganic iodide with a half-time of 12 d. Of iodine entering blood from Other, 20% moves to the upper large intestine contents, 24% returns to the thyroid gland, and 56% moves to the urinary bladder contents. The corresponding transfer coefficients for adults are as follows: Blood to Thyroid, 0.8318 d^{-1}; Blood to Urinary Bladder Contents, 1.9408 d^{-1}; Thyroid to Other, 0.0087 d^{-1}; Other to Blood, 0.0462 d^{-1}; Other to Upper Large Intestine Contents (ULI), 0.0116 d^{-1}.
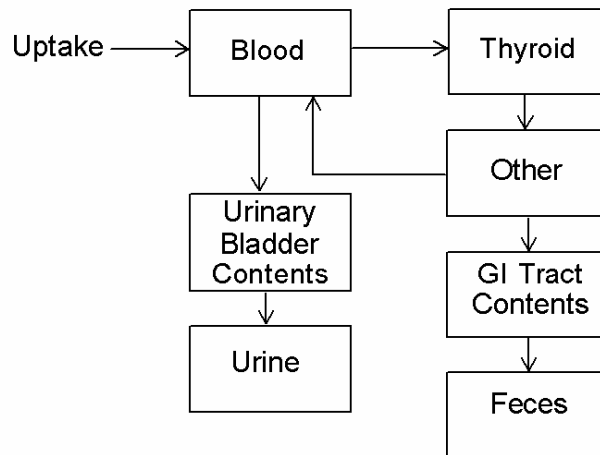
Figure B-3. Structure of the ICRP's systemic biokinetic for iodine (ICRP 1989, 1993).

Low variant: The structure of the ICRP's model is used. The removal half-time from blood is 12 h. Of iodine leaving blood, 15% goes to the thyroid gland and the rest to to the urinary bladder contents. Iodine is removed from the thyroid gland to Other with a biological half-time of 50 d. Iodine is removed from Other with a half-time of 7 d, with 80% going to blood and 20% to feces. Radioactive progeny are assigned the biokinetics of iodine, except that xenon is assumed to escape from the body without decay.

High variant: The structure of the ICRP's model is used. The removal half-time from blood is 3 h. Of iodine leaving blood, 35% goes to the thyroid gland and the rest to urine. Iodine is removed from the thyroid gland to Other with a biological half-time of 120 d. Iodine is removed from Other with a half-time of 20 d, with 80% going to blood and 20% to feces. Radioactive progeny are assigned the biokinetics of iodine, except that xenon is assumed to escape from the body without decay.

Cesium

There have been numerous studies of the biological behavior of radiocesium in human subjects exposed under natural or controlled conditions (Leggett 1986, ICRP 1989, Leggett et al. 2003). It has been established that cesium is somewhat uniformly distributed in soft tissues by a few days after intake and that whole-body retention can be approximated reasonably well by a single biological half-time, although one or two additional short-term half-times have been identified in some injection studies. Comparative data for healthy adult males and females reveal that the mean half-time for females is consistently 15-30% lower than that for males. The pattern of change with age in the retention half-time during growth is also well established. Thus, there are sufficient high-quality human data on cesium to characterize typical whole-body retention of this element within narrow bounds, for children as well as for adults of both genders. Experimental findings for ^{137}Cs indicate that there may be considerable migration of the short-lived daughter ^{137m}Ba after its production in the body.

In the ICRP's biokinetic model for cesium (ICRP 1989, 1993), activity leaves blood with a half-time of 0.25 d and is uniformly distributed in the body. Activity deposited in tissues is divided into two retention components, with fractions 0.1 and 0.9 removed with half-times 2 and 110 d, respectively. Activity removed from tissues transfers to the urinary bladder contents or upper large intestine contents. A urinary to fecal excretion ratio of 4:1 is assigned.

Low variant: This is a modification of the ICRP's model in which the short-term component is increased from 10% to 20% of cesium entering the circulation, the half-time of that component is decreased from 2 d to 1 d, and the long-term half-time is reduced from 110 d to 70 d. Radioactive progeny are assigned the biokinetics of cesium.

High variant: The ICRP's model for cesium is used, but independent kinetics of radioactive progeny is assumed.

Barium

The distribution, retention, and excretion of injected or ingested barium have been studied in a number of adult human subjects (Leggett 1992, ICRP 1993, Newton et al. 2001). Useful information on the systemic biokinetics of barium also comes from human studies involving radium, which has been shown to be a close physiological analogue of barium, and from comparative studies of barium and other alkaline earth elements in laboratory animals. In extrapolating the data for barium or radium from animals to humans, it must be considered that

66

secretion of these elements into the gastrointestinal tract is much greater in humans than in most laboratory animals, resulting in less recycling and substantially smaller net retention of barium in humans after a few days than is observed in most laboratory animals. It appears that little barium remains in soft tissues by a few days after injection, but there may be small, insoluble deposits that remain for many years. Systemic barium is contained mainly in the skeleton within a few hours or days after uptake to blood. Skeletal retention of barium in the fully mature human may decrease from one-fourth or more of injected activity in the first 3-4 d to roughly 5% at one month and 1% at 10-15 y. A portion of barium deposited on bone surfaces returns to blood over a period of hours or days, and a portion moves from bone surface to bone volume over a period of days. Some of the volume deposit may return to blood by ion exchange processes over a period of weeks or months. Activity remaining in bone after a few months is removed over a period of years at rates consistent with bone turnover rates.

The generic model structure for calcium-like elements (Figure B-1) is applied to barium (ICRP 1993). The ICRP's transfer coefficients for barium are listed in Table B-3.

Table B-3. Transfer coefficients (d^{-1}) in the ICRP's model for barium.[a]

Path of movement	Transfer coefficient (d^{-1})
Plasma to urinary bladder contents	2.2400E+00
Plasma to upper large intestine contents	2.0160E+01
Plasma to trab bone surface	9.7200E+00
Plasma to cort bone surface	7.7800E+00
Plasma to ST0	2.3000E+01
Plasma to ST1	7.0000E+00
Plasma to ST2	1.4000E-01
Trabecular bone surface to plasma	5.7800E-01
Trabecular bone surface to exch volume	1.1600E-01
Cortical bone surface to plasma	5.7800E-01
Cortical bone surface to exch volume	1.1600E-01
ST0 to Plasma	7.6700E+00
ST1 to Plasma	6.9300E-01
ST2 to Plasma	3.8000E-04
Exch trabecular bone volume to surface	9.7000E-03
Exch to nonexch trabecular bone volume	4.2000E-03
Exch cortical bone volume to surface	9.7000E-03
Exch to nonexch cortical bone volume	4.2000E-03
Nonexch cortical bone volume to plasma	8.2100E-05
Nonexch trabecular bone volume to plasma	4.9300E-04

[a] exch = exchangeable, nonexch = nonexchangeable

Low variant: This is a modification of the ICRP's model for barium described above. The transfer coefficients from the short- and intermediate-term soft-tissue compartments, ST0 and ST1, to blood are multiplied by 5. Transfer rates describing removal from all bone compartments are multiplied by 2. Independent kinetics of chain members is assumed; the model for lanthanum as a daughter is applied to subsequent chain members.

High variant: This is a modification of the ICRP's model for barium described above. The transfer coefficients from the short- and intermediate-term soft-tissue compartments, ST0 and ST1, to blood are multiplied by 0.2. Transfer rates describing removal from all bone compartments are multiplied by 0.5. Independent kinetics of chain members is assumed; the model for lanthanum as a daughter is applied to subsequent chain members.

Lanthanide elements

Data on the systemic biokinetics of the lanthanide elements were reviewed by Taylor and Leggett (2003). Knowledge of the behavior of the lanthanide elements comes mainly from studies on laboratory animals, particularly rats. Data on rats suggest a trend with decreasing ionic radius in the biokinetics of these elements. That is, if lanthanide element A has a greater ionic radius than lanthanide element B, then A is likely to have greater uptake by liver, lower uptake by bone, and a lower urinary excretion rate than B. Limited human data on the behavior of lanthanide elements in humans appear to be reasonably consistent with the rat data regarding early distribution and excretion. Where data are available for several species, the rat appears to be broadly representative of other non-human species with regard to initial liver uptake of the lanthanide elements, although there are likely to be species differences in the rate of loss of lanthanides from the liver and perhaps other organs. Among the studied species, the beagle could be a reasonable model for man with regard to the rate of loss of the lanthanides from the body, based on broad similarities in the behavior of frequently studied actinides in beagles and man.

The biokinetics of promethium has been studied in controlled studies on human subjects and large animals as well as in rats. While the biokinetic data base for promethium is more nearly complete than those for most lanthanide elements, some important gaps remain for promethium. Selection of parameter values for promethium as well as other lanthanide elements relies to some extent on information on the actinide elements. A rapid decline in the urinary excretion rate of promethium over the first several weeks in humans and large animals suggests that the rate of return to blood from liver and soft tissues (and presumably to a lesser extent from bone) is slower for promethium than americium, for example. Also, the fairly high rate of fecal excretion during the first two weeks suggests a relatively high rate of loss in bile during that time, but the slow total-body loss over the first year indicates that the biliary secretion rate could not remain at a high level for an extended period. The collective data on promethium in laboratory animals and man indicate that the content of liver is initially higher than that of skeleton. A division of 45%-35% between liver and skeleton seems reasonably consistent with these data. The parameter values in the americium model for kidneys and urinary bladder are consistent with

urinary excretion data and kidney retention data for promethium, with the exception that a slightly higher deposition fraction in the long-term kidney compartment is indicated for promethium (1% for promethium versus 0.5% for americium). Information on the behavior of promethium in soft tissues comes mainly from studies on rats.

Limited data are available on the early excretion of injected lanthanum by human subjects. However, development of a systemic model for lanthanum must rely largely on lanthanum-specific data for laboratory animals, together with extrapolation of data for other lanthanides and actinides. The division of lanthanum between liver and skeleton appears to depend on the route of administration (Moskalev 1961, Cuddihy and Boecker 1970). The results indicate that the systemic distribution is influenced by the chemical nature of lanthanum presented to the biological system and that injection studies could be misleading to some extent with regard to applications to inhalation or ingestion exposures.

There is little direct information on the behavior of cerium in humans. External measurements were made on a subject who was accidentally exposed while grinding and polishing uranium metal. The data are difficult to interpret but indicate that cerium was tenaciously retained in the lungs and may have translocated to a small extent to the liver and skeleton. There is also some information on retention of environmental cerium, presumably from weapons tests, in the lungs and lymph notes of a few subjects. These data indicate that a portion of the environmental cerium was tenaciously retained in the lungs. Data on laboratory animals indicate that the systemic biokinetics of cerium fits into the same broad pattern that has been observed for lanthanides, rare earths, and actinides. That is, cerium is lost from the body at a slow rate, with liver and skeleton containing most of the systemic cerium. Two different patterns of removal from the liver are observed in different species: fast removal from livers of rodents and some larger animals, and slow removal from livers of dogs, swine, and hamsters. Data for human subjects generally fit the same pattern as dogs, swine, and hamsters.

Results of various experimental studies indicate fairly strong physiological similarities among different lanthanide pairs. Studies on rats indicate that the biokinetics of praseodymium is very similar to that of its close chemical analogue, cerium (Durbin 1960, 1962). Data for rats (Durbin 1960, 1962) indicate that the biokinetics of samarium is very similar to that of promethium. In rats and dogs exposed by inhalation to an aerosol containing $^{145}Sm_2O_3$ and $^{143}Pm_2O_3$ and sacrificed at 0, 14, and 30 days, the biokinetics of absorbed ^{145}Sm was virtually identical to that of absorbed ^{143}Pm (Shipler *et al*. 1976). Data for rats (Durbin 1960, 1962; Moskalev *et al*. 1972) indicate that the biokinetics of europium at early times is fairly similar to that of promethium and samarium. Apparent differences are that deposition in the liver may be lower and deposition in "other" and urinary bladder contents may be higher for europium. Data for rats (Durbin 1960, 1962; Ando *et al*. 1989) indicate that gadolinium has higher deposition in the skeleton and urinary bladder and lower deposition in the liver than promethium and samarium.

In rats (Durbin 1960, 1962), neodymium showed broadly similar biokinetics to that of other lanthanides. However, neodymium had noticeably lower liver uptake and higher urinary excretion than its closest neighbors in the periodic chart and thus did not closely fit the trend with ionic radius suggested by the collective data for the lanthanides. Unpublished data on human subjects indicate that excretion of neodymium during the first few days after intravenous injection is similar to that measured for promethium (Palmer *et al*. 1970) and lower than that measured in rats (Durbin 1960, 1962).

In rats, the lanthanide elements terbium, dysprosium, holmium, erbium, thulium, ytterbium, and lutetium showed similar biokinetics (Durbin 1960, 1962; Moskalev *et al*. 1972; Ando *et al*. 1989). Compared with gadolinium, these elements showed higher deposition in the skeleton (roughly 60%), lower deposition in the liver (roughly 10%), and similar initial deposition in the urinary bladder (15-28%).

Because members of lanthanide chains are generally also lanthanide elements, the assumption of shared kinetics seems reasonable for these chains.

The ICRP's models for lanthanide elements depict one-directional flow from blood to tissues to excretion pathways (urinary bladder contents and upper large intestine contents). Parameter values for individual lanthanide elements are summarized below.

ICRP model for lanthanum: Activity leaves blood with a half-time of 0.25 d, with 60% going to liver, 20% to bone, and 20% to Other. The removal half-time from all tissues is 3500 d. A urinary to fecal excretion ratio of 1:1 is assigned. Lanthanum isotopes are uniformly distributed on bone surfaces (ICRP 1981, 1994b).

ICRP model for cerium: Activity leaves blood with a half-time of 0.25 d, with 50% going to liver, 30% to bone, and 20% to Other. The removal half-time from all tissues is 3500 d. A urinary to fecal excretion ratio of 1:9 is assigned. Cerium isotopes with half-life less than 15 d are uniformly distributed on bone surfaces, and all others are distributed in bone volume (ICRP 1989, 1993).

ICRP model for praseodymium: Activity leaves blood with a half-time of 0.25 d, with 60% going to liver, 25% to bone, 5% to kidneys, and 10% to excretion pathways. The removal half-time from liver and bone is 3500 d and from kidneys is 10 d. A urinary to fecal excretion ratio of 1:1 is assigned. Praseodymium isotopes are uniformly distributed on bone surfaces (ICRP 1981, 1994b).

ICRP model for neodymium, promethium, and samarium: Activity leaves blood with a half-time of 0.25 d, with 45% going to liver, 45% to bone, and 10% to excretion pathways. The removal half-time from all tissues is 3500 d. A urinary to fecal excretion ratio of 1:1 is assigned. Isotopes of these elements are assumed to be uniformly distributed on bone surfaces (ICRP 1981, 1994b).

ICRP model for europium: Activity leaves blood with a half-time of 0.25 d, with 40% going to liver, 40% to bone, 6% to kidneys, and 14% to excretion pathways. The removal half-time from liver and bone is 3500 d and from kidneys is 10 d. A urinary to fecal excretion ratio of 1:1 is assigned. Europium is uniformly distributed on bone surfaces (ICRP 1981, 1994b).

ICRP model for gadolinium: Activity leaves blood with a half-time of 0.25 d, with 45% going to liver, 30% to bone, 3% to kidneys, and 22% to excretion pathways. The removal half-time from liver and bone is 3500 d and from kidneys is 10 d. A urinary to fecal excretion ratio of 1:1 is assigned. Gadolium is uniformly distributed on bone surfaces (ICRP 1981, 1994b).

ICRP model for terbium: Activity leaves blood with a half-time of 0.25 d, with 25% going to liver, 50% to bone, 5% to kidneys, and 20% to excretion pathways. The removal half-time from liver and bone is 3500 d and from kidneys is 10 d. A urinary to fecal excretion ratio of 1:1 is assigned. Terbium is uniformly distributed on bone surfaces (ICRP 1981, 1994b).

ICRP model for dysprosium: Activity leaves blood with a half-time of 0.25 d, with 10% going to liver, 60% to bone, 2% to kidneys, and 28% to excretion pathways. The removal half-time from liver and bone is 3500 d and from kidneys is 10 d. A urinary to fecal excretion ratio of 1:1 is assigned. Dysprosium is uniformly distributed on bone surfaces (ICRP 1981, 1994b).

ICRP model for holmium: Activity leaves blood with a half-time of 0.25 d, with 40% going to liver, 40% to bone, 5% to pancreas, and 15% to excretion pathways. The removal half-time from all tissues is 3500 d. A urinary to fecal excretion ratio of 1:1 is assigned. Holmium is uniformly distributed on bone surfaces (ICRP 1981, 1994b).

ICRP model for erbium: Activity leaves blood with a half-time of 0.25 d, with 5% going to liver, 60% to bone, 10% to Other, and 25% to excretion pathways. The removal half-time from all tissues is 3500 d. A urinary to fecal excretion ratio of 1:1 is assigned. Erbium is uniformly distributed on bone surfaces (ICRP 1981, 1994b).

ICRP model for thulium: Activity leaves blood with a half-time of 0.25 d, with 4% going to liver, 65% to bone, 10% to Other, and 21% to excretion pathways. The removal half-time from all tissues is 3500 d. A urinary to fecal excretion ratio of 1:1 is assigned. Thulium is uniformly distributed on bone surfaces (ICRP 1981, 1994b).

ICRP model for ytterbium: Activity leaves blood with a half-time of 0.25 d, with 3% going to liver, 50% to bone, 2% to kidneys, 0.5% to spleen, and 44.5% to excretion pathways. The removal half-time from liver, bone, or spleen is 3500 d and from kidneys is 10 d. A urinary to fecal excretion ratio of 1:1 is assigned. Ytterbium is uniformly distributed on bone surfaces (ICRP 1981, 1994b).

ICRP model for lutetium: Activity leaves blood with a half-time of 0.25 d, with 2% going to liver, 60% to bone, 0.5% to kidneys, and 37.5% to excretion pathways. The removal half-time from liver, bone, or spleen is 3500 d and from kidneys is 10 d. A urinary to fecal excretion ratio of 1:1 is assigned. Lutetium is uniformly distributed on bone surfaces (ICRP 1981, 1994b).

Low variant for lanthanum, cerium, praseodymium, neodymium, promethium, samarium, europium, gadolinium: Activity leaves blood with a half-time of 1.0 d, with 15% going to cortical surfaces, 15% to trabecular surfaces, 40% to liver, 20% to excretion pathways and 10% to Other. The following removal half-times to excretion pathways are assigned: 5 y for liver and other; 20 y for cortical surface; and 5 y for trabecular surface. A urinary to fecal excretion ratio of 1:1 is assigned. Radioactive progeny are assigned the biokinetics of the parent.

Low variant for terbium, dysprosium, holmium, erbium, thulium, ytterbium, and lutetium: Activity leaves blood with a half-time of 1.0 d, with 25% going to cortical surfaces, 25% to trabecular surfaces, 10% to liver, 30% to excretion pathways, and 10% to Other. The following removal half-times to excretion pathways are assigned: 2 y for liver and other tissue; 20 y for cortical surface; and 5 y for trabecular surface. A urinary to fecal excretion ratio of 1:1 is assigned. Radioactive progeny are assigned the biokinetics of the parent.

High variant for lanthanum, cerium, praseodymium, neodymium, promethium, samarium, europium, gadolinium: Activity leaves blood with a half-time of 0.25 d, with 20% going to cortical surfaces, 20% to trabecular surfaces, 2% to red marrow, 40% to liver, 3% to kidneys, 0.05% to testes, 0.02% to ovaries, 5% to excretion pathways, and the rest (9.93%) to other soft tissues. The following removal half-times to excretion pathways are assigned: 50 y for liver, trabecular surface, red marrow, and other tissue; 200 y for cortical surface; 1 y for kidneys; 100 y for gonads. A urinary to fecal excretion ratio of 1:1 is assigned. Radioactive progeny are assigned the biokinetics of the parent.

High variant for terbium, dysprosium, holmium, erbium, thulium, ytterbium, and lutetium: Activity leaves blood with a half-time of 0.25 d, with 30% going to cortical surfaces, 30% to trabecular surfaces, 2% to red marrow, 10% to liver, 3% to kidneys, 0.05% to testes, 0.02% to ovaries, 15% to excretion pathways, and the rest (9.93%) to other soft tissues. The following removal half-times to excretion pathways are assigned: 25 y for liver, trabecular surface, red marrow, and other; 100 y for cortical surface; 0.5 y for kidneys; 50 y for gonads. A urinary to fecal excretion ratio of 1:1 is assigned. Progeny are assigned the biokinetics of the parent.

Hafnium

The systemic biokinetics of hafnium has been studied in rats, hamsters, and marmosets (ICRP 1981, Taylor et al. 1985). The skeleton appears to be an important long-term repository, although hafnium may also be tenaciously retained in liver and other soft tissues. Results of a number of studies indicate that hafnium and zirconium are close physiological analogues in a qualitative sense, and comparative data on similar chemical forms of hafnium and zirconium in rats indicate that they may have reasonably similar biokinetics as well.

In the ICRP's model for hafnium (ICRP 1981, 1994b), activity leaves blood with a half-time of 0.25 d, with 50% depositing in bone and 50% in Other. The removal half-time from bone is 8,000 d and from Other is 7 d. Activity removed from tissues transfers to excretion pathways (urinary bladder contents and upper large intestine contents). A urinary to fecal excretion ratio of 1:1 is assigned. Hafnium isotopes are uniformly distributed on bone surfaces.

Low variant: This is the same as the low variant model described earlier for yttrium and zirconium. Independent kinetics is assumed for chains involving tantalum isotopes; otherwise, radioactive progeny are assigned the biokinetics of hafnium.

High variant: This is the same as the high variant model for zirconium described earlier. Radioactive progeny are assigned the biokinetics of hafnium.

Tantalum

The systemic biokinetics of tantalum has been studied in rats (ICRP 1981). The data suggest that tantalum deposits in the skeleton to a large extent and is almost entirely removed from the body within a few months.

In the ICRP's model for tantalum (ICRP 1981, 1994b), activity leaves blood with a half-time of 0.25 d. Outflow from blood is divided as follows: bone, 30%; kidneys, 6%; Other, 64%. The removal half-time from bone is 100 d. Half the activity depositing in Kidneys or Other is removed with a half-time of 4 d and half is removed with a half-time of 100 d. Activity removed from tissues transfers to excretion pathways (urinary bladder contents and upper large intestine contents). A urinary to fecal excretion ratio of 1:1 is assigned. Tantalum isotopes with half-life <15 d are uniformly distributed on bone surfaces, and all others are distributed in bone volume.

Low variant: This is a modification of the ICRP's model for tantalum described above. Removal half-times for the short- and long-term components of soft tissues are reduced from 4 and 100 d, respectively, to 1 and 50 d, respectively. Radioactive progeny are assigned the biokinetics of tantalum.

High variant: This is a modification of the ICRP's model for the chemically similar element, niobium (described earlier). The long-term half-time in each organ is increased from 200 d to 500 d. Radioactive progeny are assigned the biokinetics of tantalum.

Tungsten

Data on the systemic biokinetics of tungsten were reviewed by Leggett (1997a). Information on the behavior of tungsten in humans consists largely of measurements of the concentration of tungsten in blood, tissues, and excreta of chronically exposed subjects. These data are sparse and difficult to interpret, and the levels and patterns of exposure of the subjects are poorly characterized. Best available information on the systemic biokinetics of tungsten comes from studies of dogs, sheep, pigs, goats, cows, and rodents. Qualitative information on the biokinetics of tungsten can also be gained from data on molybdenum, an essential element that is in many respects a close physiological analogue of tungsten.

In the ICRP's systemic model for tungsten (ICRP 1981, 1994b), activity is removed from blood with a half-time of 0.25 d, with 95% going to excretion pathways, 2.5% to bone, 1% to kidneys, 1% to liver, and 0.5% to spleen. Fractions 0.2, 0.1, and 0.7 of activity deposited in bone are removed with half-times of 5, 100, and 1000 d, respectively. Fractions 0.7 and 0.3 of activity deposited in kidneys, liver, or spleen are removed with half-times of 5 and 100 d, respectively. Activity that is promptly excreted or removed from tissues transfers directly to the urinary bladder contents or upper large intestine contents. A urinary to fecal excretion ratio of 1:1 is assigned. Tungsten isotopes with half-life less than 15 d are uniformly distributed on bone surfaces, and all others are distributed in bone volume.

A systemic model for tungsten was based on structure shown in Figure B-1, with spleen added as a separate compartment (Leggett, 1997a). Parameter values are listed in Table B-4.

Low variant: This is a modification of the model of Leggett (1997a) indicated in Table B-4. Removal half-times from skeletal compartments are decreased by a factor of 2 and removal half-times from soft-tissue compartments are decreased by a factor of 3.

High variant: This is a modification of the model of Leggett (1997a). Removal half-times from skeletal compartments are increased by a factor of 2 and removal half-times from soft-tissue compartments are increased by a factor of 3.

Table B-4. Transfer coefficients (d⁻¹) for a systemic biokinetic model for tungsten (Leggett 1997a) based on the model framework shown in Figure B-1.[a]

Path of movement	Transfer coefficient (d⁻¹)
Plasma to ST0	4.9920E+00
Plasma to RBC	5.8240E-02
Plasma to urinary bladder contents	8.7360E+00
Plasma to urinary path	5.2416E-01
Plasma to other kidney tissue	5.8240E-02
Plasma to upper large intestine contents	5.8240E-01
Plasma to spleen	5.8240E-03
Plasma to liver 1	4.6592E-01
Plasma to ST1	2.6208E-01
Plasma to ST2	2.3296E-02
Plasma to trabecular bone surface	5.1769E-01
Plasma to cortical bone surface	4.1415E-01
ST0 to plasma	8.3178E+00
RBC to plasma	3.4657E-01
Urinary path to urinary bladder contents	1.3863E+00
Other kidney tissue to plasma	1.9000E-03
Liver 1 to plasma	3.1192E-01
Liver 1 to liver 2	3.4657E-02
ST1 to plasma	6.9315E-02
ST2 to excreta	1.9000E-03
Spleen to plasma	1.9000E-03
Trabecular bone surface to plasma	5.7762E-01
Trabecular bone surface to exch volume	1.1552E-01
Cortical bone surface to plasma	5.7762E-01
Cortical bone surface to exch volume	1.1552E-01
Liver 2 to plasma	1.9000E-03
Nonexch trabecular bone volume to plasma	4.9300E-04
Nonexch cortical bone volume to plasma	8.2100E-05
Exch trabecular bone volume to surface	2.7730E-03
Exch trabecular bibe volume to nonexch volume	4.1590E-03
Exch cortical bone volume to surface	2.7730E-03
Exch cortical bone volume to nonexch volume	4.1590E-03

[a]Exch = exchangeable, nonexch = nonexchangeable

Rhenium

Information on the systemic biokinetics of rhenium comes mainly from studies on rats. It appears from these studies that the biokinetics of rhenium is similar to that of the chemically related element technetium, for which more information is available (ICRP 1980).

The ICRP's model for rhenium (ICRP 1980, 1994b) is the same as the model for technetium described earlier.

Low variant: This is a modification of the ICRP's model (ICRP Publication 30, Part 2,1980). Uptake by thyroid is reduced from 4% to 1%, with the difference distributed among compartments of "Other". All transfer coefficients from tissue compartments are multiplied by a factor of 4.

High variant: This is a modification of the ICRP's model (ICRP Publication 30, Part 2,1980). All transfer coefficients from tissue compartments are divided by a factor of 4.

Osmium

Information on the systemic biokinetics of osmium is sparse. The ICRP interpreted short-term observations of osmium in rats as indicating that its behavior does not differ markedly from that of other platinum metals (ICRP 1980). Its early behavior also resembles that of the chemically similar element, ruthenium. The limited data suggest, however, that osmium may be excreted more rapidly than either ruthenium or iridium.

The ICRP's systemic model for osmium is the same at that for iridium (described later).

Low variant: This is a modification of the low variant for rhodium. Transfer coefficients describing outflow from all tissue compartments to excretion pathways are increased by a factor of 2.

High variant: This is a modification of the ICRP's model for iridium (described below). Transfer coefficients describing outflow from all tissue compartments to excretion pathways are decreased by a factor of 2.

Iridium

The systemic behavior of iridium has been studied in various animal species, including monkeys and dogs (ICRP 1980). Liver, kidneys, and spleen show higher concentrations of injected or absorbed iridium than other organs. The retention times in these organs roughly paralleled that in the whole body. The long-term biological half-time, representing about 60-90% of the total, varied from about 3 months to about 1 year in different species, with no apparent trend with body size.

In the ICRP's model for iridium (ICRP 1980, 1994b), activity leaves blood with a half-time of 0.25 d, with 20% going to liver, 4% to kidneys, 2% to spleen, 54% to Other, and 20% to excretion pathways (urinary bladder contents and upper large intestine contents). Fractions 0.2 and 0.8 of activity deposited in any tissue are removed to excretion pathways with biological half-times of 8 and 200 d, respectively. A urinary to fecal excretion ratio of 1:1 is assigned.

Low variant: This is a modification of the ICRP's model for iridium. Transfer coefficients from all tissue compartments to excretion pathways are increased by a factor of 2.

76

High variant: This is a modification of the ICRP's model for iridium. Transfer coefficients from all tissue compartments to excretion pathways are decreased by a factor of 3.

Platinum

Data on the systemic biokinetics of platinum were reviewed in ICRP Publication 30, Part 3 (1981). Relatively detailed data for rats are reasonably consistent with more limited information on other species, including man. About 10-30% of the amount reaching blood is excreted during the first day, and most of the rest is retained with a half-time on the order of a week. There is also extended retention of a small percentage of absorbed or injected platinum, but long-term components are poorly characterized.

In the ICRP's model for platinum (ICRP 1981, 1994b), activity leaves blood with a half-time of 0.25 d, with 10% going to liver, 10% to kidneys, 1% to spleen, 0.1% to adrenal glands, 58.9% to Other, and 20% to excretion pathways (urinary bladder contents and upper large intestine contents). Fractions 0.95 and 0.05 of activity deposited in any tissue are removed to excretion pathways with biological half-times of 8 and 200 d, respectively. A urinary to fecal excretion ratio of 1:1 is assigned.

The long-term removal half-time is based on analogy with the chemically similar element, iridium (ICRP 1981).

Low variant: This is a modification of the ICRP's model for platinum described above. Transfer coefficients from all tissue compartments to excretion pathways are increased by a factor of 2.

High variant: This is a modification of the ICRP's model for platinum. Transfer coefficients for the short-term compartments are decreased by a factor of 2, and transfer coefficients for the long-term compartments are increased by a factor of 5.

Gold

Data for patients receiving gold treatment for rheumatoid arthritis indicate that gold is retained in the body with a half-life of about 3 d and is excreted in urine. Similar half-times have been found in other studies with gold salts (ICRP 1980).

In the ICRP's model for gold (ICRP 1981, 1994b), it is assumed that gold entering blood is instantaneously distributed uniformly thoughout the body and removed from tissues to the urinary bladder contents with a half-time of 3 d.

Low variant: The ICRP's model is modified by decreasing the removal half-time to 2 d.

High variant: The ICRP's model is modified by assuming two components of retention: 99% of deposited activity is removed with a half-time of 4 d and 1% with a half-time of 1 y.

Mercury

Whole-body retention, excretion rates, and long-term distribution data for mercury are available from studies on human subjects, but information on the time-dependent distribution comes mainly from studies on laboratory animals (ICRP 1980, Friberg et al. 1986). Mercury is distributed throughout all tissues, with highest concentrations usually found in the kidneys. The biokinetics differs for organic and inorganic mercury, and the distribution of organic compounds depends on the compound administered and the animal species studied. The kidneys and brain appear to be important repositories for organic mercury. Controlled studies on human subjects suggest a half-life in the total body of about 40 d for inorganic mercury and about 80 d for methyl mercury. It may be that these values apply to most but not all of the body burden. In view of the mass of mercury in Reference Man (ICRP 1975) and the fact that some mercury is still detectable in urine several years after exposure, the ICRP (1980) assigned nearly 5% to a uniformly distributed compartment with removal half-time to excretion of 10,000 d. Thus, despite the sizable database on mercury, there remain substantial uncertainties in its systemic biokinetics.

In the ICRP's systemic model for inorganic mercury (ICRP 1980, 1994b), activity leaves blood with a half-time of 0.25 d, with 8% going to kidneys and 92% to Other. Fractions 0.95 and 0.05 of activity deposited in any tissue are removed to excretion pathways (urinary bladder contents and upper large intestine contents) with biological half-times of 40 d and 10,000 d, respectively. A urinary to fecal excretion ratio of 1:1 is assigned.

In the ICRP's systemic model for organic mercury (ICRP 1980, 1994b), activity leaves blood with a half-time of 0.25 d, with 8% going to kidneys, 20% to brain, and 72% to Other. Fractions 0.95 and 0.05 of activity deposited in any tissue are removed to excretion pathways (urinary bladder contents and upper large intestine contents) with biological half-times of 80 d and 10,000 d, respectively. A urinary to fecal excretion ratio of 1:1 is assigned.

Low variant for inorganic mercury (excluding mercury vapor): Mercury is removed from blood with a half-time of 0.25 d, with 10% going to kidneys and 90% to other tissues. For each organ, the fraction 0.99 is removed to excretion pathways with a half-time of 20 d, and 0.01 is removed with a half-time of 10,000 d. A urinary to fecal excretion ratio of 1:1 is assigned.

High variant for inorganic mercury (excluding mercury vapor): Mercury is removed from blood with a half-time of 0.25 d, with 10% going to kidneys and 90% to other tissues. For each organ, the fraction 0.8 is removed to excretion pathways with a half-time of 80 d, and 0.2 is removed with a half-time of 10 y. A urinary to fecal excretion ratio of 1:1 is assigned.

Low variant for mercury vapor: It is assumed that 80% of mercury reaching blood is transported to the lungs and then exhaled as indicated in the ICRP's model for mercury vapor. The rest behaves as indicate in the low variant model for inorganic mercury.

High variant for mercury vapor: It is assumed that 50% of mercury reaching blood is transported to the lungs and then exhaled as indicated in the ICRP's model for mercury vapor. The rest behaves as indicated in the high variant model for inorganic mercury.

Low variant for organic mercury: Mercury is removed from blood with a half-time of 0.25 d, with 5% going to kidneys, 2% to brain, and 93% to other tissues. For each organ, the fraction 0.99 is removed to excretion pathways with a half-time of 40 d, and 0.01 is removed with a half-time of 10,000 d. A urinary to fecal excretion ratio of 1:1 is assigned.

High variant for organic mercury: Mercury is removed from blood with a half-time of 0.25 d, with 15% going to kidneys, 20% to brain, and 65% to other tissues. For each organ, the fraction 0.8 is removed to excretion pathways with a half-time of 160 d, and 0.2 is removed with a half-time of 10 y (3650 d). A urinary to fecal excretion ratio of 1:1 is assigned.

Thallium

The systemic biokinetics of thallium has been studied extensively in various species including man (ICRP 1981). Its behavior is broadly similar to that of potassium, but thallium is removed from the body at a higher rate than potassium. Thallium is rapidly removed from plasma, and its early distribution is determined largely by the distribution of cardiac output.

In the ICRP's systemic model for thallium (ICRP 1981, 1994b), activity reaching blood is instantaneously distributed among body tissues, with 3% depositing in the kidneys and 97% in Other. The removal half-time from tissues to excretion pathways (urinary bladder contents and upper large intestine contents) is 10 d. A urinary to fecal excretion ratio of 1:1 is assigned.

Low variant: Thallium leaves blood at the rate 1000 d^{-1} and is uniformly distributed in the body. The removal half-time to excretion pathways is 6 d. A urinary to fecal ratio of 1:1 is assigned.

High variant: Thallium leaves blood at the rate 1000 d^{-1}, with 5% depositing in the kidneys and the remainder being uniformly distributed in the body. The removal half-time to excretion pathways is 16 d. A urinary to fecal excretion ratio of 1:1 is assigned.

Lead

The ICRP's current systemic biokinetic model for lead (ICRP 1993) synthesizes a large amount of experimental, environmental, and occupational data on the biological behavior of this element in the body. These data include results of lead tracer studies on human subjects; measurements of lead in autopsy samples from environmentally and occupationally exposed persons; results of lead balance studies on human subjects; results of detailed experimental studies on nonhuman

primates, dogs, and other laboratory animals; and extensive experimental, environmental, and occupational data on chemically and physiologically related elements. Consistency of predictions of the model with various types of data derived under a wide variety of conditions gives reasonably high confidence in model predictions, particularly for adults. The database for lead and the basis for the ICRP's systemic model for lead are summarized by Leggett (1993).

The structure of the ICRP's model for lead (ICRP 1993) is the generic model structure for volume seekers shown in Figure B-1. Parameter values are listed in Table B-5.

Table B-5. Transfer coefficients (d^{-1}) in the ICRP's model for lead.[a]

Path of movement	Transfer coefficient (d^{-1})
RBC to plasma	0.139
Trabecular or cortical bone surface to plasma	0.5
Nonexch trabecular bone volume to plasma	0.000493
Nonexch cortical bone volume to plasma	0.0000821
Liver 1 to plasma	0.0312
Liver 2 to plasma	0.0019
Other kidney tissue to plasma	0.0019
ST0 to plasma	7.39
ST1 to plasma	0.00416
ST2 to plasma	0.00038
Plasma to RBC	28.0
Plasma to trabecular bone surface	4.86
Trab or cort exch bone volume to bone surface	0.0185
Plasma to cortical bone surface	3.89
Trab or cort bone surface to exch bone volume	0.5
Trab or cort exch bone volume to nonexch volume	0.0046
Plasma to liver 1	4.9
Liver 1 to liver 2	0.00693
Plasma to urinary path	2.45
Plasma to other kidney tissues	0.0245
Plasma to ST0	22.16
Plasma to ST1	0.7
Plasma to ST2	0.14
Plasma to U bladder contents	1.75
Urinary path to urinary bladder contents	0.139
Liver 1 to small intestine contents	0.0312
Plasma to upper large intestine contents	0.7
Plasma to sweat	0.42
ST1 to excreta	0.00277

[a]RBC = red blood cells, exch = exchangeable, nonexch = nonexchangeable, trab = trabecular, cort = cortical

Low variant: This is a modification of the ICRP's model for lead indicated above. Transfer coefficients describing removal from all bone volume compartments and all soft tissue compartments other than the rapid turnover extracellular fluid compartment (ST0) are multiplied by 2. Independent kinetics of chain members is assumed.

High variant: This is a modification of the ICRP's model for lead. Transfer coefficients describing removal from all bone volume compartments and all soft tissue compartments other than the rapid turnover extracellular fluid compartment (ST0) are divided by 2. Independent kinetics of chain members is assumed.

Bismuth

The biokinetics of bismuth has been studied extensively in human subjects and laboratory animals (ICRP 1980; ICRP 1993, pp. 76-77). Interpretation of the data is complicated by variability in the biokinetics of bismuth with the physical and chemical form administered. The studies generally indicate that most of the bismuth reaching blood is lost from the body over a period of days, but a small portion may be tenaciously retained. All studied forms of bismuth show high deposition in the kidneys. Some studies also indicate elevated deposition in the liver, spleen, and other organs of the reticuloendothelial (RE) system, but this may depend on the chemical form administered. Most forms of bismuth are rapidly cleared from blood. It appears that bismuth is excreted mainly in urine, but the rate of urinary excretion varies substantially with the chemical form introduced into blood. Fecal excretion is typically about 10% of total excretion. For the sparingly soluble bismuth compounds that have been used in clinical applications, there is tenacious retention of a few percent of the administered bismuth.

In the ICRP's systemic model for bismuth (ICRP 1980, 1994b), activity leaves blood with a half-time of 0.01 d, with 40% going to kidneys, 30% to Other, and 30% to excretion pathways (urinary bladder contents and upper large intestine contents). Fractions 0.6 and 0.4 of activity deposited in any tissue are removed to excretion pathways with biological half-times of 0.6 d and 5 d, respectively. A urinary to fecal excretion ratio of 1:1 is assigned.

Low variant: This is a modification of the ICRP's model for bismuth described above. The longer-term removal half-time is assumed to be 3 d rather than 5 d. The urinary-to-fecal ratio is assumed to be 9 rather than 1.

High variant: This is a modification of the ICRP's model for bismuth. The initial distribution is the same as in the ICRP's model, but for any organ or tissue, fractions 0.6 and 0.35 and 0.05 are assumed to be retained with biological half-times of 1 d and 20 d, and 1 y, respectively.

Polonium

The systemic biokinetics of polonium has been studied in accidentally exposed persons, in controlled experiments involving a few unhealthy human subjects, and in several types of laboratory animals including non-human primates and dogs (ICRP 1993, Leggett and Eckerman 2001). The urinary excretion rate of polonium appears to be species dependent, resulting in a species-dependent removal half-time from the body. Estimates of biological half-times of polonium in accidentally exposed humans, based mainly on excretion data for these persons, usually have been in the range 20-60 d. There is a large body of data on urinary excretion of polonium by human subjects, but much of the data may be unreliable due to recovery problems in a widely-used method of measuring polonium in urine. Comparative data on man, baboons, and dogs indicate that the early systemic distribution is similar in the three species. Results of some injection studies may be complicated by the formation of polonium aggregates and subsequently higher uptake of polonium by organs containing elements of the reticuloendothelial system.

In the ICRP's systemic model for polonium (ICRP 1993), activity leaves blood with a half-time of 0.25 d, with 30% going to liver, 10% to kidneys, 5% to spleen, 10% to red marrow, and 45% to Other. The removal half-time from all tissues to excretion pathways (urinary bladder contents and upper large intestine contents) is 50 d. A urinary to fecal excretion ratio of 1:2 is assigned.

Low variant: Polonium leaves plasma at a rate of 100 d^{-1}, with the fraction 10% going to red blood cells, 35% evenly divided between two liver compartments (Liver 1 and Liver 2), 10% evenly divided between two kidney compartments (Kidneys 1 and Kidneys 2), 2% to spleen, 4% to red marrow, 1.5% to bone surface (divided evenly between cortical and trabecular bone), 0.1% to testes, and 0.05% to ovaries, 5% to skin, and the remainder to Other. Polonium is removed from each compartment back to plasma with a biological half-time of 7 d, except that: polonium moves from Liver 1 to the contents of the small intestine with a half-time of 5 d; from Kidneys 1 to the urinary bladder contents with a half-time of 4 d; from bone surface to plasma with a half-time of 30 d; from skin to plasma and excreta (evenly divided) with a half-time of 50 d; and from gonads to plasma with a half-time of 50 d. Progeny are assigned the biokinetics of polonium.

High variant: This is a modification of the ICRP's model for polonium described above. Deposition in red marrow is increased from 10% to 20%; deposition in liver is increased from 30% to 40%; and the remaining 40% is assumed to be evenly distributed in other tissues. Radioactive progeny are assigned the biokinetics of polonium.

Astatine

Due to a lack of biokinetic data on astatine, the ICRP's biokinetic model (ICRP 1981, 1994b) for this element was based on analogy with two chemically similar elements, chlorine and bromine. According to the model for astatine, activity leaves blood with a half-time of 0.25 d and is distributed uniformly in the body. The removal half-time from tissues to excretion pathways

(urinary bladder contents and upper large intestine contents) is 10 d. A urinary to fecal excretion ratio of 1:1 is assigned. Uncertainties in model predictions are greater for astatine than for chlorine or bromine, both of which have been studied in human subjects.

Low variant: This is the ICRP's model with the removal half-time reduced from 10 d to 2 d. Radioactive progeny are assigned the biokinetics of astatine.

High variant: This is the ICRP's model with the removal half-time increased from 10 d to 50 d. Radioactive progeny are assigned the biokinetics of astatine.

Francium

Due to a lack of biokinetic data for francium, the ICRP (1981) assumes that its distribution in the body is similar to that of the chemically related element cesium. Francium is assumed to leave blood with a half-time of 0.25 d and to be uniformly distributed in the body. Since the isotopes of francium considered in ICRP reports are extremely short-lived, francium deposited in tissues is assumed to remain there indefinitely, i.e., to decay at the site of deposition.

Low variant: After absorption to blood, francium and all chain members behave as described by the ICRP's biokinetic model for radium (described later).

High variant: Francium leaves blood at a rate of 1000 d^{-1} and is uniformly distributed in the body. Francium and all chain members are retained indefinitely in tissues.

Radium

The systemic biokinetics of radium can be modeled reasonably well on the basis of data on radium and its physiological analogues in human subjects and laboratory animals (Leggett 1993, ICRP 1993). Measurements of whole-body retention of radium are available for a number of human subjects, but many of the subjects were unhealthy, elderly, or received relatively high doses that may have affected the bone turnover rate. Whole-body retention data for radium can be supplemented to some extent with data from controlled studies on barium, a close chemical and physiological analogue of radium. The systemic distribution of radium at early times has been determined in a few seriously ill human subjects and can also be estimated from animal data, although species differences in the behavior of radium must be taken into account. As with other alkaline earth elements, available biokinetic data for radium can be superimposed on a biologically meaningful model of calcium addition and turnover and of bone restructuring.

The ICRP's model structure for calcium-like elements (Figure B-1) is applied to radium. The ICRP's transfer coefficients for radium are listed in Table B-6.

Low variant: This is a modification of the ICRP's model for radium indicated above. Transfer coefficients describing removal from all soft tissue compartments other than rapid turnover extracellular fluid (ST0) are multiplied by 3. Transfer coefficients describing removal from bone compartments are multiplied by 2. Independent kinetics of chain members is assumed.

High variant: This is a modification of the ICRP's model for radium. Transfer coefficients describing removal from all soft tissue compartments other than the rapid turnover extracellular fluid compartment (ST0) are divided by 3. Transfer coefficients describing removal from all bone compartments are divided by 2. Independent kinetics of chain members is assumed.

Table B-6. Transfer coefficients (d^{-1}) in the ICRP's model for radium.[a]

Path of movement	Transfer coefficient (d^{-1})
Plasma to urinary bladder contents	6.0600E-01
Plasma to upper large intestine contents	2.1790E+01
Plasma to trabecular bone surface	9.7200E+00
Plasma to cortical bone surface	7.7800E+00
Plasma to ST0	2.2680E+01
Plasma to ST1	7.0000E+00
Plasma to ST2	7.0000E-02
Plasma to liver 1	3.5000E-01
Trabecular bone surface to plasma	5.7800E-01
Trabecular bone surface to exch volume	1.1600E-01
Cortical bone surface to plasma	5.7800E-01
Cortical bone surface to exch volume	1.1600E-01
ST0 to plasma	7.5600E+00
ST1 to plasma	6.9300E-01
ST2 to plasma	3.8000E-04
Liver 1 to plasma	1.3900E-02
Exch trabecular bone volume to surface	1.8500E-02
Exch to nonexch trabecular bone volume	4.6000E-03
Exch cortical bone volume to surface	1.8500E-02
Exch to nonexch cortical bone volume	4.6000E-03
Nonexch cortical bone volume to plasma	8.2100E-05
Nonexch trabecular bone volume to plasma	4.9300E-04

[a]exch = exchangeable, nonexch = nonexchangeable

Thorium

Data on the systemic biokinetics of thorium were reviewed by the ICRP (1995a) and by Leggett (1997b). Direct information on the biokinetics of thorium in the human body comes from an experimental study involving elderly human subjects, long-term measurements of ^{227}Th or ^{228}Th in the bodies and excreta of occupationally exposed persons, and measurements of thorium isotopes in autopsy samples from non-occupationally exposed subjects. The biokinetics of thorium has also been examined in some detail in experimental studies on laboratory animals including dogs. Thorium is tenaciously retained in the body and has a much higher affinity for bone than for other tissues. The biokinetics of thorium is broadly similar to that of plutonium, but thorium accumulates in the liver to a much smaller extent and has higher urinary clearance

and lower fecal clearance from blood than plutonium. An important uncertainty in estimates of dose from some thorium isotopes is the behavior of radioactive progeny produced *in vivo*, because members of some thorium chains representing a substantial portion of potentially deposited energy have much different chemical properties from thorium.

The structure of the ICRP's systemic biokinetic model for thorium (ICRP 1995a) is shown in Figure B-4, and parameter values of the model are listed in Table B-7. The model structure is a generic framework for bone-surface seeking radionuclides introduced in ICRP Publication 67 (1993), where it was applied to plutonium, americium, and neptunium.
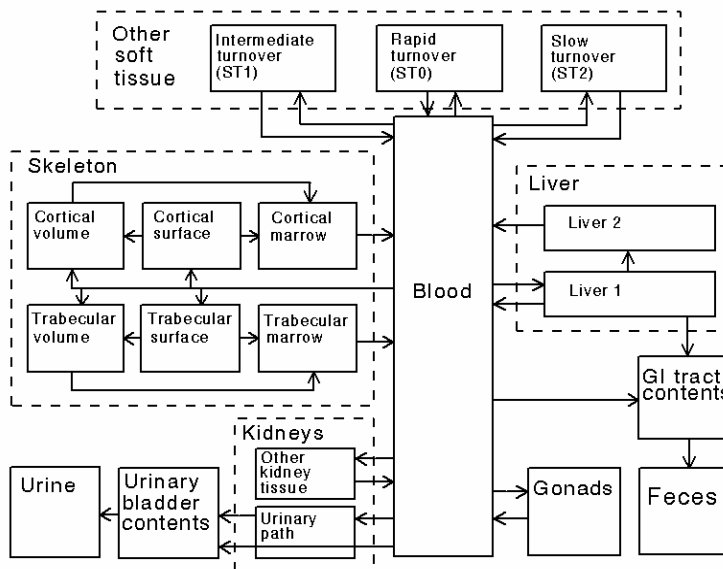
Figure B-4. ICRP's generic model structure for bone-surface-seeking radionuclides (ICRP 1993).

Low variant: The low variant model is a modification of the ICRP's model for thorium indicated above. The transfer coefficient describing transfer from blood to urinary bladder contents is increased to represent an increase from 5.5% to 10% in the percentage of thorium going from blood to urine. The coefficient describing transfer from blood to intermediate-term soft-tissue (ST1) is decreased to represent a decrease of 4.5% in the deposition percentage for ST1. Removal half-times from all bone and soft tissue compartments are one-half the ICRP's values; i.e., all transfer coefficients for bone and soft-tissue compartments are doubled. Independent kinetics of chain members is assumed. The ICRP's "independent kinetics" models for thorium chain members are applied (ICRP 1995a).

85

High variant: The high variant model is a modification of the ICRP's model for thorium. The transfer coefficient describing flow from blood to urinary bladder contents is decreased to represent a decrease from 5.5% to 3% in the percentage of thorium going from blood to urine. The coefficient describing transfer from blood to ST1 is increased to reflect a 2.5% increase in deposition in ST1 compared with the ICRP model. Removal half-times from all bone and soft tissue compartments are two times the ICRP value; i.e., all transfer coefficients for bone and soft-tissue compartments are halved. Independent kinetics of chain members is assumed (based on the ICRP models for members of thorium chains), but a minimal removal half-time of 10 d is assumed for chain members (excluding radon) that are produced at sites other than blood, red blood cells, or the rapid-turnover soft-tissue compartment (ST0). That is, element-specific removal half-times are used for radionuclides produced in the body, but any element-specific half-time less than 10 d is changed to 10 d.

Table B-7. Transfer coefficients (d^{-1}) in the ICRP's model for thorium.[a]

Path of movement	Transfer coefficient (d^{-1})
Blood to liver 1	0.0970
Blood to cortical bone surface	0.6793
Blood to trabecular bone surface	0.6793
Blood to urinary bladder contents	0.1067
Blood to urinary path	0.0679
Blood to other kidney tissue	0.0194
Blood to upper large intestine contents	0.00970
Blood to testes	0.00068
Blood to ovaries	0.00021
Blood to ST0	0.832
Blood to ST1	0.243
Blood to ST2	0.0388
ST0 to blood	0.462
Urinary path to urinary bladder contents	0.0462
Other kidney tissue to blood	0.00038
ST1 to blood	0.00095
ST2 to blood	0.000019
Trabecular bone surface to volume	0.000247
Trabecular bone surface to bone marrow	0.000493
Cortical bone surface to volume	0.0000411
Cortical bone surface to bone marrow	0.0000821
Trabecular bone volume to bone marrow	0.000493
Cortical bone volume to bone marrow	0.0000821
Bone marrow to blood	0.0076
Liver 1 to liver 2	0.00095
Liver 1 to small intestine contents	0.000475
Liver 1 to blood	0.000475
Liver 2 to blood	0.000211
Testes or ovaries to blood	0.00019

86

Uranium

Information on the systemic biokinetics of uranium comes from measurements of uranium in blood and excreta of several unhealthy human subjects who were intravenously injected with uranium; postmortem measurements of uranium in tissues of some of those subjects; postmortem measurements of uranium in tissues of occupationally and environmentally exposed subjects; data on baboons, dogs, or smaller laboratory animals exposed to uranium for experimental purposes; and consideration of the physiological processes thought to determine retention and translocation of uranium in the body (Leggett 1994, ICRP 1995a). Data from controlled studies on human subjects may not be typical because of their state of health or the fact that the subjects were administered relatively high masses of uranium, which may have altered the kinetics of uranium to some extent, particularly in the kidneys. Another difficulty is that the postmortem data are not sufficiently detailed in some cases to allow a close determination of the total uranium content of some massive tissues such as the skeleton, muscle, fat, and skin. Postmortem measurements of uranium in tissues of occupationally and environmentally exposed subjects provide the best available information on the long-term distribution of uranium in the human body but are limited by the small numbers of subjects examined; uncertainties in the exposure histories of those subjects; uncertainties in estimates of total-organ contents of the subjects based on small samples of tissue, particularly skeletal tissues; and technical difficulties in measuring the typically low concentrations of uranium in tissues of environmentally exposed subjects. Studies on baboons, dogs, monkeys, sheep, and small animals may be used to fill gaps in the data on humans but, in addition to uncertainties regarding interspecies extrapolation of results, have many of the same problems that complicate the human studies. For example, many of the animal studies involved relatively high masses of uranium, limited sampling of bone and massive soft tissues. Regarding dose estimates for injected uranium, important uncertainties are skeletal retention at times remote from injection, the residence time of uranium on or near bone surfaces, and the cumulative activity of uranium in soft tissues other than liver and kidneys.

The generic structure for calcium-like elements is applied by the ICRP to uranium (ICRP 1993). The ICRP's transfer coefficients for uranium are listed in Table B-8.

Low variant: The low variant model is a modification of the ICRP's model for uranium. Removal half-times are divided by 2 for compartments in bone and by 3 for intermediate- and long-term retention compartments of Other (ST1 and ST2). Independent kinetics of decay chain members is assumed.

High variant: The high variant model is also a modification of the ICRP's model for uranium. Removal half-times are multiplied by 10 for compartments in bone surface, by 2 for compartments in bone volume, and by 3 for intermediate- and long-term retention compartments of Other (ST1 and ST2). Independent kinetics of decay chain members is assumed.

Table B-8. Transfer coefficients (d⁻¹) in the ICRP's model for uranium.[a]

Path of movement	Transfer coefficient (d^{-1})
Plasma to ST0	10.50
Plasma to RBC	2.45E-01
Plasma to urinary bladder contents	15.43
Plasma to urinary path	2.94
Plasma to other kidney tissue	1.22E-02
Plasma to upper large intestine contents	1.22E-01
Plasma to liver 1	3.67E-01
Plasma to ST1	1.63
Plasma to ST2	7.35E-02
Plasma to trabecular bone surfaces	2.04
Plasma to cortical bone surfaces	1.63
ST0 to plasma	8.32
RBC to plasma	3.47E-01
Urinary path to urinary bladder contents	9.90E-02
Other kidney tissue to plasma	3.80E-04
Liver 1 to plasma	9.20E-02
Liver 1 to liver 2	6.93E-03
ST1 to plasma	3.47E-02
ST2 to plasma	1.90E-05
Bone surfaces to plasma	6.93E-02
Bone surfaces to exch bone volume	6.93E-02
Liver 2 to plasma	1.90E-04
Nonexch trabecular volume to plasma	4.93E-04
Nonexch cortical volume to plasma	8.21E-05
Exch bone volume to bone surface	1.73E-02
Exch bone vol to nonexch bone volume	5.78E-03

[a]RBC = red blood cells, exch = exchangeable, nonexch = nonexchangeable

Neptunium

Data on the biological behavior of neptunium were reviewed in ICRP Publication 56 (ICRP 1989). The systemic biokinetics of neptunium is reasonably well understood, particularly over the first few weeks after intake. The division of neptunium among excretion pathways, skeleton, liver, kidney, other soft tissues, and excretion is known reasonably well from combined data on human subjects, non-human primates, swine, and rodents. It appears that roughly half of absorbed neptunium is deposited in the skeleton, less than 10% is deposited in the liver, roughly 5% is deposited in kidneys and other soft tissues, and the rest is excreted within a few days, mainly in urine. Like other transuranic elements, neptunium is deposited on bone surfaces, and formation of aggregates in bone marrow following bone remodeling is evident. Information on removal half-times from specific compartments, particularly soft-tissue compartments, is weaker than information on the initial distribution of neptunium in the body and its rate of excretion. Long-term retention of neptunium in the liver must be based on animal data, together with comparative autopsy data on [237]Np and [239]Pu in environmentally exposed humans.

The structure of the ICRP's systemic biokinetic model for neptunium (ICRP 1993) is the generic structure for bone-surface-seeking radionuclides shown in Figure B-4. Parameter values of the model are listed in Table B-9.

Low variant: This is a modification of the ICRP's model for neptunium. Transfer coefficients describing outflow from blood (representing deposition fractions) are left unchanged. Removal half-times from bone and soft-tissue compartments other than liver are divided by 2. The removal half-time from the long-term retention compartment of liver is reduced from 1 y to 0.5 y. Independent kinetics of chain members is assumed.

High variant: This is a modification of the ICRP's model for neptunium. Transfer coefficients representing deposition fractions are left unchanged. Removal half-times from bone and soft-tissue compartments other than the long-term retention compartment of liver are multiplied by 2. The removal half-time from the long-term retention compartment of liver is increased from 1 y to 5 y. Radioactive progeny are assigned the biokinetics of neptunium.

Table B-9. Transfer coefficients (d^{-1}) in the ICRP's model for neptunium.[a]

Path of movement	Transfer coefficient (d^{-1})
Blood to liver 1	0.194
Blood to cortical bone surface	0.393
Blood to trabecular bone surface	0.4804
Blood to urinary bladder contents	0.6211
Blood to urinary path	0.0291
Blood to other kidney tissue	0.0097
Blood to upper large intestine contents	0.01359
Blood to testes	0.00068
Blood to ovaries	0.00021
Blood to ST0	0.832
Blood to ST1	0.1611
Blood to ST2	0.0388
ST0 to blood	0.693
Urinary path to urinary bladder contents	0.0495
Other kidney tissue to blood	0.00139
ST1 to blood	0.00693
ST2 to blood	0.000019
Trabecular bone surface to volume	0.000247
Trabecular bone surface to bone marrow	0.000493
Cortical bone surface to volume	0.0000411
Cortical bone surface to bone marrow	0.0000821
Trabecular bone volume to bone marrow	0.000493
Cortical bone volume to bone marrow	0.0000821
Bone marrow to blood	0.0076
Liver 1 to liver 2	0.00177
Liver 1 to small intestine contents	0.000133
Liver 2 to blood	0.0019
Testes or ovaries to blood	0.00019

Plutonium

The systemic biokinetics of plutonium has been investigated extensively in controlled studies on human subjects, follow-up studies of acutely or chronically exposed workers, and numerous studies of the fate of inhaled, ingested, or injected plutonium in different animal species (ICRP 1993, Leggett 2003, 2005). It is well established that absorbed or intravenously injected plutonium is tenaciously retained in the body and that most of the systemic burden is sequestered in skeleton and liver at all times after exposure. The division of activity between the liver and skeleton shows considerable variability from one plutonium worker to another. It appears that, on average, the liver contains more plutonium than the skeleton in the early months or years after intake but the skeleton contains more than the liver at times remote from intake. The qualitative behavior of plutonium after deposition on bone surfaces (gradual burial in bone volume or removal to bone marrow or plasma) is understood from observations of plutonium and related elements in laboratory animals and man. However, the rates of removal of plutonium from bone surfaces and burial in bone volume are not well established and are important sources of uncertainty in estimates of cumulative activity of plutonium isotopes on bone surface. Predictions of uptake and retention of plutonium by the gonads are based largely on animal data. The rate of urinary excretion of plutonium as a function of time after uptake to blood is now reasonably well established, and there is information on the time-dependent urinary-to-fecal excretion ratio.

The structure of the ICRP's systemic biokinetic model for plutonium (ICRP 1993) is the generic structure for bone-surface-seeking radionuclides shown in Figure B-4. Parameter values of the model are listed in Table B-10.

Low variant: The low variant is a modification of the ICRP's current model for plutonium (ICRP 1993). All transfer coefficients from blood to other compartments are the same as in the ICRP's model; i.e., the removal half-time from blood remains at 0.75 d, and none of the deposition fractions are changed. However, removal half-times from all bone and soft tissue compartments are 0.5 times the ICRP's value; i.e., all transfer coefficients for bone and soft-tissue compartments are doubled.

High variant: The high variant is also a modification of the ICRP's current model for plutonium (ICRP 1993). The removal half-time from blood is 0.75 d. The circulation includes the rapid-turnover soft-tissue compartment ST0, which is assumed to receive 30% of activity leaving blood. The term "activity leaving the circulation" refers to activity leaving blood but not entering ST0. Of activity leaving the circulation, 50% is assigned to liver, 10% to cortical bone surface, and 20% to trabecular bone surface; the deposition fractions for other compartments are the same as in the ICRP's current model. All rates of transfer of material out of skeletal compartments or soft tissue compartments ST0, ST1, and ST2 are 0.5 times the ICRP's values; i.e., the removal half-times are doubled. The removal half-times from liver compartments are 1.5 times the ICRP's values. All other transfer coefficients in the high variant model are the same as in the ICRP's model.

Table B-10. Transfer coefficients (d^{-1}) in the ICRP's model for plutonium.[a]

Path of movement	Transfer coefficient (d^{-1})
Blood to liver 1	0.1941
Blood to cortical bone surface	0.1294
Blood to trabecular bone surface	0.1941
Blood to urinary bladder contents	0.0129
Blood to urinary path	0.00647
Blood to other kidney tissue	0.00323
Blood to upper large intestine contents	0.0129
Blood to testes	0.00023
Blood to ovaries	0.000071
Blood to ST0	0.2773
Blood to ST1	0.0806
Blood to ST2	0.0129
ST0 to blood	0.693
Urinary path to urinary bladder contents	0.01386
Other kidney tissue to blood	0.00139
ST1 to blood	0.000475
ST1 to urinary bladder contents	0.000475
ST2 to blood	0.000019
Trabecular bone surface to volume	0.000247
Trabecular bone surface to bone marrow	0.000493
Cortical bone surface to volume	0.0000411
Cortical bone surface to bone marrow	0.0000821
Trabecular bone volume to bone marrow	0.000493
Cortical bone volume to bone marrow	0.0000821
Bone marrow to blood	0.0076
Liver 1 to liver 2	0.00177
Liver 1 to small intestine contents	0.000133
Liver 2 to blood	0.000211
Testes or ovaries to blood	0.00019

Americium

There is a fairly large body of information on the biokinetics of americium in human subjects, including *in vivo* measurements, excretion data, and autopsy data on workers (Leggett 1992b, ICRP 1993). Additionally, there have been several studies of the distribution and excretion of americium injected into beagles, non-human primates, and other laboratory animals, and there have been controlled studies of the biokinetics of the similarly behaving elements, curium and plutonium, in humans as well as laboratory animals (Leggett 1992b, ICRP 1993). Compared with plutonium, however, there is considerably less information with which to check model predictions of time-dependent urinary excretion.

The structure of the ICRP's systemic biokinetic model for americium (ICRP 1993) is the generic structure for bone-surface-seeking radionuclides shown in Figure B-4. Parameter values of the model are listed in Table B-11.

Table B-11. Transfer coefficients (d^{-1}) in the ICRP's model for americium.[a]

Path of movement	Transfer coefficient (d^{-1})
Blood to liver 1	11.6
Blood to cortical bone surface	3.49
Blood to trabecular bone surface	3.49
Blood to urinary bladder contents	1.63
Blood to urinary path	0.466
Blood to other kidney tissue	0.116
Blood to upper large intestine contents	0.303
Blood to testes	0.0082
Blood to ovaries	0.0026
Blood to ST0	10.0
Blood to ST1	1.67
Blood to ST2	0.466
ST0 to blood	1.386
Urinary path to urinary bladder contents	0.099
Other kidney tissue to blood	0.00139
ST1 to blood	0.0139
ST2 to blood	0.000019
Trabecular bone surface to volume	0.000247
Trabecular bone surface to bone marrow	0.000493
Cortical bone surface to volume	0.0000411
Cortical bone surface to bone marrow	0.0000821
Trabecular bone volume to bone marrow	0.000493
Cortical bone volume to bone marrow	0.0000821
Bone marrow to blood	0.0076
Liver 1 to small intestine contents	0.000049
Liver 1 to blood	0.00185
Testes or ovaries to blood	0.00019

Low variant: This is a modification of the ICRP's current model for americium (ICRP 1993). Transfer coefficients describing outflow from blood, or deposition fractions, are the same as in the ICRP's model, except that deposition in urinary bladder contents is increased from 7% to 10% and deposition in the intermediate-term soft-tissue compartment, ST1, is decreased by 3% to achieve mass balance. Removal half-times from all bone and soft tissue compartments are 0.5 times the ICRP's value; i.e., all transfer coefficients for bone and soft-tissue compartments are doubled.

High variant: This is a modification of the ICRP's current model for americium (ICRP 1993). Transfer coefficients describing outflow from blood, or deposition fractions, are the same as in the ICRP's model, except that deposition in urinary bladder contents is decreased from 7% to 4% and deposition in the intermediate-term soft-tissue compartment, ST1, is increased by 3% to achieve mass balance. Removal half-times from all bone and soft tissue compartments are 2 times the ICRP's value; i.e., all transfer coefficients for bone and soft-tissue compartments are halved.

Curium

Curium is a close physiological analogue of americium (ICRP 1995b). There are fewer worker data for curium than americium, but the retention and excretion of curium has been measured in a controlled study on human subjects. There have been several studies of the biokinetics of curium in laboratory animals, including baboons and dogs. Uncertainties in the biokinetics are similar for curium and americium.

The ICRP's systemic biokinetic for curium (ICRP 1995b) is identical to the model for americium described earlier.

Low variant: This is the same as the low variant for americium.

High variant: This is the same as the high variant for americium.

Other actinide elements

The following summary of information on the systemic biokinetics of the remaining actinide elements (atomic numbers 97-101) is taken from a recent review (Leggett 2001).

The behavior of californium has been studied in a number of different animal species, and there are limited observations on the fate of californium in accidentally exposed human subjects. Beagle studies provide relatively detailed information on the biokinetics of californium and also provide comparisons with other actinide elements, particularly americium. The behavior of californium appears to be broadly similar to that of americium, but californium may have higher deposition in bone, lower deposition in liver, and somewhat faster losses in urine and feces than americium.

There is information on the biokinetics of actinium and protactinium in laboratory animals and limited observations on human subjects. Data on laboratory animals suggest that the behavior of actinium is broadly similar to that of americium, and the behavior of protactinium is broadly similar to that of thorium. External measurements as well as bioassay measurements on workers accidentally exposed to isotopes of actinium and protactinium also provide some support for these assumptions.

The biokinetics of einsteinium has been studied in mice, miniature swine, and beagles. Comparative data for americium, californium, and einsteinium indicate that skeletal deposition increases in the order americium < californium < einsteinium. The initial urinary excretion rate appears to be much greater, and the initial fecal excretion rate much lower, for einsteinium than for californium or americium.

The biokinetics of berkelium has been studied in rats and beagles and to a limited extent in accidentally exposed human subjects. Comparative data for berkelium and einsteinium indicate that these elements have broadly similar biokinetics, but berkelium has a lower rate of urinary

excretion, lower deposition in the skeleton, greater deposition in the liver, and perhaps greater deposition in the kidneys than einsteinium.

No useful biokinetic data on fermium or mendelevium were found. Biokinetic models for these elements must be developed by analogy with other actinide elements. A reasonable assumption may be that their biokinetics is the same as that of einsteinium, the nearest element in the periodic chart for which data are available.

The ICRP's biokinetic model for actinium and protactinium are inconsistent with current information and were not used in Federal Guidance Report No. 13 (EPA 1999) or in the present report. In both reports, the models described earlier for americium and thorium were applied to actinium and protoactinium, respectively. For isotopes of both elements, independent kinetics of radioactive progeny was assigned.

The ICRP applies a common biokinetic model to berkelium, californium, einsteinium, fermium, and mendelevium (ICRP 1988, 1994b). According to that model, activity leaves blood with a half-time of 0.25 d, with 65% going to bone, 25% to liver, 0.011% to ovaries, 0.035% to testes, and 9.954% to excretion pathways (urinary bladder contents and upper large intestine contents). The removal half-time from bone and liver to excretion pathways is 50 y and 20 y, respectively. Permanent retention in ovaries and testes is assumed. A urinary to fecal excretion ratio of 1:1 is assigned. Isotopes of all of these elements are assumed to be uniformly distributed on bone surfaces.

Low variant for actinium: This is the ICRP's model for neptunium, with independent kinetics of chain members. The assumed behavior of daughters is as described in ICRP Publication 69 (1995a) for thorium chains.

High variant for actinium: This is the same as the high variant model for plutonium, with chain members having the biokinetics of the parent.

Low variant for protactinium. This is the model for neptunium, with independent kinetics of chain members. The assumed behavior of daughters is as described in ICRP Publication 69 (1995a) for thorium chains.

High variant for protactinium. This is the same as the high variant model for thorium, but with chain members assigned the biokinetics of the parent.

Low variant for berkelium, californium, einsteinium: Activity leaves blood with a half-time of 1.0 d. Of activity leaving blood, 20% goes to cortical surfaces, 20% to trabecular surfaces, 20% to liver, 30% to excretion pathways, and the rest to Other. The following removal half-times to excretion pathways are assumed: 5 y for liver and other; 20 y for cortical surface; and 5 y for

trabecular surface. A urinary to fecal excretion ratio of 1:1 is assigned. Chain members produced in the body are assigned the biokinetics of the parent.

High variant for berkelium, californium, einsteinium: Activity leaves blood with a half-time of 0.25 d. Of activity leaving blood, 20% goes to cortical surfaces, 20% to trabecular surfaces, 2% to red marrow, 40% to liver, 3% to kidneys, 0.05% to testes, 0.02% to ovaries, 5% to excretion pathways, and the rest to Other.. The following removal half-times to excretion pathways are assumed: 50 y for liver, trabecular surface, red marrow, and other; 200 y for cortical surface; 1 y for kidneys; 100 y for gonads. A urinary to fecal excretion ratio of 1:1 is assigned. Chain members produced in the body are assigned the biokinetics of the parent.

Low variant for fermium and mendelevium: Activity leaves blood with a half-time of 1.0 d. Of activity leaving blood, 25% goes to cortical surfaces, 25% to trabecular surfaces, 10% to liver, 30% to excretion pathways, and 10% to Other. The following removal half-times to excretion pathways are assumed: 2 y for liver and other; 20 y for cortical surface; and 5 y for trabecular surface. A urinary to fecal excretion ratio of 1:1 is assigned. Chain members produced in the body are assigned the biokinetics of the parent.

High variant for fermium and mendelevium: Activity leaves blood with a half-time of 0.25 d. Of activity leaving blood, 20% goes to cortical surfaces, 20% to trabecular surfaces, 2% to red marrow, 40% to liver, 3% to kidneys, 0.05% to testes, 0.02% to ovaries, 5% to excretion pathways, and 9.93% to Other. The following removal half-times to excretion pathways are assumed: 50 y for liver, trabecular surface, red marrow, and other; 200 y for cortical surface; 1 y for kidneys; 100 y for gonads.   A urinary to fecal excretion ratio of 1:1 is assigned. Chain members produced in the body are assigned the biokinetics of the parent.

APPENDIX C: UNCERTAINTIES ASSIGNED TO
GASTROINTESTINAL UPTAKE OF ELEMENTS

The uncertainty in fractional uptake from the gastrointestinal tract to blood (f_1 value) varies considerably from one element to another. In a relative sense (that is, when expressed as a multiple of the ICRP's value), uncertainties in the f_1 values are smallest for elements that are known to be nearly completely absorbed, including hydrogen, carbon, sodium, chlorine, potassium, bromine, rubidium, molybdenum, iodine, cesium, thallium, fluorine, sulfur, and germanium. Average uptake from the gastrointestinal tract is also reasonably well established for several frequently studied elements whose absorption is incomplete but represents at least a few percent of intake, such as copper, zinc, magnesium, technetium, arsenic, calcium, strontium, barium, radium, lead, iron, manganese, cobalt, and uranium. Relative uncertainties generally are greater for the remaining elements, usually because there is little direct information on man, there are substantial inconsistencies in reported absorption fractions, and/or absorption is too low to be determined with much precision under most conditions. Absorption of a few poorly absorbed elements such as thorium, plutonium, americium, and curium has been studied under controlled conditions in human subjects, and average uptake in the adult appears to be better established for these elements than for most poorly absorbed elements. Relative uncertainties may be greatest for several elements whose absorption has not been studied in man but for which animal data or other evidence indicates absorption on the order of at most a few hundredths of a percent.

The authors' assessments of the uncertainties in f_1 values for ingested radionuclides are summarized in Table C-1. As a first step in the derivation of a range of dose estimates for ingestion or inhalation of a radionuclide, three equally likely f_1 values were considered: the ICRP's value, a "low variant", and a "high variant".   In most cases, the lower end of the "most likely" range indicated in Table C-1 was taken as the low variant, and the higher end of that range was taken as the high variant. Thus, the three values usually had the relation low variant < ICRP value < high variant, as the names might suggest. However, in cases where the ICRP's value for an element was at least as great as the upper end of the most likely range, the high variant was selected as a central value from the range of most likely values. In such cases, the three values had the order low variant < high variant < ICRP value.

For each element, a continuous distribution of possible f_1 values was assigned in the form of a trapezoid with the base representing the assumed range of possible values and the plateau (top, flat portion) representing the most likely range of values. Thus, a trapezoidal distribution of possible f_1 values was defined by four numbers, $a < b < c < d$, where a and d represent the lowest and highest plausible values, respectively, and the interval from b to c represents the most likely range with all values in that range considered equally likely. The element-specific values a, b, c, and d were taken from Table C-1. For a given element, "Low" and "High" values in Table C-1 were used as the endpoints a and b, respectively, of the base of the trapezoid; the endpoints of the "Most Likely" interval indicated in Table C-1 were used as the endpoints b and c,

respectively, of the plateau; and the height of the trapezoid is calculated as the value that gives a trapezoidal area of 1.0.

The ICRP's values listed in Table C-1 are for ingestion rather than inhalation of radionuclides. For some elements, the ICRP uses a lower f_1 value for activity moving from the lungs to the gastrointestinal tract after inhalation of relatively insoluble forms (Type M or Type S). For inhalation, the low and high variants were the same as those used for ingestion of radionuclides, and the low variant was sometimes greater than the ICRP value.

Table C-1. Uncertainties in f_1 values.

Element	Gastrointestinal absorption fraction				Comments
	ICRP	Low	Most likely	High	
H, C, Na, Cl, K, Br, Rb, Mo, I, Cs, Tl	1.0	0.7	0.8-1.0	1.0	Evidence of nearly complete absorption.
F, S, Ge	1.0	0.5	0.6-0.9	1.0	Evidence of high absorption, but often substantially less than 100%.
At, Fr	1.0	0.2	0.6-0.9	1.0	f_1 based on chemical analogy.
Hg (methyl)	1.0	0.5	0.6-1.0	1.0	Nearly complete absorption observed in man and other primates.
P, Se	0.8	0.5	0.6-0.9	1.0	Absorption nearly complete but may be reduced by some dietary constituents.
Re	0.8	0.1	0.4-0.8	1.0	f_1 based on chemical similarity to Tc; f_1 for Tc later reduced from 0.8 to 0.5 but Re was not revisited.
Cu	0.5	0.3	0.4-0.7	0.9	Reasonably consistent human data.
Zn	0.5	0.2	0.3-0.5	0.6	Reasonably consistent human data.
Mg	0.5	0.2	0.3-0.6	0.7	Absorption apparently depends strongly on level of Mg in diet.
Tc	0.5	0.3	0.4-0.8	1.0	Human and animal data; central estimate complicated by high variability.
Po	0.5	0.05	0.2-0.8	0.95	Absorption apparently depends strongly on ingested material.
As	0.5	0.2	0.4-0.9	1.0	Animal data plus limited human data give wide range of values.
Hg (organic, other than methyl)	0.4	0.1	0.2-0.6	0.8	Some data on man.
Ca	0.3	0.25	0.3-0.4	0.5	Much data on human subjects.
Sr	0.3	0.1	0.15-0.3	0.4	Reasonably consistent human data from controlled and environmental studies.
Te	0.3	0.1	0.2-0.4	0.6	Broadly consistent data for several non-human species.

Table C-1 (continued)

Element	Gastrointestinal absorption fraction				Comments
	ICRP	Low	Most likely	High	
W	0.3	0.1	0.2-0.5	0.7	Data for several non-human species, plus balance data for humans.
Ra	0.2	0.1	0.15-0.25	0.3	Reasonably consistent data for man, but no definitive studies.
Ba	0.2	0.08	0.1-0.2	0.4	Human data highly variable but suggestabsorption similar to Ra and Sr.
Pb	0.2	0.08	0.1-0.2	0.3	Plentiful but variable human data.
Fe	0.1	0.04	0.06-0.15	0.2	Much human data. Absorption depends on gender, type of food ingested, and other factors.
Mn	0.1	0.01	0.05-0.15	0.2	Based on variable results of human and animal studies.
Co	0.1	0.02	0.05-0.2	0.3	Based on data for humans. Absorption varies substantially with ingested form.
Au	0.1	0.02	0.05-0.15	0.3	Limited human and animal data.
Sb	0.1	0.002	0.01-0.1	0.2	Based on highly variable animal data.
Cr (hexavalent)	0.1	0.02	0.05-0.15	0.25	Data for humans and rats.
Ni	0.05	0.005	0.01-0.03	0.06	Reasonably consistent human data.
Ru	0.05	0.001	0.005-0.07	0.15	Data for several animal species and one human subject.
Cd	0.05	0.005	0.01-0.05	0.3	Animal and human data.
Ag	0.05	0.01	0.005-0.01	0.1	Animal data.
Bi	0.05	0.001	0.005-0.05	0.1	Semi-quantitative data for humans.
Rh	0.05	0.0005	0.005-0.07	0.3	Analogy with Ru.
Al	0.01	0.0001	0.001-0.01	0.02	Based largely on animal data.
V	0.01	0.0001	0.001-0.01	0.15	Data for humans and animals indicate low but variable absorption.
Zr	0.01	0.0001	0.0005-0.005	0.01	Based on rat data.
Si	0.01	0.001	0.005-0.5	0.6	Data for various non-human species. Possibility of elevated absorption suggested by limited data on man.
Ti	0.01	0.001	0.005-0.03	0.05	Based mainly on data for sheep and semi-quantitative information on man.

Table C-1 (continued)

Element	Gastrointestinal absorption fraction				Comments
	ICRP	Low	Most likely	High	
Nb	0.01	0.0001	0.005-0.02	0.05	Data for various non-human species.
Ir	0.01	0.0001	0.005-0.02	0.05	Data for various non-human species.
Pt	0.01	0.00005	0.005-0.02	0.1	Based on data for rats.
Os	0.01	0.00002	0.005-0.02	0.2	Based on chemical analogy with Ir.
In	0.02	0.001	0.01-0.05	0.2	Based on limited data on rats.
Sn	0.02	0.005	0.01-0.05	0.1	Based on data for non-human species.
U	0.02	0.003	0.01-0.02	0.04	No definitive studies, but much human and animal data.
Hg (inorganic)	0.02	0.001	0.01-0.05	0.2	Data for laboratory animals and human subjects.
Cr (trivalent)	0.01	0.002	0.005-0.03	0.05	Data for humans and rats.
Be	0.005	0.001	0.003-0.01	0.1	Data for several non-human species. Relatively high absorption in monkeys.
Pd	0.005	0.0005	0.002-0.01	0.1	Based on limited data on rats.
Hf	0.002	0.0001	0.0005-0.005	0.01	f_1 originally based on analogy with Zr. Broadly consistent data now available for Hf in rodents.
Ga	0.001	0.00001	0.0001-0.005	0.05	Semi-quantiative data for rats.
Ta	0.001	0.0001	0.0005-0.01	0.05	Based on limited data on rats.
Th, Np, Pu, Am, Cm, Nd	0.0005	0.00005	0.0001-0.001	0.003	Based on human and animal data.
Pm	0.0001	0.00001	0.0001-0.001	0.003	Mainly animal data. Limited human data indicate extremely low absorption.
La, Ce, Pa, Eu, Es, Cf, Bk, Lu, Pr, Yb, Tb, Ho	0.0005	0.00001	0.0001-0.001	0.003	Based on animal data.
Sm, Gd, Dy, Er, Tm, Fm, Md, Ac	0.0005	0.00001	0.0001-0.001	0.005	Little or no quantitative information. Based mainly on chemical analogy.
Y	0.0001	0.00001	0.0001-0.001	0.01	Based on largely semi-quantitative information from animal studies.
Sc	0.0001	0.00001	0.0001-0.001	0.01	Based on chemical similarity to Y.

APPENDIX D. UNCERTAINTIES IN MORTALITY RISK COEFFICIENTS FOR INGESTION AND INHALATION INTAKES OF RADIONUCLIDES

Judgments concerning the minimal uncertainty in the mortality risk coefficient are tabulated by nuclide in terms of relative broad, semi-quantitative "uncertainty categories" identified by letters *A-E*. Category A represents the most narrowly determined risk coefficients, Category E represents the least well characterized coefficients, and Categories B, C, and D represent intermediate, declining levels of precision. The categories are related to the intervals specified by the sample quantile of values derived through Monte Carlo simulation. The ratio, Q_{95}/Q_5, where Q_5 and Q_{95} are the 5% and 95% sample quantile of the risk coefficient, respectively, are used to assign the coefficient to one of the five categories *A-E* as indicated below.

Definition of Uncertainty Categories

Uncertainty category	Definition
A	$Q_{95}/Q_5 < 15$
B	$15 \leq Q_{95}/Q_5 < 35$
C	$35 \leq Q_{95}/Q_5 < 50$
D	$50 \leq Q_{95}/Q_5 < 150$
E	$Q_{95}/Q_5 \geq 150$

Uncertainties in the risk coefficient for ingestion intakes are given in Table D.1. For 110 radionuclides the uncertainties were judged to be difficult to quantify and their assigned category is further marked by a plus sign; e.g., see V-49. The dominant source of uncertainty, if any, is indicated in the tables. The last column of the table lists as high those radionuclides for which the uncertainties are sensitive to the specific energy (*SE*) formulation. With only one exception, uncertainties with "high" *SE* variation were assigned to categories *D* and *E*.

Table D.2 gives the uncertainties in the risk coefficient for inhalation intakes. The various particulate forms (Type F, M and S) are addresses as well as vapor and other forms where applicable. The dominant source of uncertainty and the sensitive to the specific energy (SE) formulation are listed in the table.

Table D-1. Uncertainty categories for risk coefficients for ingestion.

Nuclide	Category	Nuclide	Category	Nuclide	Category
H-3 (HTO)	A	Fe-55	A	As-76	B
H-3 (OBT)	B	Fe-59	A	As-77	B
Be-7	A	Fe-60	C	As-78	B
Be-10	B	Co-55	A	Se-70	B
C-11	B	Co-56	A	Se-73	A
C-14	B	Co-57	A	Se-73m	A
F-18	A	Co-58	A	Se-75	A
Na-22	A	Co-58m	C	Se-79	B
Na-24	A	Co-60	B	Se-81	C
Mg-28	A	Co-60m	D	Se-81m	B
Al-26	A	Co-61	B	Se-83	B
Si-31	B	Co-62m	B	Br-74	B
Si-32	E	Ni-56	A	Br-74m	B
P-32	A	Ni-57	A	Br-75	B
P-33	A	Ni-59	C	Br-76	A
S-35	B	Ni-63	C	Br-77	A
S-35	A	Ni-65	B	Br-80	C
Cl-36	B	Ni-66	B	Br-80m	A
Cl-38	B	Cu-60	B	Br-82	A
Cl-39	B	Cu-61	A	Br-83	B
K-40	A	Cu-64	B	Br-84	B
K-42	A	Cu-67	B	Rb-79	B
K-43	A	Zn-62	A	Rb-81	A
K-44	B	Zn-63	B	Rb-81m	A
K-45	B	Zn-65	A	Rb-82m	A
Ca-41	A	Zn-69	B	Rb-83	A
Ca-45	A	Zn-69m	B	Rb-84	A
Ca-47	A	Zn-71m	A	Rb-86	A
Sc-43	B	Zn-72	A	Rb-87	A
Sc-44	A	Ga-65	B	Rb-88	C
Sc-44m	B	Ga-66	B	Rb-89	B
Sc-46	A	Ga-67	B	Sr-80	B
Sc-47	B	Ga-68	B	Sr-81	B
Sc-48	A	Ga-70	C	Sr-82	A
Sc-49	B	Ga-72	B	Sr-83	A
Ti-44	C	Ga-73	B	Sr-85	A
Ti-45	B	Ge-66	A	Sr-85m	A
V-47	B	Ge-67	B	Sr-87m	A
V-48	A	Ge-68	C	Sr-89	A
V-49	D	Ge-69	A	Sr-90	A
Cr-48	A	Ge-71	C	Sr-91	B
Cr-49	B	Ge-75	B	Sr-92	B
Cr-51	B	Ge-77	A	Y-86	A
Mn-51	B	Ge-78	A	Y-86m	A
Mn-52	A	As-69	B	Y-87	B
Mn-52m	B	As-70	B	Y-88	A
Mn-53	C	As-71	A	Y-90	B
Mn-54	A	As-72	A	Y-90m	B
Mn-56	B	As-73	B	Y-91	B
Fe-52	A	As-74	A	Y-91m	A

Nuclide	Category	Nuclide	Category	Nuclide	Category
Y-92	B	Rh-101m	A	Sn-117m	C
Y-93	B	Rh-102	C	Sn-119m	C
Y-94	B	Rh-102m	B	Sn-121	C
Y-95	C	Rh-103m	E	Sn-121m	B
Zr-86	A	Rh-105	B	Sn-123	B
Zr-88	A	Rh-106	C	Sn-123m	B
Zr-89	A	Rh-106m	A	Sn-125	B
Zr-93	C	Rh-107	B	Sn-126	B
Zr-95	B	Pd-100	A	Sn-127	B
Zr-97	B	Pd-101	B	Sn-128	B
Nb-88	B	Pd-103	D	Sb-115	B
Nb-89b	B	Pd-107	E	Sb-116	B
Nb-89a	B	Pd-109	B	Sb-116m	A
Nb-90	A	Ag-102	B	Sb-117	B
Nb-93m	D	Ag-103	B	Sb-118m	A
Nb-94	B	Ag-104	A	Sb-119	C
Nb-95	A	Ag-104m	B	Sb-120b	A
Nb-95m	C	Ag-105	A	Sb-120a	B
Nb-96	A	Ag-106	B	Sb-122	B
Nb-97	B	Ag-106m	A	Sb-124	A
Nb-98	B	Ag-108m	B	Sb-124n	B
Mo-90	A	Ag-110m	A	Sb-125	B
Mo-93	B	Ag-111	B	Sb-126	A
Mo-93m	A	Ag-112	B	Sb-126m	B
Mo-99	A	Ag-115	B	Sb-127	B
Mo-101	B	Cd-104	A	Sb-128b	A
Tc-93	A	Cd-107	C	Sb-128a	B
Tc-93m	A	Cd-109	B	Sb-129	B
Tc-94	A	Cd-113	C	Sb-130	B
Tc-94m	B	Cd-113m	C	Sb-131	B
Tc-95	A	Cd-115	B	Te-116	A
Tc-95m	A	Cd-115m	A	Te-121	A
Tc-96	A	Cd-117	B	Te-121m	C
Tc-96m	A	Cd-117m	A	Te-123	E
Tc-97	B	In-109	A	Te-123m	C
Tc-97m	B	In-110b	A	Te-125m	B
Tc-98	B	In-110a	B	Te-127	B
Tc-99	B	In-111	A	Te-127m	B
Tc-99m	A	In-112	B	Te-129	B
Tc-101	C	In-113m	B	Te-129m	B
Tc-104	B	In-114m	B	Te-131m	A
Ru-94	A	In-115	E	Te-131	B
Ru-97	A	In-115m	B	Te-132	A
Ru-103	B	In-116m	B	Te-133	B
Ru-105	B	In-117	B	Te-133m	B
Ru-106	B	In-117m	B	Te-134	B
Rh-99	A	In-119m	C	I-120	B
Rh-99m	A	Sn-110	A	I-120m	B
Rh-100	A	Sn-111	B	I-121	B
Rh-101	C	Sn-113	B	I-123	B

Nuclide	Category	Nuclide	Category	Nuclide	Category
I-124	C	Ce-141	C	Eu-152m	B
I-125	D	Ce-143	B	Eu-154	B
I-126	D	Ce-144	B	Eu-155	C
I-128	C	Pr-136	B	Eu-156	B
I-129	D	Pr-137	B	Eu-157	B
I-130	B	Pr-138m	A	Eu-158	B
I-131	C	Pr-139	B	Gd-145	B
I-132	B	Pr-142	B	Gd-146	B
I-132m	B	Pr-142m	B	Gd-147	A
I-133	C	Pr-143	B	Gd-148	E
I-134	B	Pr-144	C	Gd-149	B
I-135	B	Pr-145	B	Gd-151	C
Cs-125	B	Pr-147	B	Gd-152	E
Cs-127	A	Nd-136	B	Gd-153	B
Cs-129	A	Nd-138	B	Gd-159	B
Cs-130	B	Nd-139	B	Tb-147	A
Cs-131	A	Nd-139m	A	Tb-149	A
Cs-132	A	Nd-141	B	Tb-150	A
Cs-134	A	Nd-147	B	Tb-151	B
Cs-134m	B	Nd-149	B	Tb-153	B
Cs-135	A	Nd-151	B	Tb-154	A
Cs-135m	A	Pm-141	B	Tb-155	B
Cs-136	A	Pm-143	A	Tb-156	A
Cs-137	A	Pm-144	A	Tb-156m	B
Cs-138	B	Pm-145	B	Tb-156n	B
Ba-126	B	Pm-146	A	Tb-157	C
Ba-128	B	Pm-147	D	Tb-158	B
Ba-131	A	Pm-148	B	Tb-160	B
Ba-131m	C	Pm-148m	B	Tb-161	C
Ba-133	A	Pm-149	B	Dy-155	A
Ba-133m	B	Pm-150	B	Dy-157	A
Ba-135m	B	Pm-151	B	Dy-159	B
Ba-139	B	Sm-141	B	Dy-165	B
Ba-140	B	Sm-141m	B	Dy-166	B
Ba-141	B	Sm-142	B	Ho-155	B
Ba-142	B	Sm-145	B	Ho-157	B
La-131	B	Sm-146	E	Ho-159	B
La-132	A	Sm-147	E	Ho-161	B
La-135	B	Sm-151	D	Ho-162	B
La-137	B	Sm-153	B	Ho-162m	B
La-138	B	Sm-155	C	Ho-164	C
La-140	B	Sm-156	B	Ho-164m	B
La-141	B	Eu-145	A	Ho-166	B
La-142	B	Eu-146	A	Ho-166m	B
La-143	B	Eu-147	B	Ho-167	B
Ce-134	B	Eu-148	A	Er-161	A
Ce-135	B	Eu-149	B	Er-165	B
Ce-137	B	Eu-150b	B	Er-169	D
Ce-137m	C	Eu-150a	B	Er-171	B
Ce-139	B	Eu-152	A	Er-172	B

Nuclide	Category	Nuclide	Category	Nuclide	Category
Tm-162	B	Ta-180	B	Ir-192m	C
Tm-166	A	Ta-180m	B	Ir-194	B
Tm-167	C	Ta-182	B	Ir-194m	A
Tm-170	B	Ta-182m	C	Ir-195	B
Tm-171	D	Ta-183	C	Ir-195m	B
Tm-172	B	Ta-184	B	Pt-186	A
Tm-173	B	Ta-185	B	Pt-188	B
Tm-175	B	Ta-186	B	Pt-189	B
Yb-162	B	W-176	A	Pt-191	B
Yb-166	B	W-177	A	Pt-193	D
Yb-167	B	W-178	B	Pt-193m	D
Yb-169	C	W-179	B	Pt-195m	D
Yb-175	C	W-181	B	Pt-197	C
Yb-177	B	W-185	B	Pt-197m	B
Yb-178	B	W-187	B	Pt-199	B
Lu-169	A	W-188	B	Pt-200	B
Lu-170	A	Re-177	B	Au-193	B
Lu-171	B	Re-178	B	Au-194	A
Lu-172	B	Re-181	B	Au-195	C
Lu-173	B	Re-182b	B	Au-198	B
Lu-174m	D	Re-182a	A	Au-198m	B
Lu-174	B	Re-184	B	Au-199	C
Lu-176	B	Re-184m	C	Au-200	B
Lu-176m	B	Re-186	B	Au-200m	B
Lu-177	C	Re-186m	D	Au-201	C
Lu-177m	B	Re-187	D	Hg-193	B
Lu-178	B	Re-188	B	Hg-193m	B
Lu-178m	B	Re-188m	B	Hg-194	C
Lu-179	B	Re-189	B	Hg-195	B
Hf-170	B	Os-180	B	Hg-195m	C
Hf-172	B	Os-181	A	Hg-197	C
Hf-173	B	Os-182	B	Hg-197m	C
Hf-175	B	Os-185	B	Hg-199m	B
Hf-177m	B	Os-189m	E	Hg-203	B
Hf-178m	B	Os-191	D	Hg-193	B
Hf-179m	B	Os-191m	D	Hg-193m	A
Hf-180m	B	Os-193	B	Hg-194	B
Hf-181	B	Os-194	C	Hg-195	A
Hf-182	C	Ir-182	B	Hg-195m	A
Hf-182m	B	Ir-184	A	Hg-197	A
Hf-183	B	Ir-185	B	Hg-197m	A
Hf-184	B	Ir-186a	A	Hg-199m	B
Ta-172	B	Ir-186b	A	Hg-203	A
Ta-173	B	Ir-187	B	Hg-193	B
Ta-174	B	Ir-188	A	Hg-193m	B
Ta-175	A	Ir-189	C	Hg-194	C
Ta-176	A	Ir-190	B	Hg-195	B
Ta-177	B	Ir-190n	A	Hg-195m	B
Ta-178b	B	Ir-190m	B	Hg-197	B
Ta-179	B	Ir-192	B	Hg-197m	B

Nuclide	Category	Nuclide	Category	Nuclide	Category
Hg-199m	B	Ra-226	C	Pu-240	D
Hg-203	A	Ra-227	B	Pu-241	D
Tl-194	A	Ra-228	C	Pu-242	D
Tl-194m	B	Ac-224	D	Pu-243	B
Tl-195	A	Ac-225	C	Pu-244	D
Tl-197	A	Ac-226	D	Pu-245	B
Tl-198	A	Ac-227	E	Pu-246	B
Tl-198m	A	Ac-228	B	Am-237	B
Tl-199	A	Th-226	E	Am-238	A
Tl-200	A	Th-227	C	Am-239	C
Tl-201	A	Th-228	D	Am-240	B
Tl-202	A	Th-229	D	Am-241	D
Tl-204	A	Th-230	D	Am-242	B
Pb-195m	B	Th-231	D	Am-242m	D
Pb-198	A	Th-232	D	Am-243	D
Pb-199	A	Th-234	B	Am-244	B
Pb-200	A	Pa-227	E	Am-244m	C
Pb-201	A	Pa-228	B	Am-245	B
Pb-202	A	Pa-230	B	Am-246	B
Pb-202m	A	Pa-231	E	Am-246m	B
Pb-203	B	Pa-232	B	Cm-238	B
Pb-205	B	Pa-233	C	Cm-240	D
Pb-209	B	Pa-234	B	Cm-241	B
Pb-210	C	U-230	D	Cm-242	D
Pb-211	B	U-231	C	Cm-243	D
Pb-212	B	U-232	B	Cm-244	D
Pb-214	B	U-233	C	Cm-245	D
Bi-200	A	U-234	C	Cm-246	D
Bi-201	A	U-235	C	Cm-247	D
Bi-202	A	U-236	C	Cm-248	D
Bi-203	A	U-237	C	Cm-249	B
Bi-205	A	U-238	B	Cm-250	D
Bi-206	A	U-239	B	Bk-245	C
Bi-207	A	U-240	B	Bk-246	A
Bi-210	B	Np-232	B	Bk-247	E
Bi-210m	B	Np-233	B	Bk-249	D
Bi-212	B	Np-234	A	Bk-250	B
Bi-213	C	Np-235	C	Cf-244	E
Bi-214	C	Np-236a	D	Cf-246	E
Po-203	A	Np-236b	B	Cf-248	D
Po-205	A	Np-237	D	Cf-249	E
Po-207	A	Np-238	B	Cf-250	D
Po-210	C	Np-239	C	Cf-251	D
At-207	A	Np-240	B	Cf-252	D
At-211	B	Pu-234	B	Cf-253	D
Fr-222	E	Pu-235	B	Cf-254	E
Fr-223	D	Pu-236	D	Es-250	A
Ra-223	C	Pu-237	B	Es-251	C
Ra-224	B	Pu-238	D	Es-253	E
Ra-225	C	Pu-239	D	Es-254	D

Nuclide	Category	Nuclide	Category	Nuclide	Category
Es-254m	D	Fm-254	E	Md-257	C
Fm-252	E	Fm-255	E	Md-258	D
Fm-253	D	Fm-257	D		

Table D-1 (Continued)

Table D-2. Uncertainty categories for risk coefficients for inhalation.

Nuclide	Type	Category	Nuclide	Type	Category	Nuclide	Type	Category
H-3	F	B	P-33	S	B	Sc-46	F	A
H-3	M	C	S-35	F	E	Sc-46	M	B
H-3	S	B	S-35	M	B	Sc-46	S	A
H-3	V	A	S-35	S	B	Sc-47	F	C
H-3	G	B	S-35	V	D	Sc-47	M	B
H-3	G	B	S-35	V	A	Sc-47	S	B
Be-7	F	A	Cl-36	F	C	Sc-48	F	B
Be-7	M	A	Cl-36	M	C	Sc-48	M	A
Be-7	S	A	Cl-36	S	B	Sc-48	S	A
Be-10	F	B	Cl-38	F	B	Sc-49	F	B
Be-10	M	B	Cl-38	M	A	Sc-49	M	A
Be-10	S	B	Cl-38	S	A	Sc-49	S	A
C-11	F	B	Cl-39	F	B	Ti-44	F	C
C-11	M	A	Cl-39	M	A	Ti-44	M	B
C-11	S	A	Cl-39	S	A	Ti-44	S	B
C-14	F	D	K-40	F	B	Ti-45	F	B
C-14	M	B	K-40	M	C	Ti-45	M	A
C-14	S	B	K-40	S	B	Ti-45	S	A
C-11	G	A	K-42	F	B	V-47	F	B
C-14	G	C	K-42	M	A	V-47	M	A
C-11	G	A	K-42	S	A	V-47	S	A
C-14	G	B	K-43	F	C	V-48	F	B
F-18	F	B	K-43	M	A	V-48	M	A
F-18	M	A	K-43	S	A	V-48	S	A
F-18	S	A	K-44	F	B	V-49	F	B
Na-22	F	B	K-44	M	A	V-49	M	B
Na-22	M	B	K-44	S	A	V-49	S	B
Na-22	S	B	K-45	F	B	Cr-48	F	B
Na-24	F	B	K-45	M	A	Cr-48	M	A
Na-24	M	A	K-45	S	A	Cr-48	S	A
Na-24	S	A	Ca-41	F	B	Cr-49	F	B
Mg-28	F	B	Ca-41	M	B	Cr-49	M	A
Mg-28	M	A	Ca-41	S	B	Cr-49	S	A
Mg-28	S	A	Ca-45	F	B	Cr-51	F	A
Al-26	F	B	Ca-45	M	B	Cr-51	M	A
Al-26	M	B	Ca-45	S	B	Cr-51	S	A
Al-26	S	B	Ca-47	F	C	Mn-51	F	B
Si-31	F	B	Ca-47	M	A	Mn-51	M	A
Si-31	M	A	Ca-47	S	A	Mn-51	S	A
Si-31	S	A	Sc-43	F	B	Mn-52	F	A
Si-32	F	E	Sc-43	M	A	Mn-52	M	A
Si-32	M	D	Sc-43	S	A	Mn-52	S	A
Si-32	S	B	Sc-44	F	B	Mn-52m	F	B
P-32	F	C	Sc-44	M	A	Mn-52m	M	A
P-32	M	B	Sc-44	S	A	Mn-52m	S	A
P-32	S	B	Sc-44m	F	B	Mn-53	F	B
P-33	F	D	Sc-44m	M	A	Mn-53	M	C
P-33	M	B	Sc-44m	S	A	Mn-53	S	B

Nuclide	Type	Category	Nuclide	Type	Category	Nuclide	Type	Category
Mn-54	F	A	Ni-57	F	B	Zn-71m	F	B
Mn-54	M	B	Ni-57	M	A	Zn-71m	M	A
Mn-54	S	A	Ni-57	S	A	Zn-71m	S	A
Mn-56	F	B	Ni-59	F	C	Zn-72	F	B
Mn-56	M	A	Ni-59	M	B	Zn-72	M	A
Mn-56	S	A	Ni-59	S	B	Zn-72	S	A
Fe-52	F	B	Ni-63	F	C	Ga-65	F	B
Fe-52	M	A	Ni-63	M	B	Ga-65	M	A
Fe-52	S	A	Ni-63	S	B	Ga-65	S	A
Fe-55	F	A	Ni-65	F	B	Ga-66	F	B
Fe-55	M	A	Ni-65	M	A	Ga-66	M	A
Fe-55	S	B	Ni-65	S	A	Ga-66	S	A
Fe-59	F	A	Ni-66	F	C	Ga-67	F	C
Fe-59	M	B	Ni-66	M	A	Ga-67	M	B
Fe-59	S	A	Ni-66	S	A	Ga-67	S	B
Fe-60	F	C	Ni-56	V	A	Ga-68	F	B
Fe-60	M	B	Ni-57	V	B	Ga-68	M	A
Fe-60	S	B	Ni-59	V	C	Ga-68	S	A
Co-55	F	B	Ni-63	V	B	Ga-70	F	B
Co-55	M	A	Ni-65	V	B	Ga-70	M	A
Co-55	S	A	Ni-66	V	B	Ga-70	S	A
Co-56	F	A	Cu-60	F	B	Ga-72	F	B
Co-56	M	B	Cu-60	M	A	Ga-72	M	A
Co-56	S	A	Cu-60	S	A	Ga-72	S	A
Co-57	F	B	Cu-61	F	B	Ga-73	F	C
Co-57	M	B	Cu-61	M	A	Ga-73	M	A
Co-57	S	A	Cu-61	S	A	Ga-73	S	A
Co-58	F	B	Cu-64	F	C	Ge-66	F	B
Co-58	M	B	Cu-64	M	A	Ge-66	M	A
Co-58	S	A	Cu-64	S	A	Ge-66	S	A
Co-58m	F	B	Cu-67	F	D	Ge-67	F	B
Co-58m	M	B	Cu-67	M	B	Ge-67	M	A
Co-58m	S	A	Cu-67	S	B	Ge-67	S	A
Co-60	F	A	Zn-62	F	B	Ge-68	F	D
Co-60	M	B	Zn-62	M	A	Ge-68	M	C
Co-60	S	B	Zn-62	S	A	Ge-68	S	B
Co-60m	F	B	Zn-63	F	B	Ge-69	F	C
Co-60m	M	B	Zn-63	M	A	Ge-69	M	A
Co-60m	S	B	Zn-63	S	A	Ge-69	S	A
Co-61	F	B	Zn-65	F	A	Ge-71	F	C
Co-61	M	A	Zn-65	M	A	Ge-71	M	B
Co-61	S	A	Zn-65	S	A	Ge-71	S	B
Co-62m	F	B	Zn-69	F	B	Ge-75	F	B
Co-62m	M	A	Zn-69	M	A	Ge-75	M	A
Co-62m	S	A	Zn-69	S	A	Ge-75	S	A
Ni-56	F	B	Zn-69m	F	C	Ge-77	F	C
Ni-56	M	A	Zn-69m	M	A	Ge-77	M	A
Ni-56	S	A	Zn-69m	S	A	Ge-77	S	A

Nuclide	Type	Category	Nuclide	Type	Category	Nuclide	Type	Category
Ge-78	F	B	Se-81m	F	C	Rb-83	F	A
Ge-78	M	A	Se-81m	M	A	Rb-83	M	A
Ge-78	S	A	Se-81m	S	A	Rb-83	S	A
As-69	F	B	Se-83	F	B	Rb-84	F	A
As-69	M	A	Se-83	M	A	Rb-84	M	A
As-69	S	A	Se-83	S	A	Rb-84	S	A
As-70	F	B	Br-74	F	B	Rb-86	F	B
As-70	M	A	Br-74	M	A	Rb-86	M	B
As-70	S	A	Br-74	S	A	Rb-86	S	B
As-71	F	B	Br-74m	F	B	Rb-87	F	B
As-71	M	A	Br-74m	M	A	Rb-87	M	B
As-71	S	A	Br-74m	S	A	Rb-87	S	B
As-72	F	B	Br-75	F	B	Rb-88	F	B
As-72	M	A	Br-75	M	A	Rb-88	M	A
As-72	S	A	Br-75	S	A	Rb-88	S	A
As-73	F	D	Br-76	F	B	Rb-89	F	B
As-73	M	B	Br-76	M	A	Rb-89	M	A
As-73	S	B	Br-76	S	A	Rb-89	S	A
As-74	F	C	Br-77	F	B	Sr-80	F	B
As-74	M	B	Br-77	M	A	Sr-80	M	A
As-74	S	A	Br-77	S	A	Sr-80	S	A
As-76	F	B	Br-80	F	B	Sr-81	F	B
As-76	M	A	Br-80	M	A	Sr-81	M	A
As-76	S	A	Br-80	S	A	Sr-81	S	A
As-77	F	C	Br-80m	F	C	Sr-82	F	B
As-77	M	B	Br-80m	M	A	Sr-82	M	B
As-77	S	B	Br-80m	S	A	Sr-82	S	B
As-78	F	B	Br-82	F	B	Sr-83	F	B
As-78	M	A	Br-82	M	A	Sr-83	M	A
As-78	S	A	Br-82	S	A	Sr-83	S	A
Se-70	F	B	Br-83	F	C	Sr-85	F	A
Se-70	M	A	Br-83	M	A	Sr-85	M	B
Se-70	S	A	Br-83	S	A	Sr-85	S	A
Se-73	F	B	Br-84	F	B	Sr-85m	F	B
Se-73	M	A	Br-84	M	A	Sr-85m	M	A
Se-73	S	A	Br-84	S	A	Sr-85m	S	A
Se-73m	F	B	Rb-79	F	B	Sr-87m	F	B
Se-73m	M	A	Rb-79	M	A	Sr-87m	M	A
Se-73m	S	A	Rb-79	S	A	Sr-87m	S	A
Se-75	F	B	Rb-81	F	C	Sr-89	F	B
Se-75	M	B	Rb-81	M	A	Sr-89	M	B
Se-75	S	A	Rb-81	S	A	Sr-89	S	B
Se-79	F	B	Rb-81m	F	C	Sr-90	F	A
Se-79	M	B	Rb-81m	M	B	Sr-90	M	B
Se-79	S	B	Rb-81m	S	B	Sr-90	S	B
Se-81	F	B	Rb-82m	F	B	Sr-91	F	B
Se-81	M	A	Rb-82m	M	A	Sr-91	M	A
Se-81	S	A	Rb-82m	S	A	Sr-91	S	A

Nuclide	Type	Category	Nuclide	Type	Category	Nuclide	Type	Category
Sr-92	F	B	Zr-93	F	C	Mo-93m	F	B
Sr-92	M	A	Zr-93	M	B	Mo-93m	M	A
Sr-92	S	A	Zr-93	S	B	Mo-93m	S	A
Y-86	F	B	Zr-95	F	B	Mo-99	F	C
Y-86	M	A	Zr-95	M	B	Mo-99	M	A
Y-86	S	A	Zr-95	S	A	Mo-99	S	B
Y-86m	F	B	Zr-97	F	B	Mo-101	F	B
Y-86m	M	A	Zr-97	M	A	Mo-101	M	A
Y-86m	S	A	Zr-97	S	A	Mo-101	S	A
Y-87	F	B	Nb-88	F	B	Tc-93	F	A
Y-87	M	A	Nb-88	M	A	Tc-93	M	A
Y-87	S	A	Nb-88	S	A	Tc-93	S	A
Y-88	F	A	Nb-89b	F	B	Tc-93m	F	A
Y-88	M	A	Nb-89b	M	A	Tc-93m	M	A
Y-88	S	A	Nb-89b	S	A	Tc-93m	S	A
Y-90	F	B	Nb-89a	F	B	Tc-94	F	A
Y-90	M	A	Nb-89a	M	A	Tc-94	M	A
Y-90	S	A	Nb-89a	S	A	Tc-94	S	A
Y-90m	F	B	Nb-90	F	B	Tc-94m	F	B
Y-90m	M	A	Nb-90	M	A	Tc-94m	M	A
Y-90m	S	A	Nb-90	S	A	Tc-94m	S	A
Y-91	F	B	Nb-93m	F	C	Tc-95	F	A
Y-91	M	B	Nb-93m	M	B	Tc-95	M	A
Y-91	S	B	Nb-93m	S	B	Tc-95	S	A
Y-91m	F	A	Nb-94	F	B	Tc-95m	F	B
Y-91m	M	A	Nb-94	M	B	Tc-95m	M	B
Y-91m	S	A	Nb-94	S	B	Tc-95m	S	A
Y-92	F	B	Nb-95	F	B	Tc-96	F	A
Y-92	M	A	Nb-95	M	B	Tc-96	M	A
Y-92	S	A	Nb-95	S	A	Tc-96	S	A
Y-93	F	B	Nb-95m	F	C	Tc-96m	F	A
Y-93	M	A	Nb-95m	M	B	Tc-96m	M	A
Y-93	S	A	Nb-95m	S	B	Tc-96m	S	A
Y-94	F	B	Nb-96	F	B	Tc-97	F	B
Y-94	M	A	Nb-96	M	A	Tc-97	M	D
Y-94	S	A	Nb-96	S	A	Tc-97	S	B
Y-95	F	B	Nb-97	F	B	Tc-97m	F	D
Y-95	M	A	Nb-97	M	A	Tc-97m	M	B
Y-95	S	A	Nb-97	S	A	Tc-97m	S	B
Zr-86	F	B	Nb-98	F	B	Tc-98	F	C
Zr-86	M	A	Nb-98	M	A	Tc-98	M	C
Zr-86	S	A	Nb-98	S	A	Tc-98	S	B
Zr-88	F	A	Mo-90	F	B	Tc-99	F	D
Zr-88	M	A	Mo-90	M	A	Tc-99	M	B
Zr-88	S	A	Mo-90	S	A	Tc-99	S	B
Zr-89	F	B	Mo-93	F	B	Tc-99m	F	C
Zr-89	M	A	Mo-93	M	B	Tc-99m	M	A
Zr-89	S	A	Mo-93	S	B	Tc-99m	S	A

Nuclide	Type	Category	Nuclide	Type	Category	Nuclide	Type	Category
Tc-101	F	B	Rh-103m	M	B	Ag-108m	M	B
Tc-101	M	A	Rh-103m	S	B	Ag-108m	S	B
Tc-101	S	A	Rh-105	F	D	Ag-110m	F	B
Tc-104	F	B	Rh-105	M	B	Ag-110m	M	B
Tc-104	M	A	Rh-105	S	B	Ag-110m	S	A
Tc-104	S	A	Rh-106m	F	B	Ag-111	F	C
Ru-94	F	B	Rh-106m	M	A	Ag-111	M	B
Ru-94	M	A	Rh-106m	S	A	Ag-111	S	B
Ru-94	S	A	Rh-107	F	B	Ag-112	F	B
Ru-97	F	B	Rh-107	M	A	Ag-112	M	A
Ru-97	M	A	Rh-107	S	A	Ag-112	S	A
Ru-97	S	A	Pd-100	F	B	Ag-115	F	B
Ru-103	F	D	Pd-100	M	A	Ag-115	M	A
Ru-103	M	B	Pd-100	S	A	Ag-115	S	A
Ru-103	S	B	Pd-101	F	B	Cd-104	F	B
Ru-105	F	C	Pd-101	M	A	Cd-104	M	A
Ru-105	M	A	Pd-101	S	A	Cd-104	S	A
Ru-105	S	A	Pd-103	F	D	Cd-107	F	D
Ru-106	F	C	Pd-103	M	B	Cd-107	M	B
Ru-106	M	C	Pd-103	S	B	Cd-107	S	B
Ru-106	S	B	Pd-107	F	D	Cd-109	F	B
Ru-94	V	B	Pd-107	M	C	Cd-109	M	B
Ru-97	V	B	Pd-107	S	B	Cd-109	S	B
Ru-103	V	C	Pd-109	F	C	Cd-113	F	B
Ru-105	V	B	Pd-109	M	A	Cd-113	M	B
Ru-106	V	C	Pd-109	S	A	Cd-113	S	B
Rh-99m	F	B	Ag-102	F	A	Cd-113m	F	B
Rh-99m	M	A	Ag-102	M	A	Cd-113m	M	B
Rh-99m	S	A	Ag-102	S	A	Cd-113m	S	B
Rh-99	F	C	Ag-103	F	B	Cd-115	F	C
Rh-99	M	B	Ag-103	M	A	Cd-115	M	A
Rh-99	S	A	Ag-103	S	A	Cd-115	S	A
Rh-100	F	B	Ag-104	F	A	Cd-115m	F	B
Rh-100	M	A	Ag-104	M	A	Cd-115m	M	B
Rh-100	S	A	Ag-104	S	A	Cd-115m	S	B
Rh-101	F	D	Ag-104m	F	B	Cd-117	F	C
Rh-101	M	B	Ag-104m	M	A	Cd-117	M	A
Rh-101	S	B	Ag-104m	S	A	Cd-117	S	A
Rh-101m	F	B	Ag-105	F	A	Cd-117m	F	B
Rh-101m	M	A	Ag-105	M	A	Cd-117m	M	A
Rh-101m	S	A	Ag-105	S	A	Cd-117m	S	A
Rh-102	F	D	Ag-106	F	B	In-109	F	B
Rh-102	M	B	Ag-106	M	A	In-109	M	A
Rh-102	S	A	Ag-106	S	A	In-109	S	A
Rh-102m	F	C	Ag-106m	F	A	In-110b	F	A
Rh-102m	M	B	Ag-106m	M	A	In-110b	M	A
Rh-102m	S	B	Ag-106m	S	A	In-110b	S	A
Rh-103m	F	C	Ag-108m	F	C	In-110a	F	B

Nuclide	Type	Category	Nuclide	Type	Category	Nuclide	Type	Category
In-110a	M	A	Sn-121	M	B	Sb-122	M	A
In-110a	S	A	Sn-121	S	B	Sb-122	S	A
In-111	F	B	Sn-121m	F	B	Sb-124	F	B
In-111	M	A	Sn-121m	M	B	Sb-124	M	B
In-111	S	A	Sn-121m	S	B	Sb-124	S	A
In-112	F	B	Sn-123	F	B	Sb-124n	F	B
In-112	M	A	Sn-123	M	B	Sb-124n	M	A
In-112	S	A	Sn-123	S	B	Sb-124n	S	A
In-113m	F	B	Sn-123m	F	B	Sb-125	F	C
In-113m	M	A	Sn-123m	M	A	Sb-125	M	B
In-113m	S	A	Sn-123m	S	A	Sb-125	S	B
In-114m	F	A	Sn-125	F	B	Sb-126	F	B
In-114m	M	B	Sn-125	M	B	Sb-126	M	B
In-114m	S	B	Sn-125	S	A	Sb-126	S	A
In-115	F	D	Sn-126	F	B	Sb-126m	F	B
In-115	M	B	Sn-126	M	B	Sb-126m	M	A
In-115	S	B	Sn-126	S	B	Sb-126m	S	A
In-115m	F	C	Sn-127	F	B	Sb-127	F	C
In-115m	M	A	Sn-127	M	A	Sb-127	M	B
In-115m	S	A	Sn-127	S	A	Sb-127	S	B
In-116m	F	B	Sn-128	F	B	Sb-128b	F	B
In-116m	M	A	Sn-128	M	A	Sb-128b	M	A
In-116m	S	A	Sn-128	S	A	Sb-128b	S	A
In-117	F	B	Sb-115	F	B	Sb-128a	F	B
In-117	M	A	Sb-115	M	A	Sb-128a	M	A
In-117	S	A	Sb-115	S	A	Sb-128a	S	A
In-117m	F	C	Sb-116	F	B	Sb-129	F	B
In-117m	M	A	Sb-116	M	A	Sb-129	M	A
In-117m	S	A	Sb-116	S	A	Sb-129	S	A
In-119m	F	B	Sb-116m	F	B	Sb-130	F	B
In-119m	M	A	Sb-116m	M	A	Sb-130	M	A
In-119m	S	A	Sb-116m	S	A	Sb-130	S	A
Sn-110	F	B	Sb-117	F	B	Sb-131	F	B
Sn-110	M	A	Sb-117	M	A	Sb-131	M	A
Sn-110	S	A	Sb-117	S	A	Sb-131	S	A
Sn-111	F	B	Sb-118m	F	A	Te-116	F	B
Sn-111	M	A	Sb-118m	M	A	Te-116	M	A
Sn-111	S	A	Sb-118m	S	A	Te-116	S	A
Sn-113	F	B	Sb-119	F	B	Te-121	F	B
Sn-113	M	B	Sb-119	M	A	Te-121	M	A
Sn-113	S	B	Sb-119	S	A	Te-121	S	A
Sn-117m	F	D	Sb-120b	F	B	Te-121m	F	C
Sn-117m	M	B	Sb-120b	M	A	Te-121m	M	B
Sn-117m	S	B	Sb-120b	S	A	Te-121m	S	A
Sn-119m	F	B	Sb-120a	F	B	Te-123	F	E
Sn-119m	M	B	Sb-120a	M	A	Te-123	M	D
Sn-119m	S	B	Sb-120a	S	A	Te-123	S	B
Sn-121	F	D	Sb-122	F	B	Te-123m	F	C

113

Nuclide	Type	Category	Nuclide	Type	Category	Nuclide	Type	Category
Te-123m	M	B	Te-133m	V	B	I-135	M	A
Te-123m	S	B	Te-134	V	A	I-135	S	A
Te-125m	F	D	I-120	F	B	I-120	V	A
Te-125m	M	B	I-120	M	A	I-120m	V	A
Te-125m	S	B	I-120	S	A	I-121	V	A
Te-127	F	C	I-120m	F	B	I-123	V	B
Te-127	M	A	I-120m	M	A	I-124	V	C
Te-127	S	A	I-120m	S	A	I-125	V	D
Te-127m	F	C	I-121	F	B	I-126	V	D
Te-127m	M	B	I-121	M	A	I-128	V	B
Te-127m	S	B	I-121	S	A	I-129	V	D
Te-129	F	B	I-123	F	C	I-130	V	B
Te-129	M	A	I-123	M	A	I-131	V	C
Te-129	S	A	I-123	S	A	I-132	V	A
Te-129m	F	C	I-124	F	C	I-132m	V	A
Te-129m	M	B	I-124	M	A	I-133	V	B
Te-129m	S	B	I-124	S	A	I-134	V	A
Te-131	F	B	I-125	F	D	I-135	V	B
Te-131	M	A	I-125	M	B	I-120	V	B
Te-131	S	A	I-125	S	B	I-120m	V	B
Te-131m	F	B	I-126	F	C	I-121	V	B
Te-131m	M	A	I-126	M	B	I-123	V	C
Te-131m	S	A	I-126	S	B	I-124	V	D
Te-132	F	B	I-128	F	B	I-125	V	D
Te-132	M	A	I-128	M	A	I-126	V	D
Te-132	S	A	I-128	S	A	I-128	V	B
Te-133	F	B	I-129	F	D	I-129	V	D
Te-133	M	A	I-129	M	B	I-130	V	C
Te-133	S	A	I-129	S	B	I-131	V	D
Te-133m	F	B	I-130	F	B	I-132	V	B
Te-133m	M	A	I-130	M	A	I-132m	V	B
Te-133m	S	A	I-130	S	A	I-133	V	C
Te-134	F	B	I-131	F	C	I-134	V	B
Te-134	M	A	I-131	M	A	I-135	V	C
Te-134	S	A	I-131	S	B	Cs-125	F	B
Te-116	V	A	I-132	F	B	Cs-125	M	A
Te-121	V	B	I-132	M	A	Cs-125	S	A
Te-121m	V	C	I-132	S	A	Cs-127	F	B
Te-123	V	E	I-132m	F	B	Cs-127	M	A
Te-123m	V	C	I-132m	M	A	Cs-127	S	A
Te-125m	V	C	I-132m	S	A	Cs-129	F	B
Te-127	V	A	I-133	F	B	Cs-129	M	A
Te-129	V	B	I-133	M	A	Cs-129	S	A
Te-129m	V	B	I-133	S	A	Cs-130	F	B
Te-131	V	B	I-134	F	B	Cs-130	M	A
Te-131m	V	B	I-134	M	A	Cs-130	S	A
Te-132	V	B	I-134	S	A	Cs-131	F	B
Te-133	V	A	I-135	F	B	Cs-131	M	A

Nuclide	Type	Category	Nuclide	Type	Category	Nuclide	Type	Category
Cs-131	S	A	Ba-139	S	A	Ce-137m	S	B
Cs-132	F	A	Ba-140	F	C	Ce-139	F	B
Cs-132	M	A	Ba-140	M	B	Ce-139	M	B
Cs-132	S	A	Ba-140	S	B	Ce-139	S	B
Cs-134	F	A	Ba-141	F	B	Ce-141	F	C
Cs-134	M	B	Ba-141	M	A	Ce-141	M	B
Cs-134	S	B	Ba-141	S	A	Ce-141	S	B
Cs-134m	F	D	Ba-142	F	B	Ce-143	F	C
Cs-134m	M	B	Ba-142	M	A	Ce-143	M	A
Cs-134m	S	B	Ba-142	S	A	Ce-143	S	A
Cs-135	F	B	La-131	F	B	Ce-144	F	B
Cs-135	M	B	La-131	M	A	Ce-144	M	B
Cs-135	S	B	La-131	S	A	Ce-144	S	B
Cs-135m	F	A	La-132	F	B	Pr-136	F	B
Cs-135m	M	A	La-132	M	A	Pr-136	M	A
Cs-135m	S	A	La-132	S	A	Pr-136	S	A
Cs-136	F	B	La-135	F	B	Pr-137	F	B
Cs-136	M	A	La-135	M	A	Pr-137	M	A
Cs-136	S	A	La-135	S	A	Pr-137	S	A
Cs-137	F	A	La-137	F	B	Pr-138m	F	B
Cs-137	M	B	La-137	M	B	Pr-138m	M	A
Cs-137	S	B	La-137	S	B	Pr-138m	S	A
Cs-138	F	B	La-138	F	B	Pr-139	F	B
Cs-138	M	A	La-138	M	B	Pr-139	M	A
Cs-138	S	A	La-138	S	A	Pr-139	S	A
Ba-126	F	B	La-140	F	B	Pr-142	F	B
Ba-126	M	A	La-140	M	A	Pr-142	M	A
Ba-126	S	A	La-140	S	A	Pr-142	S	A
Ba-128	F	B	La-141	F	B	Pr-142m	F	B
Ba-128	M	A	La-141	M	A	Pr-142m	M	A
Ba-128	S	A	La-141	S	A	Pr-142m	S	A
Ba-131	F	C	La-142	F	B	Pr-143	F	C
Ba-131	M	B	La-142	M	A	Pr-143	M	B
Ba-131	S	A	La-142	S	A	Pr-143	S	B
Ba-131m	F	B	La-143	F	B	Pr-144	F	B
Ba-131m	M	B	La-143	M	A	Pr-144	M	A
Ba-131m	S	B	La-143	S	A	Pr-144	S	A
Ba-133	F	A	Ce-134	F	B	Pr-145	F	B
Ba-133	M	B	Ce-134	M	A	Pr-145	M	A
Ba-133	S	B	Ce-134	S	A	Pr-145	S	A
Ba-133m	F	C	Ce-135	F	B	Pr-147	F	B
Ba-133m	M	B	Ce-135	M	A	Pr-147	M	A
Ba-133m	S	A	Ce-135	S	A	Pr-147	S	A
Ba-135m	F	C	Ce-137	F	B	Nd-136	F	B
Ba-135m	M	B	Ce-137	M	A	Nd-136	M	A
Ba-135m	S	B	Ce-137	S	A	Nd-136	S	A
Ba-139	F	B	Ce-137m	F	C	Nd-138	F	B
Ba-139	M	A	Ce-137m	M	B	Nd-138	M	A

Table D-2 (continued)

Nuclide	Type	Category	Nuclide	Type	Category	Nuclide	Type	Category
Nd-138	S	A	Pm-150	S	A	Eu-149	S	A
Nd-139	F	B	Pm-151	F	C	Eu-150b	F	B
Nd-139	M	A	Pm-151	M	A	Eu-150b	M	A
Nd-139	S	A	Pm-151	S	A	Eu-150b	S	A
Nd-139m	F	B	Sm-141	F	B	Eu-150a	F	C
Nd-139m	M	A	Sm-141	M	A	Eu-150a	M	A
Nd-139m	S	A	Sm-141	S	A	Eu-150a	S	A
Nd-141	F	B	Sm-141m	F	B	Eu-152	F	B
Nd-141	M	A	Sm-141m	M	A	Eu-152	M	A
Nd-141	S	A	Sm-141m	S	A	Eu-152	S	A
Nd-147	F	C	Sm-142	F	B	Eu-152m	F	B
Nd-147	M	B	Sm-142	M	A	Eu-152m	M	A
Nd-147	S	B	Sm-142	S	A	Eu-152m	S	A
Nd-149	F	C	Sm-145	F	B	Eu-154	F	B
Nd-149	M	A	Sm-145	M	B	Eu-154	M	A
Nd-149	S	A	Sm-145	S	A	Eu-154	S	B
Nd-151	F	B	Sm-146	F	D	Eu-155	F	B
Nd-151	M	A	Sm-146	M	C	Eu-155	M	B
Nd-151	S	A	Sm-146	S	B	Eu-155	S	B
Pm-141	F	B	Sm-147	F	D	Eu-156	F	B
Pm-141	M	A	Sm-147	M	C	Eu-156	M	B
Pm-141	S	A	Sm-147	S	B	Eu-156	S	A
Pm-143	F	A	Sm-151	F	C	Eu-157	F	C
Pm-143	M	A	Sm-151	M	B	Eu-157	M	A
Pm-143	S	A	Sm-151	S	B	Eu-157	S	A
Pm-144	F	A	Sm-153	F	D	Eu-158	F	B
Pm-144	M	A	Sm-153	M	A	Eu-158	M	A
Pm-144	S	A	Sm-153	S	B	Eu-158	S	A
Pm-145	F	B	Sm-155	F	B	Gd-145	F	B
Pm-145	M	B	Sm-155	M	A	Gd-145	M	A
Pm-145	S	B	Sm-155	S	A	Gd-145	S	A
Pm-146	F	B	Sm-156	F	B	Gd-146	F	A
Pm-146	M	A	Sm-156	M	A	Gd-146	M	B
Pm-146	S	A	Sm-156	S	A	Gd-146	S	A
Pm-147	F	B	Eu-145	F	A	Gd-147	F	B
Pm-147	M	B	Eu-145	M	A	Gd-147	M	A
Pm-147	S	B	Eu-145	S	A	Gd-147	S	A
Pm-148	F	B	Eu-146	F	A	Gd-148	F	D
Pm-148	M	A	Eu-146	M	A	Gd-148	M	C
Pm-148	S	A	Eu-146	S	A	Gd-148	S	B
Pm-148m	F	A	Eu-147	F	B	Gd-149	F	B
Pm-148m	M	B	Eu-147	M	A	Gd-149	M	A
Pm-148m	S	A	Eu-147	S	A	Gd-149	S	B
Pm-149	F	C	Eu-148	F	A	Gd-151	F	B
Pm-149	M	A	Eu-148	M	A	Gd-151	M	B
Pm-149	S	A	Eu-148	S	A	Gd-151	S	B
Pm-150	F	B	Eu-149	F	B	Gd-152	F	D
Pm-150	M	A	Eu-149	M	B	Gd-152	M	C

Nuclide	Type	Category	Nuclide	Type	Category	Nuclide	Type	Category
Gd-152	S	B	Tb-161	S	B	Ho-167	S	A
Gd-153	F	B	Dy-155	F	B	Er-161	F	B
Gd-153	M	B	Dy-155	M	A	Er-161	M	A
Gd-153	S	B	Dy-155	S	A	Er-161	S	A
Gd-159	F	C	Dy-157	F	B	Er-165	F	B
Gd-159	M	A	Dy-157	M	A	Er-165	M	A
Gd-159	S	A	Dy-157	S	A	Er-165	S	A
Tb-147	F	B	Dy-159	F	B	Er-169	F	D
Tb-147	M	A	Dy-159	M	B	Er-169	M	B
Tb-147	S	A	Dy-159	S	A	Er-169	S	B
Tb-149	F	D	Dy-165	F	C	Er-171	F	C
Tb-149	M	B	Dy-165	M	A	Er-171	M	A
Tb-149	S	B	Dy-165	S	A	Er-171	S	A
Tb-150	F	B	Dy-166	F	C	Er-172	F	C
Tb-150	M	A	Dy-166	M	B	Er-172	M	B
Tb-150	S	A	Dy-166	S	B	Er-172	S	B
Tb-151	F	B	Ho-155	F	B	Tm-162	F	B
Tb-151	M	A	Ho-155	M	A	Tm-162	M	A
Tb-151	S	A	Ho-155	S	A	Tm-162	S	A
Tb-153	F	B	Ho-157	F	A	Tm-166	F	B
Tb-153	M	A	Ho-157	M	A	Tm-166	M	A
Tb-153	S	A	Ho-157	S	A	Tm-166	S	A
Tb-154	F	B	Ho-159	F	B	Tm-167	F	C
Tb-154	M	A	Ho-159	M	A	Tm-167	M	B
Tb-154	S	A	Ho-159	S	A	Tm-167	S	B
Tb-155	F	B	Ho-161	F	B	Tm-170	F	B
Tb-155	M	A	Ho-161	M	A	Tm-170	M	B
Tb-155	S	A	Ho-161	S	A	Tm-170	S	B
Tb-156	F	B	Ho-162	F	B	Tm-171	F	B
Tb-156	M	A	Ho-162	M	A	Tm-171	M	B
Tb-156	S	A	Ho-162	S	A	Tm-171	S	B
Tb-156m	F	B	Ho-162m	F	B	Tm-172	F	B
Tb-156m	M	A	Ho-162m	M	A	Tm-172	M	A
Tb-156m	S	A	Ho-162m	S	A	Tm-172	S	A
Tb-156n	F	C	Ho-164	F	B	Tm-173	F	C
Tb-156n	M	A	Ho-164	M	A	Tm-173	M	A
Tb-156n	S	B	Ho-164	S	A	Tm-173	S	A
Tb-157	F	B	Ho-164m	F	C	Tm-175	F	B
Tb-157	M	B	Ho-164m	M	A	Tm-175	M	A
Tb-157	S	B	Ho-164m	S	A	Tm-175	S	A
Tb-158	F	B	Ho-166	F	B	Yb-162	F	B
Tb-158	M	A	Ho-166	M	A	Yb-162	M	A
Tb-158	S	B	Ho-166	S	A	Yb-162	S	A
Tb-160	F	B	Ho-166m	F	B	Yb-166	F	B
Tb-160	M	B	Ho-166m	M	B	Yb-166	M	A
Tb-160	S	B	Ho-166m	S	A	Yb-166	S	A
Tb-161	F	C	Ho-167	F	C	Yb-167	F	B
Tb-161	M	B	Ho-167	M	A	Yb-167	M	B

Nuclide	Type	Category	Nuclide	Type	Category	Nuclide	Type	Category
Yb-167	S	B	Lu-178	S	A	Ta-172	S	A
Yb-169	F	B	Lu-178m	F	B	Ta-173	F	B
Yb-169	M	B	Lu-178m	M	A	Ta-173	M	A
Yb-169	S	B	Lu-178m	S	A	Ta-173	S	A
Yb-175	F	D	Lu-179	F	C	Ta-174	F	B
Yb-175	M	B	Lu-179	M	A	Ta-174	M	A
Yb-175	S	B	Lu-179	S	A	Ta-174	S	A
Yb-177	F	B	Hf-170	F	B	Ta-175	F	B
Yb-177	M	A	Hf-170	M	A	Ta-175	M	A
Yb-177	S	A	Hf-170	S	A	Ta-175	S	A
Yb-178	F	C	Hf-172	F	B	Ta-176	F	B
Yb-178	M	A	Hf-172	M	A	Ta-176	M	A
Yb-178	S	A	Hf-172	S	A	Ta-176	S	A
Lu-169	F	B	Hf-173	F	B	Ta-177	F	C
Lu-169	M	A	Hf-173	M	A	Ta-177	M	A
Lu-169	S	A	Hf-173	S	A	Ta-177	S	A
Lu-170	F	B	Hf-175	F	A	Ta-178b	F	C
Lu-170	M	A	Hf-175	M	B	Ta-178b	M	A
Lu-170	S	A	Hf-175	S	A	Ta-178b	S	A
Lu-171	F	B	Hf-177m	F	B	Ta-179	F	B
Lu-171	M	A	Hf-177m	M	A	Ta-179	M	B
Lu-171	S	A	Hf-177m	S	A	Ta-179	S	B
Lu-172	F	B	Hf-178m	F	B	Ta-180	F	B
Lu-172	M	A	Hf-178m	M	A	Ta-180	M	B
Lu-172	S	A	Hf-178m	S	A	Ta-180	S	B
Lu-173	F	B	Hf-179m	F	B	Ta-180m	F	C
Lu-173	M	B	Hf-179m	M	B	Ta-180m	M	A
Lu-173	S	A	Hf-179m	S	B	Ta-180m	S	B
Lu-174	F	B	Hf-180m	F	C	Ta-182	F	B
Lu-174	M	B	Hf-180m	M	A	Ta-182	M	B
Lu-174	S	B	Hf-180m	S	A	Ta-182	S	A
Lu-174m	F	B	Hf-181	F	B	Ta-182m	F	B
Lu-174m	M	B	Hf-181	M	B	Ta-182m	M	B
Lu-174m	S	B	Hf-181	S	B	Ta-182m	S	B
Lu-176	F	B	Hf-182	F	B	Ta-183	F	D
Lu-176	M	B	Hf-182	M	B	Ta-183	M	B
Lu-176	S	B	Hf-182	S	B	Ta-183	S	B
Lu-176m	F	C	Hf-182m	F	B	Ta-184	F	B
Lu-176m	M	A	Hf-182m	M	A	Ta-184	M	A
Lu-176m	S	A	Hf-182m	S	A	Ta-184	S	A
Lu-177	F	D	Hf-183	F	B	Ta-185	F	B
Lu-177	M	B	Hf-183	M	A	Ta-185	M	A
Lu-177	S	B	Hf-183	S	A	Ta-185	S	A
Lu-177m	F	B	Hf-184	F	C	Ta-186	F	B
Lu-177m	M	B	Hf-184	M	A	Ta-186	M	A
Lu-177m	S	B	Hf-184	S	A	Ta-186	S	A
Lu-178	F	B	Ta-172	F	B	W-176	F	B
Lu-178	M	A	Ta-172	M	A	W-176	M	A

118

Nuclide	Type	Category	Nuclide	Type	Category	Nuclide	Type	Category
W-177	F	B	Re-188m	M	A	Ir-187	M	A
W-177	M	A	Re-188m	S	A	Ir-187	S	A
W-178	F	E	Re-189	F	C	Ir-188	F	B
W-178	M	B	Re-189	M	A	Ir-188	M	A
W-179	F	B	Re-189	S	A	Ir-188	S	A
W-179	M	A	Os-180	F	B	Ir-189	F	C
W-181	F	B	Os-180	M	A	Ir-189	M	B
W-181	M	B	Os-180	S	A	Ir-189	S	B
W-185	F	E	Os-181	F	B	Ir-190	F	B
W-185	M	B	Os-181	M	A	Ir-190	M	B
W-187	F	D	Os-181	S	A	Ir-190	S	A
W-187	M	A	Os-182	F	B	Ir-190n	F	B
W-188	F	D	Os-182	M	A	Ir-190n	M	A
W-188	M	B	Os-182	S	A	Ir-190n	S	A
Re-177	F	B	Os-185	F	D	Ir-190m	F	B
Re-177	M	A	Os-185	M	B	Ir-190m	M	B
Re-177	S	A	Os-185	S	A	Ir-190m	S	A
Re-178	F	B	Os-189m	F	C	Ir-192	F	B
Re-178	M	A	Os-189m	M	B	Ir-192	M	B
Re-178	S	A	Os-189m	S	B	Ir-192	S	B
Re-181	F	B	Os-191	F	E	Ir-192m	F	C
Re-181	M	A	Os-191	M	B	Ir-192m	M	C
Re-181	S	A	Os-191	S	B	Ir-192m	S	B
Re-182b	F	C	Os-191m	F	D	Ir-194	F	B
Re-182b	M	A	Os-191m	M	B	Ir-194	M	A
Re-182b	S	A	Os-191m	S	B	Ir-194	S	A
Re-182a	F	B	Os-193	F	C	Ir-194m	F	B
Re-182a	M	A	Os-193	M	A	Ir-194m	M	B
Re-182a	S	A	Os-193	S	A	Ir-194m	S	A
Re-184	F	C	Os-194	F	E	Ir-195	F	C
Re-184	M	B	Os-194	M	C	Ir-195	M	A
Re-184	S	A	Os-194	S	B	Ir-195	S	A
Re-184m	F	D	Ir-182	F	B	Ir-195m	F	C
Re-184m	M	B	Ir-182	M	A	Ir-195m	M	A
Re-184m	S	A	Ir-182	S	A	Ir-195m	S	A
Re-186	F	C	Ir-184	F	B	Pt-186	F	B
Re-186	M	A	Ir-184	M	A	Pt-186	M	A
Re-186	S	A	Ir-184	S	A	Pt-186	S	A
Re-186m	F	D	Ir-185	F	B	Pt-188	F	C
Re-186m	M	C	Ir-185	M	A	Pt-188	M	B
Re-186m	S	B	Ir-185	S	A	Pt-188	S	A
Re-187	F	D	Ir-186a	F	B	Pt-189	F	C
Re-187	M	C	Ir-186a	M	A	Pt-189	M	A
Re-187	S	B	Ir-186a	S	A	Pt-189	S	A
Re-188	F	B	Ir-186b	F	B	Pt-191	F	C
Re-188	M	A	Ir-186b	M	A	Pt-191	M	A
Re-188	S	A	Ir-186b	S	A	Pt-191	S	A
Re-188m	F	B	Ir-187	F	B	Pt-193	F	B

Nuclide	Type	Category	Nuclide	Type	Category	Nuclide	Type	Category
Pt-193	M	D	Hg-193	M	A	Hg-199m	M	A
Pt-193	S	B	Hg-193	S	A	Hg-199m	S	A
Pt-193m	F	D	Hg-193m	F	B	Hg-203	F	B
Pt-193m	M	B	Hg-193m	M	A	Hg-203	M	B
Pt-193m	S	B	Hg-193m	S	A	Hg-203	S	B
Pt-195m	F	D	Hg-194	F	C	Hg-193	V	C
Pt-195m	M	B	Hg-194	M	B	Hg-193m	V	C
Pt-195m	S	B	Hg-194	S	B	Hg-194	V	C
Pt-197	F	D	Hg-195	F	C	Hg-195	V	C
Pt-197	M	A	Hg-195	M	A	Hg-195m	V	C
Pt-197	S	B	Hg-195	S	A	Hg-197	V	C
Pt-197m	F	C	Hg-195m	F	C	Hg-197m	V	C
Pt-197m	M	A	Hg-195m	M	B	Hg-199m	V	B
Pt-197m	S	A	Hg-195m	S	B	Hg-203	V	B
Pt-199	F	B	Hg-197	F	D	Tl-194	F	A
Pt-199	M	A	Hg-197	M	B	Tl-194	M	A
Pt-199	S	A	Hg-197	S	B	Tl-194	S	A
Pt-200	F	B	Hg-197m	F	D	Tl-194m	F	B
Pt-200	M	A	Hg-197m	M	B	Tl-194m	M	A
Pt-200	S	A	Hg-197m	S	B	Tl-194m	S	A
Au-193	F	C	Hg-199m	F	B	Tl-195	F	B
Au-193	M	A	Hg-199m	M	A	Tl-195	M	A
Au-193	S	A	Hg-199m	S	A	Tl-195	S	A
Au-194	F	B	Hg-203	F	C	Tl-197	F	C
Au-194	M	A	Hg-203	M	B	Tl-197	M	A
Au-194	S	A	Hg-203	S	B	Tl-197	S	A
Au-195	F	D	Hg-193	F	C	Tl-198	F	A
Au-195	M	B	Hg-193	M	B	Tl-198	M	A
Au-195	S	B	Hg-193	S	B	Tl-198	S	A
Au-198	F	C	Hg-193m	F	C	Tl-198m	F	B
Au-198	M	A	Hg-193m	M	A	Tl-198m	M	A
Au-198	S	A	Hg-193m	S	A	Tl-198m	S	A
Au-198m	F	D	Hg-194	F	B	Tl-199	F	C
Au-198m	M	B	Hg-194	M	B	Tl-199	M	A
Au-198m	S	B	Hg-194	S	B	Tl-199	S	A
Au-199	F	D	Hg-195	F	C	Tl-200	F	A
Au-199	M	B	Hg-195	M	A	Tl-200	M	A
Au-199	S	B	Hg-195	S	A	Tl-200	S	A
Au-200	F	B	Hg-195m	F	D	Tl-201	F	C
Au-200	M	A	Hg-195m	M	B	Tl-201	M	B
Au-200	S	A	Hg-195m	S	B	Tl-201	S	B
Au-200m	F	C	Hg-197	F	D	Tl-202	F	B
Au-200m	M	A	Hg-197	M	B	Tl-202	M	A
Au-200m	S	A	Hg-197	S	B	Tl-202	S	A
Au-201	F	B	Hg-197m	F	D	Tl-204	F	C
Au-201	M	A	Hg-197m	M	B	Tl-204	M	C
Au-201	S	A	Hg-197m	S	B	Tl-204	S	B
Hg-193	F	C	Hg-199m	F	B	Pb-195m	F	B

Nuclide	Type	Category	Nuclide	Type	Category	Nuclide	Type	Category
Pb-195m	M	A	Bi-202	M	A	Fr-222	M	B
Pb-195m	S	A	Bi-202	S	A	Fr-222	S	B
Pb-198	F	B	Bi-203	F	B	Fr-223	F	E
Pb-198	M	A	Bi-203	M	A	Fr-223	M	B
Pb-198	S	A	Bi-203	S	A	Fr-223	S	B
Pb-199	F	B	Bi-205	F	B	Ra-223	F	E
Pb-199	M	A	Bi-205	M	A	Ra-223	M	B
Pb-199	S	A	Bi-205	S	A	Ra-223	S	B
Pb-200	F	B	Bi-206	F	B	Ra-224	F	E
Pb-200	M	A	Bi-206	M	A	Ra-224	M	B
Pb-200	S	A	Bi-206	S	A	Ra-224	S	B
Pb-201	F	B	Bi-207	F	C	Ra-225	F	E
Pb-201	M	A	Bi-207	M	C	Ra-225	M	C
Pb-201	S	A	Bi-207	S	B	Ra-225	S	B
Pb-202	F	B	Bi-210	F	E	Ra-226	F	E
Pb-202	M	A	Bi-210	M	C	Ra-226	M	C
Pb-202	S	B	Bi-210	S	B	Ra-226	S	B
Pb-202m	F	B	Bi-210m	F	E	Ra-227	F	B
Pb-202m	M	A	Bi-210m	M	C	Ra-227	M	B
Pb-202m	S	A	Bi-210m	S	B	Ra-227	S	B
Pb-203	F	B	Bi-212	F	D	Ra-228	F	C
Pb-203	M	A	Bi-212	M	B	Ra-228	M	D
Pb-203	S	A	Bi-212	S	B	Ra-228	S	C
Pb-205	F	B	Bi-213	F	C	Ac-224	F	E
Pb-205	M	B	Bi-213	M	B	Ac-224	M	B
Pb-205	S	B	Bi-213	S	B	Ac-224	S	B
Pb-209	F	C	Bi-214	F	C	Ac-225	F	E
Pb-209	M	B	Bi-214	M	B	Ac-225	M	B
Pb-209	S	B	Bi-214	S	B	Ac-225	S	B
Pb-210	F	C	Po-203	F	B	Ac-226	F	E
Pb-210	M	D	Po-203	M	A	Ac-226	M	B
Pb-210	S	C	Po-203	S	A	Ac-226	S	B
Pb-211	F	C	Po-205	F	B	Ac-227	F	D
Pb-211	M	B	Po-205	M	A	Ac-227	M	C
Pb-211	S	B	Po-205	S	A	Ac-227	S	B
Pb-212	F	E	Po-207	F	B	Ac-228	F	C
Pb-212	M	B	Po-207	M	A	Ac-228	M	B
Pb-212	S	B	Po-207	S	A	Ac-228	S	B
Pb-214	F	D	Po-210	F	D	Th-226	F	C
Pb-214	M	B	Po-210	M	C	Th-226	M	B
Pb-214	S	B	Po-210	S	B	Th-226	S	B
Bi-200	F	B	At-207	F	D	Th-227	F	E
Bi-200	M	A	At-207	M	B	Th-227	M	B
Bi-200	S	A	At-207	S	B	Th-227	S	B
Bi-201	F	B	At-211	F	E	Th-228	F	C
Bi-201	M	A	At-211	M	B	Th-228	M	C
Bi-201	S	A	At-211	S	B	Th-228	S	B
Bi-202	F	B	Fr-222	F	C	Th-229	F	D

Nuclide	Type	Category	Nuclide	Type	Category	Nuclide	Type	Category
Th-229	M	C	U-234	M	C	Np-240	M	A
Th-229	S	B	U-234	S	B	Np-240	S	A
Th-230	F	D	U-235	F	D	Pu-234	F	D
Th-230	M	C	U-235	M	C	Pu-234	M	B
Th-230	S	B	U-235	S	B	Pu-234	S	B
Th-231	F	D	U-236	F	D	Pu-235	F	B
Th-231	M	B	U-236	M	C	Pu-235	M	A
Th-231	S	B	U-236	S	B	Pu-235	S	A
Th-232	F	C	U-237	F	E	Pu-236	F	C
Th-232	M	C	U-237	M	B	Pu-236	M	B
Th-232	S	C	U-237	S	B	Pu-236	S	B
Th-234	F	B	U-238	F	D	Pu-237	F	B
Th-234	M	B	U-238	M	C	Pu-237	M	B
Th-234	S	B	U-238	S	B	Pu-237	S	A
Pa-227	F	D	U-239	F	B	Pu-238	F	C
Pa-227	M	B	U-239	M	A	Pu-238	M	C
Pa-227	S	B	U-239	S	A	Pu-238	S	B
Pa-228	F	C	U-240	F	C	Pu-239	F	C
Pa-228	M	B	U-240	M	A	Pu-239	M	C
Pa-228	S	B	U-240	S	A	Pu-239	S	B
Pa-230	F	E	Np-232	F	C	Pu-240	F	C
Pa-230	M	C	Np-232	M	B	Pu-240	M	C
Pa-230	S	B	Np-232	S	B	Pu-240	S	B
Pa-231	F	D	Np-233	F	B	Pu-241	F	D
Pa-231	M	C	Np-233	M	A	Pu-241	M	C
Pa-231	S	B	Np-233	S	A	Pu-241	S	C
Pa-232	F	D	Np-234	F	A	Pu-242	F	C
Pa-232	M	B	Np-234	M	A	Pu-242	M	C
Pa-232	S	B	Np-234	S	A	Pu-242	S	B
Pa-233	F	B	Np-235	F	B	Pu-243	F	C
Pa-233	M	B	Np-235	M	B	Pu-243	M	A
Pa-233	S	B	Np-235	S	B	Pu-243	S	B
Pa-234	F	C	Np-236a	F	D	Pu-244	F	C
Pa-234	M	A	Np-236a	M	C	Pu-244	M	B
Pa-234	S	A	Np-236a	S	B	Pu-244	S	B
U-230	F	E	Np-236b	F	C	Pu-245	F	C
U-230	M	B	Np-236b	M	B	Pu-245	M	A
U-230	S	B	Np-236b	S	B	Pu-245	S	A
U-231	F	D	Np-237	F	D	Pu-246	F	B
U-231	M	A	Np-237	M	C	Pu-246	M	A
U-231	S	A	Np-237	S	B	Pu-246	S	B
U-232	F	C	Np-238	F	B	Am-237	F	B
U-232	M	C	Np-238	M	B	Am-237	M	A
U-232	S	C	Np-238	S	A	Am-237	S	A
U-233	F	D	Np-239	F	D	Am-238	F	B
U-233	M	C	Np-239	M	B	Am-238	M	B
U-233	S	B	Np-239	S	B	Am-238	S	B
U-234	F	D	Np-240	F	B	Am-239	F	C

Nuclide	Type	Category	Nuclide	Type	Category	Nuclide	Type	Category
Am-239	M	A	Cm-244	S	B	Cf-251	F	D
Am-239	S	A	Cm-245	F	D	Cf-251	M	C
Am-240	F	B	Cm-245	M	C	Cf-251	S	B
Am-240	M	A	Cm-245	S	B	Cf-252	F	D
Am-240	S	A	Cm-246	F	D	Cf-252	M	B
Am-241	F	D	Cm-246	M	C	Cf-252	S	B
Am-241	M	C	Cm-246	S	B	Cf-253	F	D
Am-241	S	B	Cm-247	F	D	Cf-253	M	B
Am-242	F	D	Cm-247	M	C	Cf-253	S	B
Am-242	M	B	Cm-247	S	B	Cf-254	F	D
Am-242	S	B	Cm-248	F	D	Cf-254	M	B
Am-242m	F	D	Cm-248	M	C	Cf-254	S	B
Am-242m	M	C	Cm-248	S	B	Es-250	F	D
Am-242m	S	B	Cm-249	F	B	Es-250	M	B
Am-243	F	D	Cm-249	M	A	Es-250	S	B
Am-243	M	C	Cm-249	S	A	Es-251	F	D
Am-243	S	B	Cm-250	F	C	Es-251	M	B
Am-244	F	B	Cm-250	M	C	Es-251	S	B
Am-244	M	B	Cm-250	S	B	Es-253	F	E
Am-244	S	B	Bk-245	F	D	Es-253	M	B
Am-244m	F	B	Bk-245	M	B	Es-253	S	B
Am-244m	M	B	Bk-245	S	B	Es-254	F	C
Am-244m	S	B	Bk-246	F	B	Es-254	M	B
Am-245	F	C	Bk-246	M	A	Es-254	S	B
Am-245	M	A	Bk-246	S	A	Es-254m	F	E
Am-245	S	A	Bk-247	F	D	Es-254m	M	B
Am-246	F	B	Bk-247	M	C	Es-254m	S	B
Am-246	M	A	Bk-247	S	B	Fm-252	F	E
Am-246	S	B	Bk-249	F	D	Fm-252	M	B
Am-246m	F	B	Bk-249	M	C	Fm-252	S	B
Am-246m	M	A	Bk-249	S	B	Fm-253	F	E
Am-246m	S	A	Bk-250	F	B	Fm-253	M	B
Cm-238	F	D	Bk-250	M	B	Fm-253	S	B
Cm-238	M	B	Bk-250	S	B	Fm-254	F	D
Cm-238	S	B	Cf-244	F	C	Fm-254	M	B
Cm-240	F	D	Cf-244	M	B	Fm-254	S	B
Cm-240	M	B	Cf-244	S	B	Fm-255	F	E
Cm-240	S	B	Cf-246	F	E	Fm-255	M	B
Cm-241	F	C	Cf-246	M	B	Fm-255	S	B
Cm-241	M	B	Cf-246	S	B	Fm-257	F	D
Cm-241	S	B	Cf-248	F	C	Fm-257	M	B
Cm-242	F	D	Cf-248	M	B	Fm-257	S	B
Cm-242	M	B	Cf-248	S	B	Md-257	F	D
Cm-242	S	B	Cf-249	F	D	Md-257	M	B
Cm-243	F	D	Cf-249	M	C	Md-257	S	B
Cm-243	M	C	Cf-249	S	B	Md-258	F	D
Cm-243	S	B	Cf-250	F	D	Md-258	M	B
Cm-244	F	D	Cf-250	M	C	Md-258	S	B
Cm-244	M	C	Cf-250	S	B			

REFERENCES

A. Ando, I. Ando, T. Hiraki, and K. Hisada (1989). "Relation between the Location of Elements in the Periodic Table and Various Organ-Uptake Rates", *Nucl. Med. Biol. 16*, 57-80.

J. Bäckström, L. Hammarström, and A. Nelson (1967). "Distribution of Zr and Nb in Mice", *Acta Radiol. 6*, 122-128.

L. N. Burykina (1962). "The Metabolism of Radioactive Ruthenium in the Organism of Experimental Animals", in: *The toxicology of Radioactive Substances, Vol. 1* (A. A. Letavet and E. B. Kurlyandskaya, eds). Oxford: Pergamon Press; pp. 60-76.

R.T. Clemen and R.L. Winkler (1999). "Combining Probability Distributions from Experts in Risk Analysis", *Risk Analysis 19*,187-203.

P. J. Coughtrey and M. C. Thorne (1983). *Radionuclide Distribution and Transport in Terrestrial and Aquatic Ecosystems, Vol 3* (A. A. Balkema, editor), Rotterdam.

CRC (1966). *Handbook of Probability and Statistics*, pp 258-272, (Chemical Rubber Co.)

R. B. Cuddihy and B. B. Boecker (1970). "Kinetics of Lanthanum Retention and Tissue Distribution in the Beagle Dog Following Administration of ^{140}LaCl$_3$ by Inhalation, Gavage, and Injection", *Health Phys. 19*, 419-426.

D. E. Dunning and G. Schwarz (1981). "Variability of Human Thyroid Characteristics and Estimates of Dose from Ingested ^{131}I", *Health Phys. 40*, 661-675.

P. W. Durbin (1957). "The Distribution of Radioisotopes of Some Heavy Metals in the Rat", *Univ. Calif. Pub. Pharmacol. 3*, 1-34.

P. W. Durbin (1960). "Metabolic Characteristics Within a Chemical Family", *Health Phys. 2*, 225-238.

P. W. Durbin (1962). "Distribution of the Transuranic Elements in Mammals", *Health Phys. 8*, 665-671.

EPA (1991). *Final Draft for the Drinking Water Criteria Document on Radium*, NTIS: PB 91225631 (Prepared by Life Systems, Inc., for the Environmental Protection Agency, Washington, DC).

EPA (1994). *Estimating Radiogenic Cancer Risks*, EPA 402-R-93-076 (U. S. Environmental Protection Agency, Washington, DC).

EPA (1999). *Cancer Risk Coefficients for Environmental Exposure to Radionuclides. Federal Guidance Report No. 13*, EPA 402-R-99-001 (U. S. Environmental Protection Agency, Washington, DC).

G. Etherington, M. R. Bailey, M. D. Dorrian, and A. Hodgson (1989). "A Study of the Biokinetics of Intravenously Administered Yttrium-88 in Man", in: *Radiation Protection – Theory and Practice.* Paper presented at 4th Int. Symp., Malvern, June 1989; pp. 445-448.

E. L. Etnier, C. C. Travis, and D. M. Hetrick (1984). "Metabolism of Organically Bound Tritium in Man", *Radiat. Res. 100*, 487-502.

F.N. Fritsch and R.E. Carlson (1980). "Monotone Piecewise Cubic Interpolation", *SIAM J. Numer. Anal. 17*, 238-246.

L. Friberg, G. F. Nordberg, and V. B. Vouk, editors (1986). *Handbook of the Toxicology of Metals. Vol. II: Specific Metals.* Elsevier; pp. 26-42.

J. E. Furchner and G. A. Drake (1971). "Comparative Metabolism of Radionuclides in Mammals - VI. Retention of ^{95}Nb in the Mouse, Rat, Monkey and Dog", *Health Phys. 21*, 173-180.

J. E. Furchner, C. R. Richmond, and G. A. Drake (1971). "Comparative Metabolism of Radionuclides in Mammals. VII. Retention of ^{106}Ru in the Mouse, Rat, Monkey and Dog", *Health Phys. 21*, 355-365.

A. Gelman, J. Carlin J, H. Stern, and D. Rubin (1995). *Bayesian Data Analysis*. Chapman and Hall/CRC.

G. R. Howe (1992). "Effects of Dose, Dose-Rate and Fractionation on Radiation-Induced Breast and Lung Cancers: The Canadian Fluoroscopy Study", in: *International Conference on Radiation Effects and Protection*, pp. 108-113, Japan Atomic Energy Institute, Tokyo.

Z. Hrubec, JD Boice Jr., RR Monson, and M Rosenstein (1989). "Breast Cancer after Multiple Chest Fluoroscopies: Second Follow-Up of Massachusetts Women with Tuberculosis", *Cancer Res 49*, 229-234.

ICRP (1975). International Commission on Radiological Protection, "Report of the Task Group on Reference Man", ICRP Publication 23 (Pergamon Press, Oxford).

ICRP (1979). International Commission on Radiological Protection, "Limits for Intakes by Workers", ICRP Publication 30, Part 1 (Pergamon Press, Oxford).

ICRP (1980). International Commission on Radiological Protection, "Limits for Intakes by Workers", ICRP Publication 30, Part 2 (Pergamon Press, Oxford).

ICRP (1981). International Commission on Radiological Protection, "Limits for Intakes by Workers", ICRP Publication 30, Part 3 (Pergamon Press, Oxford).

ICRP (1987). International Commission on Radiological Protection, "Radiation Dose to Patients from Radiopharmaceuticals", ICRP Publication 53 (Pergamon Press, Oxford).

ICRP (1988). International Commission on Radiological Protection, "Limits for Intakes by Workers: An Addendum", ICRP Publication 30, Part 4 (Pergamon Press, Oxford).

ICRP (1989). International Commission on Radiological Protection, "Age-Dependent Doses to Members of the Public from Intake of Radionuclides, Part 1", ICRP Publication 56 (Pergamon Press, Oxford).

ICRP (1991). International Commission on Radiological Protection, "1990 Recommendations of the International Commission on Radiological Protection", ICRP Publication 60 (Pergamon Press, Oxford).

ICRP (1993). International Commission on Radiological Protection, "Age-Dependent Doses to Members of the Public from Intake of Radionuclides, Part 2", ICRP Publication 67 (Pergamon Press, Oxford).

ICRP (1994). International Commission on Radiological Protection, "Human Respiratory Tract Model for Radiological Protection", ICRP Publication 66 (Pergamon Press, Oxford).

ICRP (1995a). International Commission on Radiological Protection, "Age-Dependent Doses to Members of the Public from Intake of Radionuclides, Part 3", ICRP Publication 69 (Pergamon Press, Oxford).

ICRP (1995b). International Commission on Radiological Protection, "Age-Dependent Doses to Members of the Public from Intake of Radionuclides, Part 4", ICRP Publication 71 (Pergamon Press, Oxford).

ICRP (1996). International Commission on Radiological Protection, "Age-Dependent Doses to Members of the Public from Intake of Radionuclides, Part 5. Compilation of Ingestion and Inhalation Dose Coefficients", ICRP Publication 72 (Pergamon Press, Oxford).

ICRP (1994b). International Commission on Radiological Protection. "Dose Coefficients for Intakes of Radionuclides by Workers", ICRP Publication 68. Oxford: Pergamon Press.

ICRP (2002). International Commission on Radiological Protection. "Basic Anatomic and Physiological Data for Use in Radiological Protection: Reference values". ICRP Publication 89. Oxford: Pergamon Press.

J. Inaba, Y. Nishimura, K.-I. Kimura, and R. Ichikawa (1982). "Whole-Body Retention and Tissue Distribution of 60Co in Rats after Oral Administration of Freshwater Fish Contaminated with ^{60}Co", *Health Phys. 43*, 247-250.

IREP (2006). Interactive RadioEpidemiological Program. NIOSH-IREP v.5.5.1. http://www.niosh-irep.com/irep_niosh

R. Kirchmann, P. Charles, R. Van Bruwaene, J. Remy, G. Koch, and J. Van den Hoek (1977). "Distribution of Tritium in the Different Organs of Calves and Pigs after Ingestion of Various Tritiated Feeds", *Curr. Top. Radiat. Res. 12*, 291-312.

C. E. Land, E. Gilbert, and J.M. Smith (2003). *Report of the NCI-CDC Working Group to Revise the 1985 Radioepidemiological Tables* (National Institutes of Health, Bethesda), NIH Publication 03-5387.

R. W. Leggett (1986). "Predicting the Retention of Cesium in Individuals", *Health Phys. 50*, 747-759.

R. W. Leggett and L. R. Williams (1986). "A Model for the Kinetics of Potassium in Healthy Humans", *Phys. Med. Biol. 31*, 23-42.

R. W. Leggett (1992). "A Generic Age-Specific Biokinetic Model for Calcium-Like Elements", *Radiat. Prot. Dosim. 41*, 183-198.

R. W. Leggett (1993). "An Age-Specific Kinetic Model of Pb Metabolism in Humans", *Environ. Health Perspect. 101*, 598-616.

R. W. Leggett (1994). "Basis for the ICRP's Age-Specific Biokinetic Model for Uranium", *Health Phys. 67*, 589-610.

R. W. Leggett (1997a). "A Model of the Distribution and Retention of Tungsten in the Human Body", *Sci. Tot. Environ. 206*, 147-165.

R. W. Leggett (1997b). "Basis and Implications of the ICRP's New Biokinetic Model for Thorium", *Health Phys. 73*, 587-600.

R. W. Leggett, A. Bouville, and K. F. Eckerman (1998). "Reliability of the ICRP's Systemic Biokinetic Models", *Radiat. Prot. Dosim. 79*, 335-342.

R. W. Leggett and K. F. Eckerman (2001). "A Systemic Biokinetic Model for Polonium", *Sci. Tot. Environ. 275*, 109-125.

R. W. Leggett and L. R. Williams (1988). "A Biokinetic Model for Rubidium in Humans", *Health Phys. 55*, 685-702.

R. W. Leggett, J. C. Barton, and K. F. Eckerman (2000). "Mathematical Models of Metal Metabolism in Hemochromatosis", in: *Hemochromatosis*, J. C. Barton and C. Q. Edwards, eds. New York: Cambridge University Press.

R. W. Leggett (2001). "Consistent Biokinetic Models for the Actinide Elements", *Rad. Prot. Env. 24*, 616-622.

R. W. Leggett, L. R. Williams, D. R. Melo, and J. L. Lipsztein (2003). "A Physiologically Based Biokinetic Model for Cesium in the Human Body", *Sci. Total Environ. 317*, 235-255.

C. W. Mays and H. Speiss (1984). "Bone sarcomas in patients given radium-224", in: *Radiation Carcinogenesis. Epidemiology and Biological Significance*, J.D. Boice and J.F. Fraumeni, eds., pp. 241-252. New York: Raven.

C. W. Mehard and B. E. Volcani (1975). "Similarity in Uptake and Retention of Trace Amounts of 31-Silicon and 68-Germanium in Rat Tissues and Cell Organelles", *Bioinorg. Chem. 5*, 107-124.

Yu. I. Moskalev (1961). "Distribution of Lanthanum-140 in the Animal Organism", in: *Distribution, Biological Effects, and Migration of Radioactive Isotopes*. AEC-tr-7512, 45-59.

Yu. I. Moskalev, G. A. Zalikin, and V. S. Stepanov (1974). "Distinctions of Distribution in the Organism of Radioactive Isotopes of Lanthanide Elements", in: *Biological Effects of Radiation from External and Internal Sources*. AEC-tr-7457.

NAS (1988). *Health Risks of Radon and Other Internally Deposited Alpha-Emitters (BEIR IV)* (National Academy of Sciences, National Academy Press, Washington, DC).

NAS (1990). *Health Effects of Exposure to Low Levels of Ionizing Radiation (BEIR V)*. (National Academy of Sciences, National Academy Press, Washington, DC).

NCHS (1992). *Vital Statistics Mortality Data, Detail, 1989*, NTIS order number for datafile tapes: PB92-504554 (U. S. Department of Health and Human Services, Public Health Service, National Center for Health Statistics, Hyattsville, MD).

NCHS (1993a). *Vital Statistics Mortality Data, Detail, 1990*, NTIS order number for datafile tapes: PB93-504777 (U. S. Department of Health and Human Services, Public Health Service, National Center for Health Statistics, Hyattsville, MD).

NCHS (1993b). *Vital Statistics Mortality Data, Detail, 1991*, NTIS order number for datafile tapes: PB93-506889 (U. S. Department of Health and Human Services, Public Health Service, National Center for Health Statistics, Hyattsville, MD).

NCRP (1980). *Influence of Dose and Its Distribution in Time on Dose-Response Relationships for Low-LET Radiations*, NCRP Report 64 (National Council on Radiation Protection and Measurements, Bethesda, MD).

NCRP (1990). *The Relative Biological Effectiveness of Radiations of Different Quality*, NCRP Report No. 104 (National Council on Radiation Protection and Measurements, Bethesda, MD).

NCRP (1997). *Uncertainties in Fatal Cancer Risk Estimates Used in Radiation Protection*, NCRP Report No. 126 (National Council on Radiation Protection and Measurements, Bethesda, MD).

D. Newton, A. K. Ancill, K. E. Naylor, and R. Eastell, R. (2001). "Long-Term Retention of Injected Barium-133 in Man", *Radiat. Prot. Dosim. 97*, 231-240.

NRC (National Research Council). 2006. *Health Risks from Exposure to Low Levels of Ionizing Radiation. BEIR VII Phase 2*. Washington, DC: National Academy Press.

NRC-CEC (1997). *Probabilistic Accident Consequence Uncertainty Analysis. Late Health Effects Uncertainty Assessment*, NUREG/CR-6555; EUR 16774; SAND97-2322 (U.S. Nuclear Regulatory Commission, Washington, DC; Office for Publications of the European Communities, Luxembourg).

NRC-CEC (1998). *Probabilistic Accident Consequence Uncertainty Analysis. Uncertainty Assessment for Internal Dosimetry*, NUREG/CR-6571; EUR 16773; SAND98-0119 (U.S. Nuclear Regulatory Commission, Washington, DC; Office for Publications of the European Communities, Luxembourg).

H. E. Palmer, I. C. Nelson, and G. H. Crook (1970). "The Uptake, Distribution, and Excretion of Promethium in Humans and the Effect of DTPA on These Parameters", *Health Phys. 18*, 53-61.

Z. Pietrzak-Flis, I. Radwan, and L. Indeka (1978). "Tritium in Rabbits after Ingestion of Freeze-Dried Tritiated Food and Tritiated Water", *Radiat. Res. 76*, 420-428.

Z. Pietrzak-Flis, I. Radwan, Z. Major, and M. Kowalska (1982). "Tritium Incorporation in Rats Chronically Exposed to Tritiated Food or Tritiated Water for Three Successive Generations", *J. Radiat. Res. 22*, 434-442.

J. W. Poston, Jr., K.A. Kodimer, W.E. Bolch, and J.W. Poston, Sr. (1996a). "Calculation of Absorbed Energy in the Gastrointestinal Tract", *Health Phys. 71*, 300-306.

J. W. Poston, Jr., K.A. Kodimer, W.E. Bolch, and J.W. Poston, Sr. (1996b). "A Revised Model for the Calculation of Absorbed Energy in the Gastrointestinal Tract", *Health Phys. 71*, 307-314.

N. D. Priest, D. Newton, J. P. Day, R. J. Talbot, and A. J. Warner (1995). "Human Metabolism of Aluminum-26 and Gallium-67 Injected as Citrates", *Human Exp. Toxicol. 14*, 287-293.

M. Rochalska and Z. Szot (1977). "The Incorporation of Organically-Bound Tritium of Food into Some Organs of the Rat", *Int. J. Radiat. Biol. 31*, 391-399.

G. E. Runkle, M. B. Snipes, R. O. McClellan, and R. G. Cuddihy (1980). "Metabolism and Dosimetry of Inhaled $^{106}RuO_4$ in Fischer-344 Rats", *Health Phys. 39*, 543-553.

D. B. Shipler, J. E. Ballou, B. I. Griffin, and I. C. Nelson (1976). "Development of a Diagnostic Model for Inhaled Promethium-147 Oxide", in: *Diagnosis and Treatment of Incorporated Radionuclides*. IAEA-SR-6/28.

J. W. Stather and J. R. Greenhalgh (1983). *The Metabolism of Iodine in Children and Adults*. UK National Radiological Protection Board Report NRPB-R140, Chilton.

R. J. Talbot, D. Newton, N. D. Priest, J. G. Austin, and J. P. Day (1995). "Inter-subject Variability in the Metabolism of Aluminum following Intravenous Injection as Citrate", *Human Exp. Toxicol. 14*, 595-599.

D. M. Taylor and R. W. Leggett (2003). "A Generic Biokinetic Model for Predicting the Behavior of the Lanthanide Elements in the Human Body". *Radiat. Prot. Dosim. 105*, 193-198.

D. M. Taylor, A. Seidel, and H. Doerfel (1985). "The Metabolism of Radiohafnium in Marmosets and Hamsters", *Int. J. Nucl. Med. Biol. 12*, 387-391.

G. A. Taylor, R. G. Pullen, A. B. Keith, and J. A.Edwardson (1992). "Germanium-68 as a Possible Marker for Silicon in Rat Brain", *Neurochem. Res. 17*, 1181-1185.

R. G. Thomas, J. E. Furchner, J. E. London, G. A. Drake, J. S. Wilson, and C. R. Richmond (1976). "Comparative Metabolism of Radionuclides in Mammals--X. Retention of Tracer-Level Cobalt in the Mouse, Rat, Monkey and Dog", *Health Phys. 31*, 323-333.

M. C. Thorne, D. Jackson, and A. D. Smith (1986). *Pharmacodynamic Models of Selected Toxic Chemicals in Man. Vol. 1: Review of Metabolic Data*, Lancaster, England: MTP Press Limited.

M. Tokunaga, C.E. Land, S. Tukoka, I. Nishimori, M. Soda and S. Akiba (1994). "Incidence of female breast cancer among atomic bomb survivors, 1950-1985", *Radiat Res 138*, 209-223.

P. L. Wright and M. C. Bell (1966). "Comparative Metabolism of Selenium and Tellurium in Sheep and Swine", *Am. J. Physiol. 211*, 6-10.

N. Yamagata, K. Iwashima, T. A. Iinuma, K. Watari, and T. Nagai (1969). "Uptake and Retention Experiments of Radioruthenium in Man - I", *Health Phys. 16*, 159-166.

N. Yamagata, K. Iwashima, T. A. Iinuma, T. Ishihara, and K. Watari (1971). "Long-Term Retention of Radioruthenium in Man", *Health Phys. 21*, 63 (abstract).

INTERNAL DISTRIBUTION

1-3. R. W. Leggett, Bldg 1060COM, MS6480
4-5. K. F. Eckerman, Bldg 1060COM, MS6480
6. Central Research Library
7. ORNL Laboratory Records-RC
8-9. ORNL Laboratory Records-OSTI

EXTERNAL DISTRIBUTION

10. A. Bouville, National Cancer Institute, 6120 Executive Boulevard, EPA Room 7094, Rockville, MD 20852
11. M. A. Boyd, U.S. EPA-6608J, 1200 Pennsylvania Avenue, NW, Washington, DC 20460
12. C. B. Nelson, RR1 Box 4140, Sedgwick, ME 04676-9724
13. N. S. Nelson, U.S. EPA-6608J, 1200 Pennsylvania Avenue, NW, Washington, DC 20460
14-19. D. J. Pawel, U.S. EPA-6608J, 1200 Pennsylvania Avenue, NW, Washington, DC 20460
20. J. S. Puskin, U.S. EPA-6608J, 1200 Pennsylvania Avenue, NW, Washington, DC 20460